Title
Protein Nanocapsule Based Protein Carriers for Industrial and Medical Applications

Author
LI, JIE

Publication Date
2015

Peer reviewed|Thesis/dissertation

UNIVERSITY OF CALIFORNIA

Los Angeles

Protein Nanocapsule Based Protein Carriers for Industrial and Medical Applications

A dissertation submitted in partial satisfaction of the

requirements for the degree Doctor of Philosophy

in Chemical Engineering

by

Jie Li

2015

ABSTRACT OF THE DISSERTATION

Protein Nanocapsules Based Protein Carriers for Industrial and Medical Applications

by

Jie Li

Doctor of Philosophy in Chemical Engineering

University of California, Los Angeles, 2015

Professor Yunfeng Lu, Chair

Proteins play the most dynamic and diverse roles among all the biomacromolecules in living organisms. With the fast development in biotechnology, protein gains more and more interests for a wide range of applications, such as biochemical synthesis, sensing, environmental protection and medical applications. However, the vulnerable nature of proteins has hindered their boarder applications. Developing vectors and stabilizers that help to more effectively deliver protein therapeutics or stabilize proteins has been an essential theme of the field.

In this dissertation, novel strategies have been developed for protein delivery by a method of *in-situ* free-radical polymerization or by a self-assembling/ crosslinking approach. Protein nanocapsules made from the *in-situ* polymerization method were also used building blocks to synthesize protein composites with dramatically enhanced stability. This dissertation research consist with four topics outlined below:

1. Organophosphorus hydrolase (OPH) nanocapsules were synthesized by *in-situ* free-radical polymerization with enhanced activity and stability. These nanocapsules are highly potent for decontamination, as well as *in vivo* detoxification of organophosphorus as prophylactics or antidotes.
2. Protein nanocapsules made by the *in-situ* polymerization technique were used as building blocks to synthesize protein-silica composites through a sol-gel process. The microenvironment around the proteins was engineered through judicious choices of the polymer monomers and the silica precursors, enabling the synthesis robust enzyme composites with high activity for various industry applications.
3. Protein nanocapsules were synthesized by assembling the proteins with self-crosslinking cell penetrating polymer (SCP). Self-crosslinking by disulfide-bond formation within the SCP leads to the formation of robust protein nanocapsules with highly retained activity. These nanocapsules

were able to be effectively internalized by cells without significant cytotoxicity, and the protein cargo could be effectively released upon exposure to glutathione that break down the disulfide bonds.

4. Protein nanocapsules with zwitterionic shells were synthesized by a self-assembling approach. The zwitterionic shells protected the nanocapsules from being uptake by macrophages, while such shells could be detached once exposing to a low pH environment. This approach provides a suitable platform towards protein therapeutics with prolonged circulation time with ability of being delivered into the cells.

Overall, this dissertation work provides novel strategies toward better protein-delivery vectors, as well as composites with better protein stability and activity, for a broad range of applications.

The dissertation of Jie Li is approved.

Tatiana Segura

Yu Huang

Yunfeng Lu, Committee-Chair

University of California, Los Angeles

2015

Table of Contents

List of Figures

List of tables

ACKNOWLEDGEMENTS

The completion of the dissertation is the most exciting moment after the five years tough but fruitful journey for my PhD study. I would like to thank and appreciate all the people who have helped and supported me during my study in UCLA.

First of all, I would like to express the deepest appreciation to my committee chair, Professor Yunfeng Lu, who is a genius of science and engineering and also a role model as an advisor. He guided me to the cutting-edge research in the field of protein delivery and demonstrated the spirit and attitude towards research. Without his guidance and persistent help, I would not have been possible to complete my dissertation.

I would like to appreciate my committee members, Professor Tatiana Segura, Professor Harold Monbouquette and Professor Yu Huang for their help with my research work and dissertation. I would especially appreciate Professor Segura, for generous guidance and supports for our lab.

I would like to express my appreciation to Dr. Juanjuan Du and Dr. Yang Liu, who convey the philosophy and method of research as senior members in our lab. I would like to thank Dr. Jing Wen, Dr. Ding Weng, Dr. Chih-ning Pao, Dr. Jing Jin, Dr. Gan Liu, Di Wu, Chaoyong Liu, Jie Ren and Shuoran Li. They provide a lot of insightful suggestions and support that motivated my research. I would also like to thank all the other Lu lab members and alumni. The five years spent with you will become good memories in my life. I would also like to express my appreciate for my friends Rui Li and Zhiping Feng, who provided a lot on lab support for cell lines and bacteria strains.

At last, I would like to thank my parents who encourage me to pursuing my PhD degree and cheer me up when I'm frustrated. They are always my strongest support to rely on.

VITA

Education:

September 2016-July 2010	B. S., Chemistry
	Nankai University
September 2016-July 2010	B. E., Chemical Engineering
	Tianjin University
	(Joint program with Nankai University)

Publication:

1. W. Wei, J. Du, J. Li, M. Yan, Q. Zhu, X. Jin, X. Zhu, Z. Hu, Y. Tang, Y. Lu, Construction of Robust Enzyme Nanocapsules for Effective Organophosphate Decontamination, Detoxification, and Protection, *Adv. Mater.*, 2013, **25**, 2212-2218.
2. J. Jin, W. Wei, J. Du, Y. Liu, J. Li, Z. Lu, Y. Lu, Development of a self-crosslinking targeting polymer for rapid gene delivery, *J. Controlled Release*, 2013, **172**, e107-e108.
3. J. Du, J. Jin, Y. Liu, J. Li, T. Tokatlian, Z. Lu, T. Segura, X.-b. Yuan, X. Yang, Y. Lu, Gold-Nanocrystal-Enhanced Bioluminescent Nanocapsules, *ACS Nano*, 2014, **8**, 9964-9969.
4. J. Li, X. Jin, Y. Liu, F. Li, L. Zhang, X. Zhu, Y. Lu, Robust enzyme-silica composites made from enzyme nanocapsules, *Chem. Commun.* (Cambridge, U. K.), 2015.
5. Y. Liu, J. Li (Equal contribution), Y. Lu, Enzyme therapeutics for systemic detoxification, *Adv. Drug. Deliv. Rev.*, 2015.

Chapter 1 Application of proteins and protein carriers

Every single living cell is made from millions of biomacromolecules. Among them, proteins have the most dynamic and diverse role of any macromolecule in the body, catalyzing biochemical reactions, forming receptors and channels in membranes, providing intracellular and extracellular scaffolding support, and transporting molecules within a cell or from one organ to another.[1] Human have widely applied proteins, particularly enzymes, in industries such as food process [2], pharmaceutical manufacture [3], biofuel production [4] and environment protection [5] due to their high activity and high specificity. On the other hand, many diseases may result when any one of these proteins contains mutations or other abnormalities, or is present in an abnormally high or low concentration and protein therapeutics represent a tremendous opportunity to directly alleviate these diseases.[1] However, due to the vulnerable nature of proteins, their application has been limited. Developing methodology to stabilize proteins as well as improve their activities remains challenging.

1.1 Enzyme immobilization

Enzyme immobilization has been extensively used to improve enzyme's thermal, solvent and long-term storage stability. Enzymes were either physically encapsulated within or chemically conjugated to solid matrices, such as polymers [6-8], silica [9, 10], organoclays [11] and carbons [12]. Sol-gel entrapment and mesoporous silica loading are two most widely used approaches. For sol-gel method, traditional way of hydrolysis and condensation of silica precursor such as tetramethyl orthosilicate (TMOS) and tetraethyl orthosilicate (TEOS) usually requires strong acid or base catalysis, which greatly comprise the activity of the native enzyme. The hydrolysis by-product, methanol and

ethanol, also decimate the delicate secondary and tertiary structure of enzyme, resulting significant decreased activity. Moreover, due to small pore size and non-open-pore structure, the substrate and product diffusion resistance is larger and most studies showed lower specific activity than that of the free enzymes in solutions [11], reflecting as significantly increased K_m. On the other hand, enzyme leaching from mesoporous silica and low loading capacities are two major problems when enzyme loading is conducted by physical adsorption.[12] While covalent immobilization can partially alleviate these problems by reaction of functional groups on the enzyme with a chemically active surface, these covalent links may also block the functional groups in the enzyme active sites or inhibit enzyme conformational mobility, resulting significantly comprised activity.[13] To endow enzymes with improved stability and accredited activity, novel strategies need to be further established.

1.2 Protein therapy

With the fast developing biotechnology and recombinant DNA and protein techniques, protein drugs now can be produced in large quantities.[13] Protein therapeutics represents a tremendous opportunity to directly alleviate diseases and can be used for treatment of endocrine and metabolic disorders [14-32], augmenting and blocking pathways [33-44], detoxification [45-54], vaccine [55-57] and diagnostics [58-60]. At present, more than 130 different proteins or peptides are approved for clinical use by the US Food and Drug Administration (FDA), and many more are under development.[1]

Protein therapy has several advantages over small-molecule drugs. First, proteins often serve a highly specific and complex set of functions that cannot be mimicked by simple chemical compounds and therefore there is less potential for protein therapeutics to

interfere with normal biological processes and cause adverse effects. Second, because the body naturally produces many of the proteins that are used as therapeutics, these agents are often well tolerated and are less likely to elicit immune responses. Third, the clinical development and FDA approval time of protein therapeutics may be faster than that of small-molecule drugs.[1]

Protein therapy also has advantages over gene therapy. Proteins have previously defined optimal doses of the individual protein for disease states with well-known biological effects, while the protein expression level by gene therapies are difficult to predicted. Also gene therapy may have risk of undesired immune and inflammatory response and potential oncogenesis related to viral vectors and currently there is no approved human gene therapy product.[61]

Table 1.1 Protein therapeutics in clinical practice.

Therapeutic	Function	Examples of clinical use
Insulin	Regulates blood glucose	Diabetes mellitus
Factor VIII and IX	Coagulation factor	Haemophilia
β-Glucocerebrosidase	Hydrolyzes glucocerebroside to glucose and ceramide	Gaucher's disease
Bevacizumab	Humanized mAb that binds all isoforms of VEGF-A	Colorectal cancer, non-small-cell lung cancer
Rituximab	Chimeric (human/mouse) mAb that binds CD20	Refractory CD 20^+ B-cell non-Hodgkin's lymphomas (NHL) in combination with chemotherapy

Interferon-α2a	Immunoregulator	Hairy cell leukemia, chronic myelogenous leukemia, Kaposi's sarcoma, chronic hepatitis C infection
Streptokinase	Plasminogen activator	Pulmonary embolism, deep vein thrombosis, arterial thrombosis or embolism
Recombinant human bone morphogenic protein 2	Bone differentiation regulator	Spinal fusion surgery, bone injury repair
Growth hormone	Anabolic and anticatabolic effector	Growth failure due to GH deficiency or chronic renal insufficiency
Uricase	Metabolizes uric acid	Hyperuricemia and gout
Adenosine deaminase	Metabolizes adenosine, prevents accumulation of adenosine	Severe combined immunodeficiency disease
Phenylalanine ammonia lyase	Metabolizes phenylalanine	Treatment for phenylketonuria
L-Asparaginase	Removing available asparagine from serum	Acute lymphocytic leukemia

Despite these tremendous advances, protein drugs possess several shortcomings that limit their usefulness, including their susceptibility to destruction by proteolytic enzymes, short circulating half-life, low solubility, rapid kidney clearance and their propensity to generate neutralizing antibodies.[62] In addition, most protein drugs must be delivered by injection, either subcutaneously or intravenously.[62] Use of an appropriate delivery carrier, which can protect protein drugs from enzymatic degradation, prolong circulation time and control release, is a promising approach for prolonged retention and biological activity of the drugs within the body.

1.3 Nanocarriers for protein delivery

Nanocarriers has been developed during the last two decades focusing on improvement of protein stability. Nanocarriers provide unquestionable advantages as it permits resolving some of the problems inherent to the therapeutic use of enzymes, as are their low stability, fast clearance, immunological disorders, allergies associated with the treatments, and the need for repeated administrations.[63] To date, various vectors have been explored to facilitate delivery of proteins, such as liposomes, polymers, mesoporous silica particles, magnetic nanoparticles and carbon nanotubes, and natural vectors such as cell-penetrating peptides, antibodies and other biomolecules.

1.3.1 Liposome

Liposomes have been used as pharmaceutical carriers during the past 30 years.[64] Liposomes are nano-sized artificial vesicles, which can be produced from natural or synthetic phospholipids. Proteins are typically located in the aqueous core, while other hydrophobic molecules can be dissolved within the bilayers of liposomes.[65] Liposomes may provide many advantages for protein therapies, including: 1) liposomes are biocompatible; 2) liposomes can stabilize the encapsulated enzymes; 3) the size, charge and surface properties of liposomes can be readily turned by introducing desired lipid moieties such as PEG-conjugated lipids, where PEG stands for poly(ethylene glycol).

A potential problem with liposome-wrapped enzymes, particularly when delivered intravenously, is the rapid removal from the circulation by the reticuloendothelial system.[66] To enhance their circulation half life, “stealth liposomes” have been designed by coating the liposomes with PEG.[67] This could be achieved either by constructing liposomes using PEG-conjugated lipids (PEG-lipid) or by post-conjugating PEG on the

liposome surface (Figure 1.1). Klibanov *et al*. first reported the preparation of PEGylated liposomes, which increased the circulation half life from less than 30 min to 5 h compared to their liposome counterparts.[68] The prolonged circulation time is attributed to the large hydrodynamic volume of the PEG chains, which shield around the liposomes and mask the liposomes from immune and metabolic systems.[69] Based on a similar mechanism, other hydrophilic polymers were also used to construct long-circulating liposomes, including poly[N-(2-hydroxypropyl) methacrylamide)] [70], poly-N-vinylpyrrolidones [71], L-amino-acid based polymers [72], and polyvinyl alcohol [73]. However, conjugating with such polymers often decreases the liposome stability because conjugation of hydrophilic polymers reduces glass-transition temperature of the liposomes. To maintain necessary stability for these liposomes, only a limited amount of polymers could be conjugated, leading to low density of the surface-grafted polymeric layer, which reduce their effects in prolonging the circulation time of liposomes

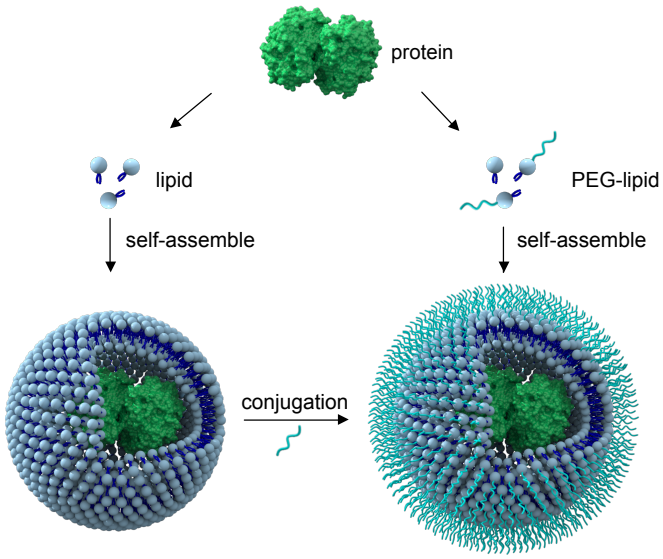

Figure 1.1 Illustration of PEG-liposome.

Because simple preparation and excellent biocompatibility, liposomes have been extensively explored as delivery carriers for many therapeutic proteins. For example, cationic liposomes constructed from trifluoroacetylated lipopolyamine (TFADODAPL) and dioleoyl phosphatidylethanolamine (DOPE) were used to deliver various different proteins, including antibodies, phycoerythrin, β-galactosidase, caspase 3, caspase 8 and gramzyme B intracellularly.[74] The majority of the internalized proteins were distributed within the cytosol, indicating successful release of the proteins during endocytosis. Cationic liposomes containing lipospermine (DOGS) were also used to deliver anionic proteins such as phycoerythrin and IgGs into the cytoplasm.[75] Uricase has been successfully encapsulated within liposomes. Studies showed that liposome-wrapped uricase exhibits more effective management of the uric-acid level than native uricase in hyperuricemia rat model due to the higher uricolytic activity.[76, 77] Consistently, L-asparaginase has also been encapsulated into liposomes, resulting in liposome-wrapped L-asparaginase with prolonged circulating time, abrogation of acute toxicity and better retained *in vivo* antitumor activity.[78, 79] However, despite the improved circulating time and therapeutic effects, the delivery efficiency is still far from optimal.

To further enhance cell uptake efficiency, cell-penetrating peptides (CPPs) such as TAT (a cell penetrating peptide derived from HIV virus with sequence of GRKKRRQRRRPPQ) were conjugated to liposomes. The first example of TAT-conjugated liposomes was reported by Torchilin *et al.*, where TAT was conjugated to liposomes with poly(ethyleneglycol) (PEG) spacer.[80] Proteins such as BSA, β-galactosidase and IgGs were delivered with high efficiency using other CPP-modified

liposomes, such as oligoarginine-modified liposomes.[81] In addition to CPPs, antibodies,[82-84] folic acid,[85] and transferrin[83, 86] were also conjugated to liposomes to facilitate their internalization and targeting process. Moreover, to realize targeted delivery, TAT and antibodies were conjugated to liposomes with short and long PEG spacers, respectively. Liposomes were able to target the cancer cell surface through antibody, while TAT were exposed and facilitate internalization after cleavage of long PEG spacers by acid-liable linker.[87]

1.3.2 Polymers

Due to versatility and easy control of the physiochemical properties, conjugating proteins with polymer has been broadly adapted for the development of therapeutic purposes. The polymers may shield the enzymes from undesired interactions with the surrounding, improve the enzyme stability, reduce immune activation, and prolong the circulation time. Polymers, particularly cationic polymers can also facilitate protein intracellular delivery. The protein delivery effects are highly dependent on the physiochemical properties of the polymers, such as hydrophilicity, chain length, chain architecture (i.e., linear versus branched) and biocompatibility, which are elaborated in detail below.[88]

1.3.2.1 Poly(ethylene glycol) (PEG)

PEG is the most commonly used polymer for the preparation of polymer-enzyme conjugates. Covalently attaching PEG to the enzymes, also termed as PEGylation, is generally achieved by reacting PEG with the reactive motifs of enzymes. Commonly, PEGylation is achieved through reacting the ε-amino groups of lysine residues. This process often results in the formation of conjugated isomers containing various PEG chains attached at different sites,[89] and further purification process is required for FDA

approval. To circumvent this limitation, site-specific PEGylation reactions have also been developed,[90] such as the methods of N-terminal PEGylation and cysteine-specific PEGylation, where the conjugation is occurred at the N-terminal α-amino groups and the residue cysteines (or cleaved disulfide bond), respectively.[91-93] Other site-specific PEGylation methods were also developed, such as conjugating PEG-alkylamine reagent onto glutamine residues by transglutaminase[91-93] and reacting (sialic acid)-PEG with the hydroxyl groups of specific serine or threonine of a glycosylated protein.[94] These site-specific strategies lead to more defined conjugating structure, facilitating their transition for clinic use.

The shielding effect of PEG is mainly attributed from its hydrogen bonding with water, although the backbone of the molecule is hydrophobic. When dispersed in aqueous solution, the PEG chains form hydrogen bonds with the surrounding water molecules.[95] Such hydrated layers effectively shield the enzymes from their surrounding, affording the enzymes with improved bioavailability, prolonged circulation time, and reduced immunogenicity and toxicity. Consistently, PEG with longer chain length and higher density offers longer circulation life. In addition, PEG chain architecture also influences the pharmacokinetics of PEGylated enzymes, and branched PEG generally exhibits longer circulation half life than linear ones with similar molecular weight.[96] Such shielding layers, however, may block active sites of the PEGylated enzymes, resulting in reduced or even completely loss of the enzyme activity. Although the improved pharmacokinetics may compensate the reduced enzyme activity in certain degree,[97, 98] reduced enzyme activity remains as a main drawback of PEGylation.[90]

PEGylated proteins have been extensively studied for therapeutics to treat metabolism

disorders and intoxication, many of which have been approved for therapeutic use.[99] Adagen (pegadamase) represents the first enzyme therapeutic approved for inherited disease,[100] followed by the approval of Oncaspar (pegaspargase),[101] both of which use PEG succinimidyl succinate as a random PEGylation reagent. Krystexxa, a PEGylated recombinant uricase was also prepared by random conjugation of PEG p-nitrophenyl carbonate ester to the lysine residues of uricase.[102] Branched PEG of 40 kDa was coupled to Interferon-α2a to make Pegasys, which only need treatment once a week for hepatitis C, showing superior efficacy compared with their unpegylated counterparts.

Other enzymes, such as arginine deiminase (ADI), phenylalanine ammonia-lyase and organophosphorus hydrolase (OPH), were also conjugated with PEG with significantly extended residence time of days, in comparison with their native enzyme counterparts with resident time of hours.[46, 103] However, there are increasing number of reports on the formation of anti-PEG antibodies when PEGylation therapeutics was used as intravenous agents.[46, 104] Developing alternative shielding layers that can further evade the immune system is essential but challenging.

1.3.2.2 Other hydrophilic polymers

Dextran, a natural and biodegradable polysaccharide, poly(vinylpyrolidone) (PVP) and poly(N-acryloylmorpholine) (PAcM), two synthetic polymer, are extensively used in large quantities as a blood expander, and are known for its negligible toxicity, low immunogenicity and antigenicity.[105-108] Recently, they have also been investigated as carriers for delivery of drugs and proteins, which are mainly achieved through conjugating dextran with the therapeutic agents.[109] Similar to PEG, conjugation of

these hydrophilic polymers endows the therapeutic agents with prolonged circulating time, increased protein stability and reduced in vivo immunogenicity. For example, Wileman *et al.* prepared asparaginase-dextran conjugates with significantly improved plasma half-life in both immune and non-immune rabbits.[110] Similarly, dextran-conjugated uricase exhibits significantly prolonged circulation time, which is over ten times of the native enzyme counterpart (7h vs 0.6h).[111] Carboxypeptidase G2 (CPG), which can enzymatically deplete an essential nutrient (folate) for the tumor cells, has only 3.1 h plasma half-life. Conjugating CPG with dextran with 40, 70, 110 or 150 kDa molecular weight results in a plasma half-life of 14.3, 16.3, 17.5 and 45.6 h in normal mice, respectively.[112] However, it has been reported that intravenous administration of dextran with high molecular weight may cause life-threatening anaphylaxis.[113] PVP-conjugated SOD was prepared with increased circulation time, reduced antigenicity and immunogenicity, and enhanced thermal stability.[114] Similar to PVP, PAcM-uricase conjugates, for example, exhibit dramatically reduced antigenicity and suppressed immunogenicity.[115] PVP-Uricase conjugates were also prepared; however, 2-folds higher of antigenicity than the native uricase was observed.[115] Therefore, more extensive studies in toxicity, immunogenicity, antigenicity, and clearance mechanism of these polymer-protein conjugates are required to understand their therapeutic potentials.

1.3.2.3 Block Copolymers

Amphiphilic block copolymers are another class of polymers commonly used as nanocarriers. Particularly, Pluronic triblock copolymers composed with poly(ethylene oxide) (PEO) and poly(propylene oxide) (PPO) have been extensively studied due to their biocompatibility, biodegradability, low toxicity and prolonged circulation time when

conjugated with proteins.[116, 117] This makes Pluronic copolymers promising carriers for delivering proteins *in vivo*. For example, organophosphorus hydrolase (OPH) was conjugated to Pluoronic F127 ($EO_{100}PO_{65}EO_{100}$), and the resulting conjugates could self-assemble into a micelle structure with a hydrophobic PPO core and OPH on the surface. The PPO core can attract hydrophobic OP molecules and the OPH on the surface facilitates its degradation, showing great promise for treatment of OP intoxication.[118] Pluronic P85 ($EO_{26}PO_{40}EO_{26}$) and L81 ($EO_6PO_{43}EO_6$) were also conjugated with superoxide dismutase (SOD), which could be used to inhibit intraneuronal superoxides.[119]

Besides Pluronic triblock copolymers, other block copolymers have also been studied as nanocarriers for antioxidant treatment. One example is vinyl sulfone (VS)-terminated block copolymers of poly(propylene sulfide) (PPS) and PEG (PPS-PEG-VS), which forms micelles with vinyl sulfone groups. SOD could be readily conjugated to the micelle surface through the Michael-type addition. The conjugated SOD could effectively eliminate superoxides, while PPS (mainly located within the micelle cores) can scavenge the toxic hydrogen peroxide produced the SOD-mediated reactions. Such a synergic effect is also observed in a cascade reactions mediated by SOD and catalase.[120]

1.3.2.4 Cationic polymer

For effective intracellular protein delivery, conjugating proteins to cationic polymeric delivery vectors is a feasible approach to increase transduction efficacy. In 2005, Futami *et al.* first reported conjugates of cationic polyethylenimine (PEI) with protein for intracellular protein delivery [121]. Enhanced green florescent protein (EGFP) conjugated with PEI shows significantly higher cell uptake than TAT-EGFP fusion

proteins. When using similar method to conjugate ribonuclease (RNase), the cytotoxicity of RNase increased dramatically. Additionally, the cytotoxicity of PEI-RNase was found to relate to the length of PEI chains, confirming the role of PEI in improving cellular uptake efficacy. β-catenins were also delivered via conjugation with PEI with high efficiency and demonstrated by activating the Wnt canonical signaling pathway (a pathway that contributes to the self-renewal of mouse hematopoietic stem cells).[122] Such a strategy was also extended to deliver antibodies with the capability to bind antigens. For example, biotin and antibodies were conjugated to PEI, respectively; after binding with streptavidin- or protein G-conjugated proteins, the PEI conjugates were delivered into cells with high efficiency.[123] Cleavable bonds such as disulfide bonds were also used for conjugation. For example, denatured p53-PEI conjugation can be delivered into cells and the unfolded proteins could refold to their native form after PEI is cleaved.[124]

1.3.2.5 Self-assembly of block copolymers with proteins

Self-assembly of block copolymers with proteins provide another approach for successful intracellular delivery of proteins. Protein denaturation is relatively small compared with covalent conjugation and the complexes are readily to dissociate once uptake by cells. Typically, one section of the polymer chain complexes with the protein through electrostatic interactions, hydrophobic interactions or other noncovalent interactions while the other hydrophilic section of the polymer helps to stabilize the assembly structure in the solutions. Particularly, the formation of protein-polymer complexes with copolymers containing a cationic block and a PEG block is of the greatest interest. The cationic block effectively binds with anionic proteins via electrostatic interaction, while

the PEG block forms an exterior hydration layer that stabilizes the complexed structure. For example, Kim *et al.* synthesized polylysine-co-poly(ethylene glycol) (PLL-PEG) block copolymer with folic acid linked to the end of the PEG chains. Assembling of such copolymer with anionic proteins resulted in highly effective protein delivery carriers.[125] Similarly, cationic proteins can be complexed with anionic copolymers. Typically, amine groups on cationic block copolymers can be modified with citraconic or cis-aconitic groups, which bear negative charged, but can be degraded in acidic endosomal environment upon endocytosis to release the cationic protein cargos.[126, 127] Such molecular modification provides enough flexibility to enable the formation of complexes with all kinds of proteins. The introduction of hydrophobic moieties into the block copolymers can further regulate the structure and increase the stability and uptake efficacy of the protein-polymer complex. For example, cationic cholesteryl group-bearing pullulans (CHPNH2) were assembled with proteins, resulting in monodispersed nanoparticles with more effective internalization than cationic liposomes and a protein transduction domain (PTD) based carrier even in the presence of serum.[128]

In addition to the non-specific assemblies mediated by electrostatic force or hydrophobic interactions, more specific affinity bindings were also utilized to form protein-polymer complexes. For example, glutathione modified PEI could bind with glutathione S-transferase-fused proteins and induce cellular uptake in mammalian cells. However, its application *in vivo* is still limited due to size effect, possible immunogenicity.[129]

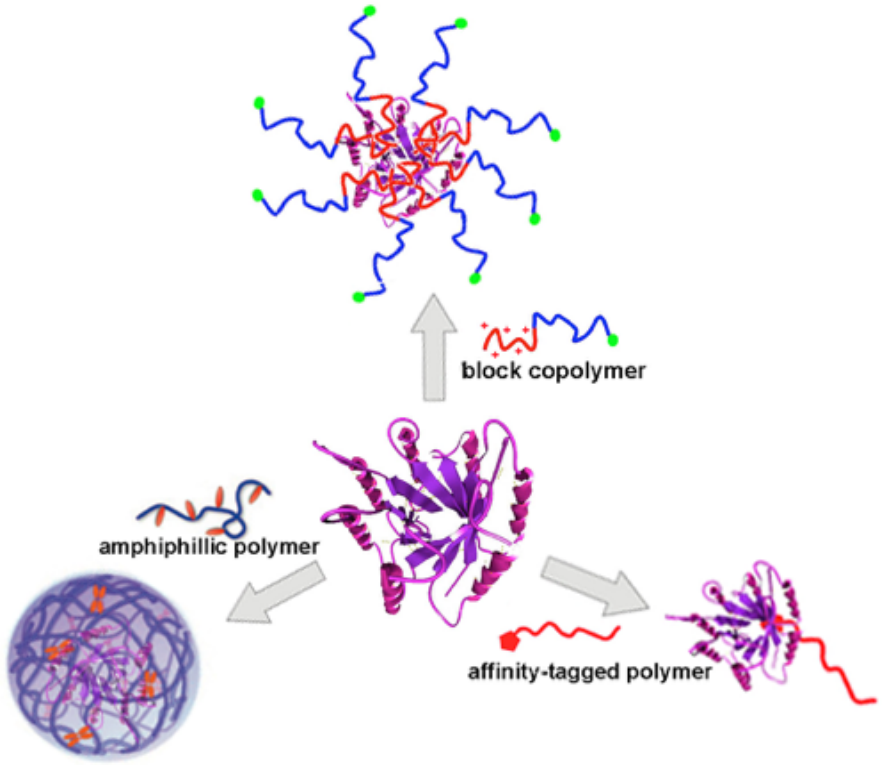

Figure 1.2 Illustration of noncovalent polymeric delivery systems.[123]

Overall, noncovalent polymeric delivery systems provide a facile strategy for intracellular protein delivery. However, the stability of the assembled complexes is often quite low. In fact, the complexes may be rapidly dissociated by dilution or competitive binding by serum proteins,[130] while strong interactions between polymers and proteins may alter the protein structures.[131]

1.3.3 Inorganic system

Besides liposome and polymer based delivery system, inorganic nanomaterials, including mesoporous silica, carbon nanotubes and magnetic nanoparticles (MNP) have also been explored for protein delivery, though to a less extent.

Gold nanoparticles (GNPs) are of interest for protein delivery due to their bioinertness, low toxicity, cellular imaging ability,[132-136] and easy synthesis and functionalization.[137, 138] The first intracellular delivery of proteins using GNPs was

reported by Tkachenko *et al.*[139]. CPP-modified BSA was absorbed onto GNP surface and delivered into cytoplasm. In addition, conjugating nuclear localization signals onto BSA led to its delivery into the nuclei. Similarly, β-galactosidase was adsorbed onto the peptide-coated GNPs with diameter of 2.5 nm and delivered into various cell lines was observed without significant toxicity to cells.[140]

Mesoporous silica prepared through co-assembly of silicates and surfactant has recently been explored as potential nanocarriers for bioactive molecules due to their unique properties, such as high surface area, large pore volume, tunable pore size, and convenient surface functionalization.[141-144] Delivery of cytochrome c was first achieved by loading proteins into MCM-41-type mesoporous silica with an average pore diameter around 5.2 nm.[145] The cytochrome c maintained its function after being delivered into the cytoplasm of human cervical cancer cells (HeLa) and being released under physiological conditions.

Carbon nanotubes (CNTs) have been extensively explored for a large spectrum of applications; their biological applications have started to emerge in recent years.[146] For example, single walled carbon nanotubes (SWNT) have been recently shown to shuttle various molecular cargos inside living cells including proteins, short peptides, and nucleic acids.[147-154] The first SWNT protein delivery system was reported by Kam *et al.*[147]. It was found that SWNT-streptavidin conjugates were internalized by human promyelocytic leukemia (HL60) cells and human T cells (Jurkat) via endocytosis. Later on, it was also found that SWNTs are genetic intracellular transporters of various types of proteins (≤80 kDa), including streptavidin, protein A, BSA, and cytochrome c, noncovalently and nonspecifically bound to nanotube sidewalls.[148] Various

mammalian cell lines, including HeLa, NIH-3T3 fibroblast, HL60, and Jurkat cells, were tested and a wide applicability was demonstrated. The internalization mechanism was verified as energy-dependent endocytosis. Further studies suggested that clathrin-dependent endocytosis is the pathway for the uptake of various SWNT-protein conjugates. [97] These results provide the first proof of concept of *in vitro* biological functionality and activity of proteins delivered by SWNT molecular transporters.

1.4 Responsive protein delivery

Stimuli-triggered release is an appealing and promising approach for protein delivery and has made protein delivery with both spatiotemporal- and dosage-controlled manners possible.[155] Both physiological and external stimuli have been extensively explored for controlling delivery of proteins, such as pH, redox potential, or enzymatic activities and external stimuli such as temperature, light, magnetic field or ultrasound.[155]

Table 2.2 Summary of recently reported stimuli-responsive nanomaterials for protein delivery.[156]

Stimulus	Nanomaterials	Model protein/peptide
pH	PIC micelles	Cytochrome C, IgG
	Cross-linked PDEAEMA-core/PAEMA-shell particles	OVA protein
	Polyaspartamide nanocapsules	BSA
	Single-protein nanocapsules	EGFP, HRP, BSA, SOD and Caspase 3
	Aldehyde-displaying silica nanoparticles	Arginase, GFP
	PAAD/PGA hydrogels	Insulin
Redox	Single-protein nanocapsules	Caspase 3
	Protein nanocapsules	MBP–APO
Enzyme	Crosslinked nano matrix	EGFP, Caspase 3, BSA and Klf4
	Protein nanocapsules	BSA, VEGF
	Gelipo	TRAIL
Temperature	Chitosan-PEG copolymer based hydrogels	BSA

	PNIPAAM hydrogels	Insulin, BSA
	PNIPAAM-grafted PPCL films	BSA
Light	Amphiphilic TiO_2 nanotubular-structured nanocarrier	HRP
	TiO_2 nanoparticles	Hemoglobin
	Lipid based nanoparticles	GFP, luciferase
	Silica-coated gold nanorods	OVA
Magnetic force	AMMHs	BSA
	Fatty acid calcium salt	Antioxidant enzymes, SOD and catalase
	Ab-MNPs	DR4
Ultrasound	PLGA nano-network	Insulin

1.4.1 pH responsive systems

Physiological pH gradient is the most explored responsive trigger to design nanosystems for controlled drug delivery to target locations, including intracellular compartments or extracellular microenvironments associated with certain pathological situations, such as cancer or inflammation.[157-159] There are two main strategies to utilize the pH stimuli: one relies on the charge or hydrophobicity change of polymers in response to the pH variation[160]; the other involves the cleavage of acid-sensitive bond, such as hydrazone, oxime, acetal or ester.[161-164]

Extensive studies have been focus on the charge reversible response for protein delivery, which relies on polymer swelling and charge repulsion. For example, chitosan swelling induced on amino-group protonation (pK_a ~6.3) leads to the release of encapsulated tumor necrosis factor alpha (TNFα) in the local acidic environment of tumor tissues.[158] PH triggered delivery of proteins into ischemic areas was achieved with piperidine- and imidazole-modified PEG–poly(β-amino ester) micelles.[159] An intracellular protein delivery strategy based on charge-conversional polyionic complex (PIC) micelles were

developed by Kataoka group.[127, 165] Proteins were encapsulated in micelle structure by electrostatic interaction between diblock copolymers with counterions which can remained stable at physiological pH (pH 7.4) and rapidly disintegrating at pH 5.5 based on a charge-conversional principle. Both Cytochrome C and IgG were controlled released into the cytoplasm of human hepatoma cell line. Hu *et al.* utilized pH-responsive cross-linked PDEAEMA-core/PAEMA-shell particles for intracellular delivery of membrane-impermeable macromolecules, including ova protein, influenza A, and siRNA.[166] The cationic shell could complex with negative charged cargos while the cross-linked poly(diethylaminoethyl methacrylate) (PDEAEMA) core were shown to elicit highly efficient endolysosomal disruption to release the cargos into the cytosol, showing dramatically lowered the dose of antigen required to elicit naïve $CD8^+$ T-cell.

Acid liable linker is another commonly used for pH-stimuli nanosystem design. For example, Wu *et al.* loaded aldehyde displaying silica nanoparticles with protein cargos by acid liable imine bond formation[167]. Arginase and EGFP were successfully escaped the lysosomes and released into cytosol of HepG2, HeLa and L929 cells through lysosomal acidity-mediated hydrolysis, where arginase efficiently induced autophagy of the host cells.

Recently the combination use of both acid liable bond as well as charge responsive swelling has been studied. Gu *et al.* utilized layer-by-layer assembly of PADH (tertiary amine and hydrazide grafted polyaspartamide) and PACA (carboxyl and aldehyde grafted polyaspartamide) on amino-functionalized silica spheres loaded with BSA to prepare biodegradable shell cross-linked nanocapsules for protein delivery[168]. PADH and PACA were assembled through electrostatic interaction and crosslinked via hydrazone

formation. BSA release rate increased significantly as pH dropped from the physiological pH to acidic pH, which result from the degradation of hydrazone bond and electrostatic repulsion of charged polymers.

1.4.2 Redox potentials responsive systems

Glutathione (GSH) is a tripeptide found at a level that is 2 to 3 orders higher (approximately 2–10 mM) in the cytosol than in the extracellular fluids (approximately 2–20 μM)[169]. Disulfide bond, which is degradable in the presence of high reduction potential but remains stable under low reduction potential, is very promising to create stable proteins carriers extracellularly but release proteins in the cytosol. Utilizing this reversible characteristic of thiol–disulfide chemistry, disulfide bonds can be incorporated into either the polymer backbone or the crosslinkers in order to design redox-responsive nanomaterials[155].

The thiolated heparin Pluronic F127 conjugate (DHP) was developed to self-assembled and oxidized to form a disulfide-crosslinked nanogel network to encapsulate RNase A. The crosslinked nanogels exhibited augmentable release responding to the GSH concentration and significantly higher cytotoxicity than non-crosslinked nanogel.[170] Zhao *et al.* reported the preparation of redox-responsive single-protein nanocapsules for intracellular protein delivery. Caspase 3[171] and apoptin[172] were non-covalently encapsulated into a positively charge polymeric shell crosslinked by disulfide linkers, which could be released in the cytoplasm and induce apoptosis in various cell lines.

The redox-responsive system can further be applied for oral protein and peptide delivery. Zheng *et al.* designed and synthesized redox-responsive silica capsules adopting the layer-by-layer technique with thiolated poly(L-aspartic acid) and thiolated chitosan for

transmucosal delivery of proteins and peptides, showing high insulin loading efficiency and regulated release according to GSH level, which is promising for oral insulin delivery.[173]

However, Mylotrag, a redox-responsive anti-CD33 antibody-linked drug developed by Celltech and approved by the Food and Drug Administration of the United States for acute myelogenous leukemia, failed to confirm benefits to patients and was withdrawn from the market. This illustrates the difficulties of drug-release control by a specific redox molecular mechanism in a complex biological environment.[157]

1.4.3 Enzymatic responsive systems

The altered expression profile of specific enzymes (such as proteases, phospholipases or glycosidases) observed in pathological conditions, such as cancer or inflammation, can be exploited to achieve enzyme-mediated protein release at desired biological target.[157] Compared with delivery approaches utilizing other internal or external stimuli, the enzyme-based approach represents an elegant biocompatible method of both high sensitivity and selectivity.[174]

Biswas *et al.* designed protein nanocapsule crosslinked by bisacrylated peptides with a specific sensitivity towards furin,[175] a ubiquitous intracellular protease expressed in many mammalian cells and overexpressed at tumor site. Both cytosolic and nuclear proteins, such as EGFP, Caspase 3, BSA and the transcription factor Klf4, were able to be delivered in active forms to different of cell lines. Wen *et al.* developed an metalloproteinases (MMP)-responsive delivery platform with controlled-releasing capability of vascular endothelial growth factor (VEGF).[176] Since matrix metalloproteinases (MMP)[177]and serine proteases, such as plasmin[178, 179], are

generally upregulated in diseased or injured tissues, they can be potentially chosen as the enzyme trigger for controlled release of growth factors in tissue engineering applications. Aimetti *et al.* designed a PEG hydrogel system with human neutrophil elastase (HNE) sensitive peptide crosslinkers synthesized *via* thiol-ene photopolymerization rendering the gel degradable at sites of inflammation. The controlled delivery of a model protein, BSA, based on this PEG hydrogel system was demonstrated. Thornton *et al.* functionalized poly (ethylene glycol acrylamide) (PEGA) hydrogel particles with peptide actuators that will release either cationic or anionic fragment, resulting in charge-induced swelling and cargo release upon exposure to the target enzyme (thermolysin).[180]

Jiang *et al.* recently reported co-delivery of tumor necrosis factor-related apoptosis inducing ligand (TRAIL) and Doxorubicin (Dox) based on Gelipo nanoparticles with assemble of CPP modified Dox loaded liposome, TRAIL protein and hyaluronic acid (HA).[156] The overexpressed hyaluronidase (HAase) in tumor area, promoted the degradation of the HA shell and released the encapsulated TRAIL for induced tumor apoptosis. The exposed liposome core could subsequently enter the tumor cell for Dox release with the aid of CPP, exhibiting a notable enhanced effect on tumor inhibition was observed after TRAIL/Dox-Gelipo treatment.

1.4.4 Thermo responsive systems

Thermoresponsive delivery is among the most investigated stimuli-responsive strategies, and has been widely explored in oncology.[157] Thermoresponsive systems are generally liposomes, or polymer micelles or nanoparticles (usually poly(*N*-isopropyl acrylamide), PNIPAM) that exhibit a lower critical solution temperature.[157] A nonlinear sharp change in the balance of hydrophilic and hydrophobic moieties with temperature triggers

the release of the cargos following a variation in the surrounding temperature. Ideally, thermosensitive nanocarriers should retain their load at body temperature (~37 °C), and rapidly release the cargo within a locally heated tumor (~40–42 °C).[157]

The most used protein loading strategy is to utilize the equilibrium swelling of a hydrogel in a protein-containing solution. Bhattarai *et al.* reported a PEG grafted chitosan copolymer designed for injectable thermo reversible hydrogel for sustained BSA release.[181] Compared with natural polymers, synthetic polymers display more potential in the development of thermal responsive protein delivery system. The most extensively studied synthetic polymer which displays a thermo responsive character in biomedical applications is poly(*N*-isopropylacrylamide) (PNIPAM), due to the fact that its LCST is 32 °C, therefore suitable for *in situ* gelling.[182] Wu and co-workers studied the interactions between proteins and PNIPAM hydrogels using insulin and BSA as model. The release of the protein was not complete as a result of the strong interaction between the polymer and the cargo protein.[183] Hu *et al.* grafted the porous polycaprolactone (PPCL) surface with ATRP initiator for subsequent surface initiated ATRP of NIPAM.[184] The resultant PNIPAM-grafted PPCL films exhibit potentials for controlled protein delivery using BSA as a model protein.

1.4.5 Photo responsive systems

Owing to their non-invasiveness and the possibility of remote spatiotemporal control, a large variety of photoresponsive systems has been engineered in the past few years to achieve on-demand drug release in response to illumination of a specific wavelength in the ultraviolet, visible or near-infrared (NIR) regions.[157]

TiO_2 have superior photocatalytic properties and biocompatibility; therefore, they are considered suitable nanocarriers for light-triggered protein delivery.[185, 186] Song *et al.* prepared TiO_2 nanotubes capped with hydrophobic octadecylphosphonic acid (OPDA) for protein delivery.[187]

Horseradish peroxidase (HRP) was demonstrated to be released by UV induced chain scission of attached organic monolayers according to the intensity of the UV light. However, most proteins were not endurable to UV irradiation.[188] Residues such as tryptophan, tyrosine, phenylalanine, and cysteine/cysteine will undergo photoinduced oxidation, and thus are the primary targets of photodegradation in proteins.[189] Thus, Visible light is more desired for protein delivery purpose. Luo and co-workers developed a visible light responsive protein delivery system based on coordination of 3, 4-dihydroxyl benzoic acid (DB) to TiO_2 nanoparticles and further grafted with hemoglobin (Hb).[190] Hb could be released with retained activity upon illumination by visible light *via* cleavage of the coordination bonds between DB and TiO_2 surfaces.

Instead of directly delivering proteins, Schroeder *et al.* developed UV controlling protein synthesis machinery based on lipid vesicle filled with amino acids, ribosomes, and plasmid caged with a UV labile cage. Active luciferase production triggered by UV were demonstrated *in vivo* by mice bioluminescence imaging, which opens new door for sustained delivery of proteins *in vivo*.

Near-infrared light (NIR) is gaining more and more attention due to its deeper tissue penetration, lower scattering properties and minimal harm to tissues compared with UV-Vis light making NIR-responsive systems extremely promising for clinical applications.[157] Tang *et al.* synthesized silica-coated gold nanorods and applied them

onto the skin surface for photothermal response to facilitate transdermal protein delivery.[191] Both a continuous-wave laser (CW-laser) and a pulsed laser enhanced the chicken ovalbumin delivery across the stratum corneum, providing an alternative approach for transdermal protein delivery and vaccination.

Although promising from a conceptual point of view, the safety and/or biodegradability of the typical materials used in light-responsive nanoparticles for drug-delivery applications (Au–Ag, gold nanorods, TiO_2, azobenzene and *o*-nitro benzyl derivatives) is still questionable. Finding biocompatible photosensitive materials will therefore be a critical part in the potential clinical translation of these systems.[157]

1.4.6 Magnetic responsive systems

Magnetically guided delivery has great potential since the response can be precisely triggered at target site and significantly lower off-target interactions.[155] Thermal response can also be created when an alternating magnetic field is applied. Furthermore, magnetic nanoparticles can be used for MRI imaging. Thus, associate diagnostics and therapy can be incorporated within a single system (the so-called theranostic approach).[192] Therefore, magnetically responsive systems allow for diversity in the drug-delivery applications.

Magnetic nanoparticles are capable of targeting specific sites to kill tumors under the guidance of a magnetic field. Thus, designing nanovehicles based on magnetic nanoparticles is a rather appealing approach in designing controlled protein delivery systems. Huang *et al.* prepared mesoporous magnetic hollow nanoparticles (MMHs) using polystyrene (PS) as templates and subsequently removed for BSA loading.[193] The amino functionalized MMHs (AMMHs) were efficient in protein loading and

capable of transporting BSA into the cells and releasing the protein cargo into cytosol and nucleus. Chorny *et al.* successfully loaded SOD and catalase into calcium oleate-based MNP by controlled aggregation/precipitation method which exhibited a strong magnetic response to release their cargo protein in plasma.[194] The combination of magnetic guidance can be promising for targeted removal of antioxidant in the circulation to protect endothelial cells from oxidative damage. Teodor *et al.* obtained L-asparaginase entrapped biocompatible hydrogel-magnetic nanoparticles by co-precipitation with hyaluronic acid and chitosan [195], which have potential application for antitumor therapy by asparagine clearance. Yoshimoto *et al.* prepared magnetic urokinase by conjugation of urokinase with magnetite through a PEG linker.[195] The magnetic urokinase can be selectively delivered to fibrin clot by magnetic force in continuously circulating plasma and exerts fibrinolytic activity without degrading fibrinogen, providing a novel view for thrombosis therapy[196]. Cho *et al.* developed a magnetic switch by conjugation of death receptor 4 (DR4) monoclonal antibodies to magnetic nanoparticles for the control of apoptosis signaling *via* a specific antigen–antibody interaction.[197] The magnetic switch turns 'ON' when applying a magnetic field to aggregate magnetic nanoparticle conjugated DR4s, promoting apoptosis *in vivo* in zebrafish with 3.5-fold morphological alteration in the tail region after applying a 0.50 T magnetic field for 24 h.

However, efforts to identify the best magnetic and irradiation technologies are needed for adequate focusing and deep penetration into the tissues to reach the diseased area with sufficient strength.[157]

1.4.7 Ultrasound responsive systems

Ultrasounds represent an effective method for attaining spatiotemporal control of drug release at the desired site, thus preventing harmful side effects to healthy tissues. The use of ultrasounds is also appealing because of their non-invasiveness, the absence of ionizing radiations, and the facile regulation of tissue penetration depth by tuning frequency, duty cycles and time of exposure.[157]

However, the report on ultrasounds triggered protein delivery is limited. Recently, Jin *et al.* reported a novel ultrasound-triggered insulin delivery system based on injectable polymeric nano-network.[198] Insulin loaded PLGA was encapsulated in either positively charged chitosan or negatively charged alginate and subsequently formed nano-network, which shows an ultrasound-triggered pulsatile insulin release profile mainly attributed to cavitation induced by focused ultrasound system (FUS). The FUS treatment on diabetic mice could perform for 10 days with similar releasing profile, indicating the potential for sustained long-term insulin delivery.

1.5 Protein nanocapsules

Recently, Lu group has developed a novel encapsulation method, where a thin polymer network is formed *in situ* around a single protein or protein complex, leading to the formation of protein nanocapsules containing a protein core and a thin polymer shell (Figure 1.3). Such nanocapsule platform has been used for both systemic and intracellular delivery of proteins.[54, 199-201] The synthesis of the protein nanocapsule involves two steps. Proteins were first conjugated with amine-reactive acrylate molecules to attach polymerizable groups onto the proteins. *In-situ* polymerization is then initiated in aqueous solution, yielding a thin polymer shell around each of the protein molecule with several advantages: 1) the crosslinked polymer shells offer enhanced stability against

proteolysis and non-physiological environments; while the shells are so thin (nanometer scale) allowing effectively transport of small-size molecular substrates crossing the shells. 2) The physicochemical properties of the nanocapsules can be easily controlled by judicious choice of monomers and crosslinkers with desired charge (neutral, positive and negative charge), degradability, and hydrophilicity. 3) In most cases, only one single protein molecule is encapsulated within each nanocapsule, resulting in small particle size (~ 20 nm) favorable for systemic circulation[202-204]. All of these advantages make enzyme nanocapsules ideal nanocarriers for protein delivery.

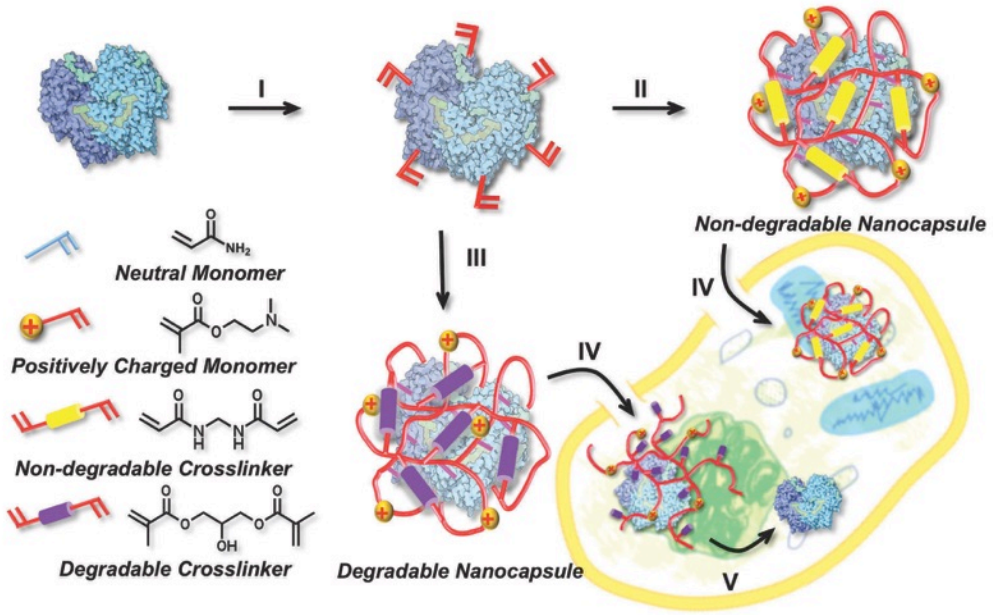

Figure 1.3 Illustration of the synthetic strategy for protein nanocapsules and their intracellular delivery.[200]

Nanocapsules with non-degradable shells can be delivered with long-term stability within the cells. This is particularly useful for proteins with small molecular substrates, since small molecular substrates can readily diffuse through the polymer shells.[123] For enzymes with macromolecular substrates, nevertheless, degradable crosslinkers can be incorporated within the polymer shells. Release of protein cargo commences upon

degradation of the polymer shells. For example, in response to the local acidic environment of endosomes, acid-degradable crosslinkers were cleaved off, releasing the incorporated caspase-3 to the cytosol to trigger cell apoptosis.[200]

Since the modification of the enzymes prior to their encapsulation may decrease the enzyme activity, a revised encapsulation protocol was also developed.[176, 205] Instead of conjugating acrylate groups to the enzyme surface, monomers and crosslinkers are adsorbed and enriched around the enzyme molecules spontaneously through electrostatic or hydrogen-bonding interactions. Subsequent polymerization yields enzyme nanocapsules with a similar core-shell structure. With the revised protocol, enzymes can retain as their intact form with highly preserved activity. This encapsulation approach becomes a platform technology for the encapsulation of proteins with different sizes, surface charges, and structures without compromising their biological activity. Wen *et al.* successfully encapsulated VEGF into MMP sensitive nanocapsule with fully retained bioactivity after release.[176] Zhao *et al.* also encapsulated Caspase 3 [171] and apoptin [172] using this noncovalent method into redox sensitive nanocapsule with disulfide crosslinker and exhibit apoptosis effect for cancer cell lines after intracellular delivery.

The enzyme nano-encapsulating platform provides a highly powerful tool towards the development of protein therapeutics. Naturally existed biochemical reactions in our body generally require cascades reactions to work synergistically (e.g. phase I and phase II detoxification system in our body).[206] In this context, ability to deliver two or more enzymes with synergic functions is essential for effective protein therapeutics and antidotes. Exemplified with alcohol detoxification, during the metabolism, alcohol is converted to acetaldehyde and acetic acid sequentially by alcohol dehydrogenase and

acetaldehyde dehydrogenase, respectively. Administrating alcohol dehydrogenase or alcohol oxidase alone reduces the blood alcohol concentration, however, generates toxic intermediates acetaldehyde and hydrogen peroxide, respectively. To address this problem, Liu *et al.* further developed a multiple-enzyme nanocapsule system which mimics the physiological alcohol detoxification process, where alcohol oxidase and catalase are co-delivered to eliminate the toxic intermediate hydrogen peroxide.[54] The antidotal effect of such multiple-enzyme nanocapsules was firstly verified with alcohol detoxification in mice by administrating the nanocapsules of alcohol oxidase (AOx) and catalase (Cat).[54] It was found that the nanocapsules of AOx-Cat complex could reduce the blood alcohol level much faster than the equivalent mixture of native AOx and Cat, or nanocapsules of AOx and Cat. Moreover, significantly lower liver damage was observed in mice administrated with the nanocapsules of AOx-Cat complex in comparison with those administrated with the equivalent enzyme mixtures. This observation confirms the effectiveness of using multiple-enzyme structure to remove toxic intermediates. This development provides a practical way to design and construct safer and more effective protein therapeutics and antidotes.

1.6 Summary

In summary, although many efforts have been put to improve the protein performance, there are still many challenges for proteins in industry and therapeutic applications.

Enzyme immobilization is widely used for food process, pharmaceutical manufacture and environmental protection. However, the current methods used for enzyme immobilization often decimate the dedicated protein structure leading to low bioactive of the enzyme composite. More efforts need to be focused on more enzyme friendly immobilization

methods, which provide optimal enzyme microenvironment that could enhance protein activity and reduce the substrate transport resistance.

Protein therapy has been a fast developing field due to their high active and specificity compared with small molecule drugs. More than 130 different proteins or peptides have been approved by FDA and more are under development, thanks to the advances in recombinant DNA and protein technology. Despite its fast growth in the recent years, the use of therapeutic proteins is still limited due to vulnerable nature of proteins, fast clearance in the blood circulation and lack of target delivery.

Various protein delivery carriers have been developed during decades. These carriers have certain merits to solve some of the problems for protein delivery. PEGylation is most widely used and most successful method, which increases protein half-life and reduces protein immunogenicity. Cationic block copolymers and liposomes can protect the proteins and increase cell internalization of proteins. Responsive delivery carriers utilizing either physiological or external stimuli can control the delivery of proteins in spatiotemporal- and dosage-controlled manners, resulting in more precise and on demand delivery of proteins. The recently developed protein nanocapsule method can integrate the above advantages of protein delivery carriers into a single protein nanocapsule by carefully choosing monomers, crosslinkers, reaction ratios and polymerization methods.

All these methods have pros and cons and new approach need to be further developed according to purpose of protein delivery. An ideal protein delivery system should have high stability in serum, low immunogenicity, on demand release and in many cases high cell penetration ability. Integration of knowledge from chemistry, biology, medical science and other fields can provide new design tools for the successful protein delivery.

Chapter 2 Protein nanocapsules for organophosphorus detoxification

2.1 Introduction

Organophosphates (OPs), a class of highly toxic synthetic compounds, are commonly used as pesticides, insecticides, and chemical warfare agents[207] (e.g., sarin and soman). Such compounds irreversibly inhibit acetylcholinesterase, a serine hydrolase that hydrolyzes the neurotransmitter acetylcholine, causing neuromuscular paralysis throughout the entire body and death by asphyxiation.[208] Developing approaches that lead to effective detection, decontamination, protection, and detoxification of OP is highly essential and challenging. For OP decontamination, both chemical and biological means have been explored. The former approach generally involves the use of chemical agents that are often toxic, corrosive or flammable, excluding them from applications for large-area decontamination, on sensitive equipment or on personnel.[209] The latter approach, on the other hand, relies on organophosphorus hydrolase (OPH), an enzyme that hydrolyzes OPs with exquisite specificity and efficiency.[210, 211] However, the use of OPH has been hampered by the fragile nature of the enzyme – similar to other enzymes, OPH often loses its activity rapidly in non-physiological environments, as well as in the presence of proteases commonly existing in biological systems. Developing an effective approach to stabilize OPH is therefore crucial towards better decontaminants, antidotes, and protection applications.

Recently, our group developed protein nanocapsules for delivery various proteins both intracellularly and systemically. Each protein molecule was surrounded by a thin polymer shell under mild conditions, with uniformed size, controlled surface properties, which is

highly stable and active. Based on this, we can apply the nanocapsule systems to obstacle the limits of using OPH as decontaminants and antidotes.

2.2 Experimental

2.2.1 Material

All chemicals were purchased from Sigma-Aldrich unless otherwise noted, and were used as received. N-(3-Aminopropyl) methacrylamide was purchased from Polymer Science, Inc. Male Balb/C mice were purchased from Chinese Academy of Sciences (SLAC Laboratory Animal Co. Ltd., Shanghai, China).

2.2.2 Instruments

UV-Visible adsorption was acquired with a Beckman Coulter DU®730 UV/Vis Spectrophotometer. TEM images were obtained on a Philips EM-120 TEM instrument. Particle size and zeta potential were measured with Malvern Nano-ZS. Agarose gel electrophoresis was obtained with an Edvotek M6Plus Electrophoresis Apparatus. Fluorescence intensities were measured with a Fujifilm BAS-5000 plate reader. Fourier Transformed Infrared Spectroscopy (FT-IR) was acquired with JASCO FT/IR-420 spectrometer.

2.2.3 OPH expression and purification

OPH from *pseudomonas diminuta* was expressed by E. coli strain BL21 (DE3) carrying pET28-derived expression vector. Bacterial cells were grown in LB medium until OD600 reached 0.8. Then, 1 mM $CoCl_2$ was added at the induction step together with 1mM IPTG (Isopropyl β-D-1-thiogalactopyranoside). The cells were then shaken under 16 °C for 16 hours. Subsequent enzyme extraction and purification were performed in 50 mM HEPES buffer (pH 8.5) at 4 °C, according to the method described by Omburo [212].

2.2.4 Preparation of nOPH

OPH was modified by reacting its surface lysine groups with N-acryloxysuccinimide (NAS) in 50 mM HEPES buffer (pH=8.5), with an OPH/NAS molar ratio of 1:5. This acryloylation was taken place under a reaction temperature of 4 ^{o}C for 2 hours. Subsequently, *in-situ* polymerization was carried out at 4 ^{o}C for another 2 hours. Briefly, monomers acrylamide (AAM) and N-3-aminopropyl methacrylamide hydrochloride (APM), cross-linker N, N'-methylene bis-acrylamide (BIS) and initiators ammonium persulfate (APS) and N, N, N', N'-tetramethylethylenediamine (TEMED) were subsequently added to the acryloylated OPH. The weight ratio of acryloylated OPH: AAM: APM: BIS: APS: TEMED was 1: 2.5: 1.25: 1: 1: 1. The mixture was stirred at 4 ºC for 2 hours. After that, the resulting nanocapsule was dialyzed against 50 mM HEPES buffer (pH= 8.5), followed by a further purification with Sephadex G-75 to remove the unreacted monomers, initiators and free enzymes.

2.2.5 Synthesis of nOPH-cellulose nanocomposites

Bacterial cellulose (BC) (5% w/v) was dissolved in the ionic liquid 1-butyl-3-methylimidazolium chloride at 80 °C. After cooling down to room temperature, the resulting solution was spread onto a glass slide, immersed into methanol to form a BC pad. Smaller pads with dimension around 5 mm × 15 mm were cut from the original one. These pads were washed extensively with DI water before the treatment with 3% $KMnO_4$ at 60 ºC for 3 hours to generate carboxylic groups. The resulted carboxylated BC pads were covalently linked with nOPH through the EDC-NHS reaction. EDC and NHS were dissolved in 1 ml 2 mg/ml nOPH with a concentration of 50 mM and 5 mM, respectively. Then, the carboxylated BC pads were incubated in the above solution to allow the

reaction to carry out for 4 hours at 4 ^{o}C before extensive wash with DI water to remove unreacted nOPH, EDC and NHS.

2.2.6 DLS measurement

DLS experiments were performed with a Zetasizer Nano instrument (Malvern Instruments Ltd., UK) equipped with a 10-mW helium-neon laser (λ = 632.8 nm) and thermoelectric temperature controller. Measurements were taken at 90° scattering angle. The samples are in a pH 7.0 10 mM phosphate buffer with a protein concentration of 1 mg/mL.

2.2.7 TEM measurement

TEM images were obtained on a Philips EM-120 transmission electro microscopy. For negative stained nanocapsules, 10 μL 1 mg/mL nOPH is dropped on a copper grid. After 5 min, the solution is drawn off from the edge of the grid with filter paper. 5 μL of 1% pH=7.0 phosphotungstic acid (PTA) solution was immediately added on top of the grid. After another 5 min, the grid is washed 3 times with DI-water and allowed to dry in air. The grid is then stored for TEM observation. The grid is then stored for TEM observation. TEM images are acquired with an acceleration voltage of 120 kV and magnification of 67000x to 100000x.

2.2.8 Infrared spectra acquisition

Fourier Transformed Infrared Spectroscopy (FT-IR) for native OPH and nOPH were acquired with KBr disks on a JASCO FT/IR-420 spectrometer.

2.2.9 Agarose gel electrophoresis

0.7 % (w/v) agarose gel is prepared in pH 7.2 1×TAE buffer. Protein nanocapsule sample with concentration of 0.2-1 mg/mL is mixed with 20% glycerol with a volume ratio of

9:1 and loaded in the gel. Electrophoresis is conducted with an Edvoket M12 electrophoresis cell under constant voltage of 110 V for 15 min.

2.2.10 Protein concentration assay

The protein content in the form of nanocapsules was determined by bicinchoninic acid (BCA) colorimetric protein assay. Briefly, a tartrate buffer (pH 11.25) containing 25 mM BCA, 3.2 nM $CuSO_4$, and appropriately diluted protein/nanocapsules was incubated at 60 ºC for 30min. After the solution was cooled to room temperature, absorbance reading at 562 nm was determined with a UV-Vis spectrometer. OPH solutions with known concentration were used as standards.

2.2.11 Protein activity and stability assay

Native OPH and OPH nanocapsules were both incubated at the same concentration at 65 °C in 10 mM HEPES buffer (pH 8.5). Samples were taken out at different time intervals during the incubation and placed immediately on ice. The organophosphate hydrolysis mediated by native OPH and OPH nanocapsules were determined by monitoring absorbance change at 405 nm in 50mM HEPES buffer (pH 8.5) with Paraoxon-ethyl as the substrate.

2.2.12 Probing local pH environment with fluorescein

To 100 μL native OPH or nOPH solutions with the same protein concentration (1 mg/mL in 10 mM pH 8.5 borate buffer), 100 μL 9 μM 5-Carboxy-fluorescein diacetate N-succinimidyl ester aqueous solution (prepared fresh) was added. The mixtures were stirred at room temperature in dark for 4 hours to allow complete reaction. After that, the solutions were diluted with 100 mM pH 7.0 phosphate buffer to a final concentration of 0.025 mg OPH/mL. The fluorescence intensity of each sample was measured with a plate

reader (λ_{ex} = 485 nm, λ_{em} = 535 nm). Each data point was done in triplicate. And free fluorescein with the same concentration was used as a control.

2.2.13 Cell proliferation assay

The toxicity of the OPH nanocapsules was assessed by the resazurin assay using native OPH as control. HeLa cells (2000 cells/well) and 3T3 cells (4000 cells/well) were seeded on a 96-well plate in 100 μL DMEM the day before exposure to OPH nanocapsules. After incubation with nanocapsules at different concentrations for 2-4 hrs, the cells were washed with 1× PBS and fresh medium was added to the cells. After another incubation for 24 hours, resazurin solution (10 μL 0.1mg/mL in PBS) was added to each well and incubated for 3 h. The cell viability was then determined by measuring the fluorescence of each well (λ_{ex} = 535 nm, λ_{em} = 585 nm) with a plate reader. Untreated cells and fresh medium were used as the 100% and 0% cell proliferation control, respectively.

2.2.14 In-vivo prophylactic experiments

Male Balb/C mice (5weeks of age) were purchased from Chinese Academy of Sciences (SLAC Laboratory Animal Co. Ltd., Shanghai, China). Animal study protocols were approved by the Animal Ethics Committee of School of Medicine, Shanghai Jiao Tong University. The mice were housed and furnished according to *The Guide for the Care and Use of Laboratory Animals* (8^{th} edition, NRC, 2011) in the Animal Center of School of Medicine, Shanghai Jiao Tong University, one week before use. Native OPH (iv, 50 units), and nOPH (iv, 50 units) were administered 5 minutes prior to the administration of paraoxon (in 6% cyclodextrin and propylene glycol solvent system [213]). The propylene glycol solvent system consisted of 40% propylene glycol, 10% ethanol, and 50% water (v/v). In the control group, mice were injected with equal volume of saline, instead of

OPH solution, before paraoxon treatment. For each group, 3 mice were used in parallel. 24-h mortality was used to evaluate the efficiency of OPH or nOPH as prophylactics. Surviving animals were observed for an additional week for late-developing toxicity. In our experiment, a dose of 0.27 mg/kg paraoxon was applied to each mouse. Mice were videotaped in the first 2 hours after injection, and another videotape was recorded after 24hours. By the end of the experiments, surviving animals were euthanized in accordance with the 1986 report of the AVMA Panel of Euthanasia.

2.3 Results and discussion

2.3.1 Synthesis of OPH nanocapsules (nOPH)

As illustrated in Figure 2.1, OPHs were firstly conjugated with polymerizable acryl groups by reacting their lysine groups with *N*-acryloxysuccinimide (NAS) (Step I); subsequent polymerization at room temperature grew a thin layer of polymer network around the conjugated OPH, leading to the formation of OPH nanocapsules (denoted as nOPHs), each of which contains an OPH core inside and a thin permeable shell outside (Step II). The polymer shells can effectively stabilize the interior OPHs while enable rapid substrate transportation, affording a novel class of biocatalytic nanocapsules with outstanding activity and stability for various applications. The broad applications of such nanocapsules are exemplified herein by the development of antidotes for OP poisoning, decontamination agents for OP spreading, and OPH building blocks for the fabrication of bioactive nanocomposites for effective OP protection.

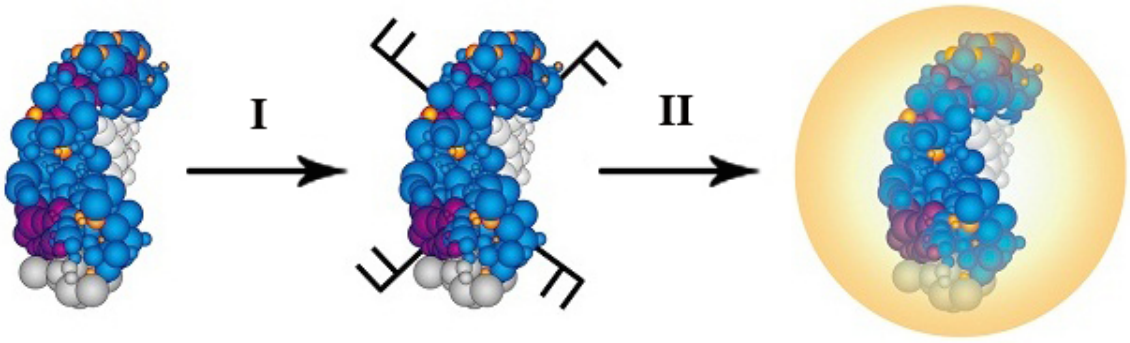

Figure 2.1 Construction of OPH nanocapsules. OPH was constructed by attaching polymerizable groups onto the enzyme surface (Step I) followed by an *in situ* polymerization (Step II) that forms a layer of polymer shell around the enzyme molecule.

2.3.2 Characterization of OPH nanocapsules

The formation of nOPH was confirmed with various characterization techniques. Figure 2.2a and 2.2b show the size distribution and zeta potential of native OPH and nOPH obtained by DLS. These nanocapsules were synthesized using acrylamide (AAM) and *N*-(3-aminopropyl) methacrylamide hydrochloride (APM) as co-monomers. The native OPH exhibits negative charge (~ -5 mV) with a size distribution centered at 5 nm, which is consistent with its molecular dimension (6.1 nm × 8.6 nm × 5.1 nm [214]). Figure 2.2c shows a representative transmission electron microscopic (TEM) image of nOPH, exhibiting spherical morphology confirms the nanocapsules diameter ~ 20 nm. For comparison, nOPH shows positive charge (~ 3 mV) and a size distribution centered at 18 nm, suggesting the successful formation of the polymer on the enzyme molecules. Successful encapsulation was also validated by agarose gel electrophoresis (Figure 2.2d), where the positive-charged nOPH migrates to cathode and the native OPH migrates to anode. Although cationic nOPH was chosen as a model system in this study, precise control over the charge of protein nanocapsules can be achieved by choosing appropriate

monomer composition.[200] FTIR spectra of nOPH show characteristic absorption at 1670 cm^{-1} and 1460 cm^{-1} confirming the formation of polymeric shells composed of polyacrylamide (Figure 2.3).[215] Combining the DLS, FTIR and TEM results, it is reasonable to conclude that the proposed polymer shells are indeed constructed around the enzyme molecules forming the nanocapsules.

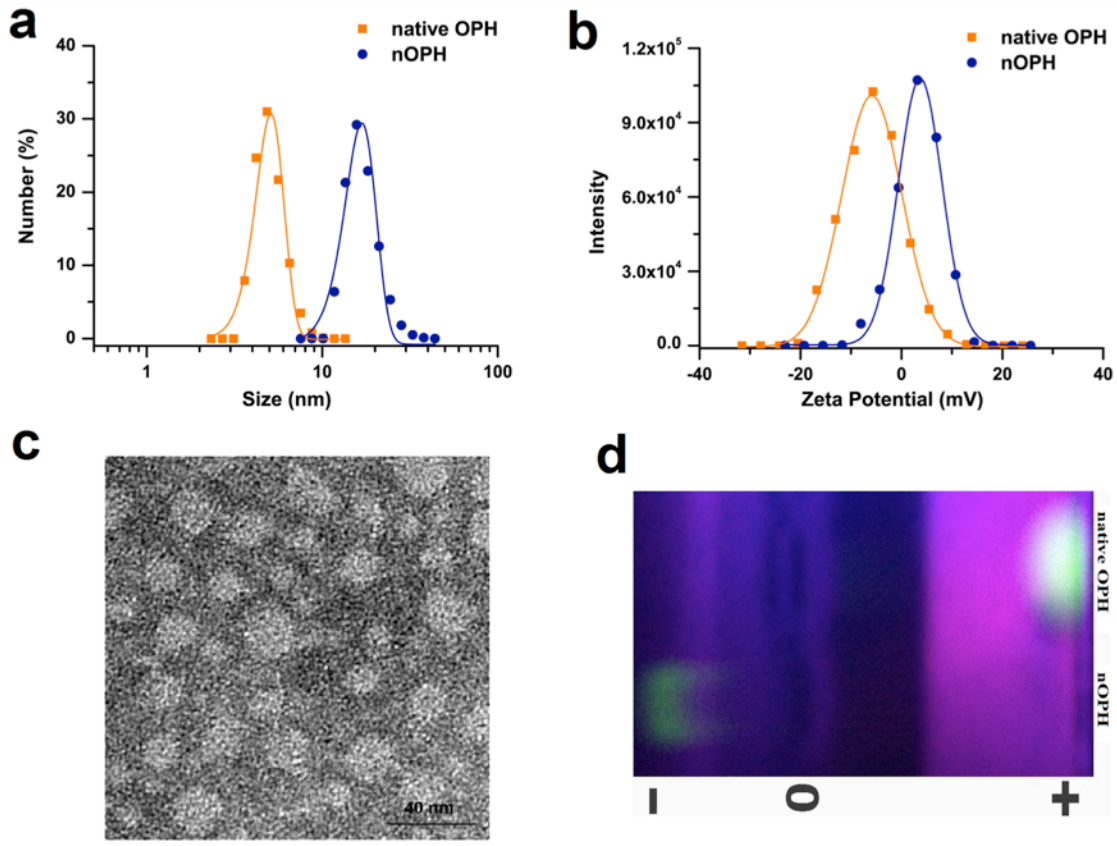

Figure 2.2 a) Particle size distributions and b) Zeta potentials of native OPH and nOPH. c) TEM image of nOPH. d) Agarose gel electrophoresis image of native OPH and nOPH.

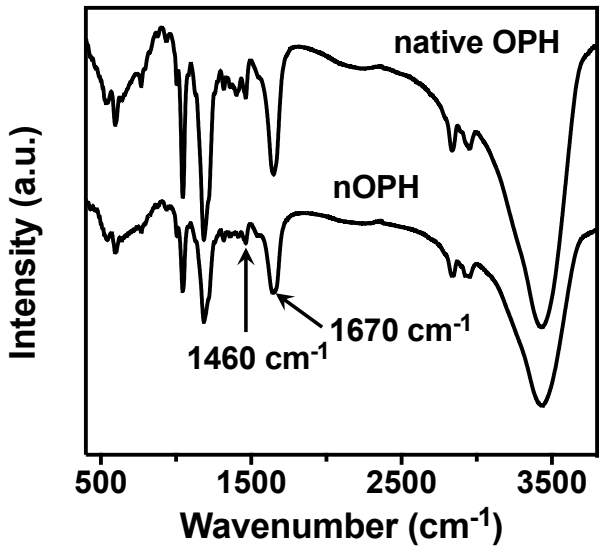

Figure 2.3 FTIR spectra of native OPH and OPH nanocapsule.

2.3.3 Activity and stability enhancement

Generally, enzyme immobilization leads to significantly increased Michaelis constant (K_m) and decreased turnover number (k_{cat}).[199, 216] Nevertheless, the native OPH exhibits a similar K_m (0.061 mM) as that of nOPH (0.071 mM), suggesting that thin polymer shells around the OPH cores do not cause any significant resistance for substrate transport. Moreover, nOPH also exhibits a higher k_{cat} than that of the native OPH (1322 s^{-1} *vs.* 594 s^{-1}), indicating enhanced catalytic activity. Figure 2.4 compares the activities of native OPH and nOPH at different pHs. While native OPH experiences a steep fall after the pH decreased below its optimum pH (~ 8.5), nOPH retains a comparatively stable activity from pH 7.8 to 9.7. This observation can be attributed to the high pKa of amine groups on the surface from poly[N-(3-aminopropyl) methacrylamide] (pKa ~10), which created an local high pH environment. To verify this hypothesis, we probe the local pH environment with fluorescein, a pH sensitive fluorescence dye with higher fluorescence emission at higher pH. Compared with free fluorescein in solution (Figure 2.5), FITC bound to nOPH emits stronger fluorescence. Nevertheless, FITC conjugated to native

OPH does not exhibit significant fluorescence enhancement. Therefore, we can conclude that, by engineering the polymer composition of nOPH, we could readily manipulate the microenvironment around the encapsulated OPH, and thus adjust the enzymatic activity.

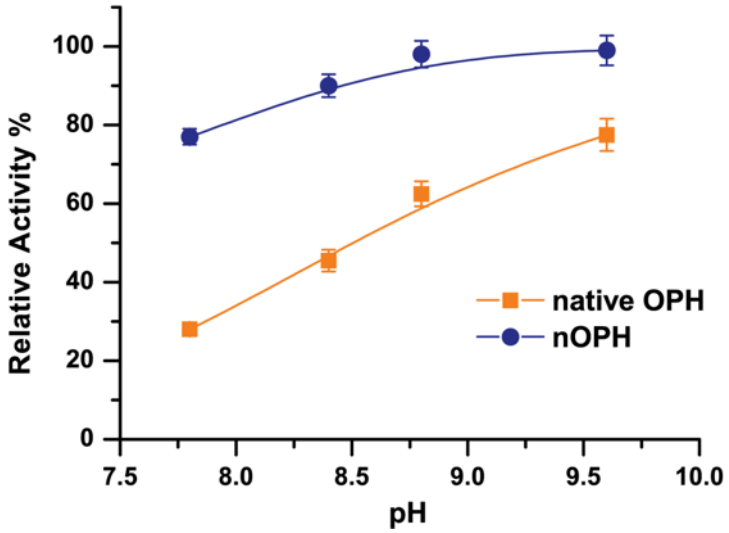

Figure 2.4 Relative enzyme activity of native OPH and nOPH under various pHs, activities were normalized using their activities at pH 10.5 as 100% standards.

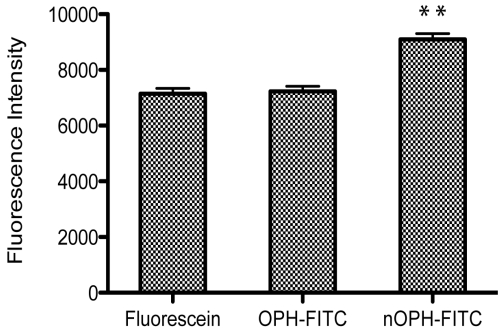

Figure 2.5 Fluorescence intensity of free fluorescein, OPH-FITC, and nOPH-FITC containing the same amount of fluorescein (n = 3, ** p < 0.01)

Besides the enhanced activity, nOPH also presents significantly improved stability against various denaturation factors, including elevated temperature and organic solvents. Figure 2.6a compares the relative stabilities of nOPH and native OPH at 65 °C. Distinct from the fast denaturation of the native OPH, which retains only 6% of the activity,

nOPH retains a 26% of initial activity. The enhanced thermal stability of nOPH is believed to be the result of multiple covalent attachments of the enzyme core to the polymer shell, which effectively hinder the OPH conformation change upon heating.

The enhanced enzyme stability in the existence of the organic solvents was demonstrated by exposing native OPH or nOPH to organic solvent-water mix solvents with different volume fractions of dimethylsulfoxide (DMSO). As shown in Figure 2.6b, after incubating with a series of DMSO/buffer solutions, the nOPH retains more than 30% of its initial activity even in the presence of 50% DMSO. In contrast, native OPH only retain 10% of their initial activity. This improved performance of nOPH can be attributed to the hydrophilic environment kept by its hydrophilic shell, which otherwise would be depleted by polar organic solvent.

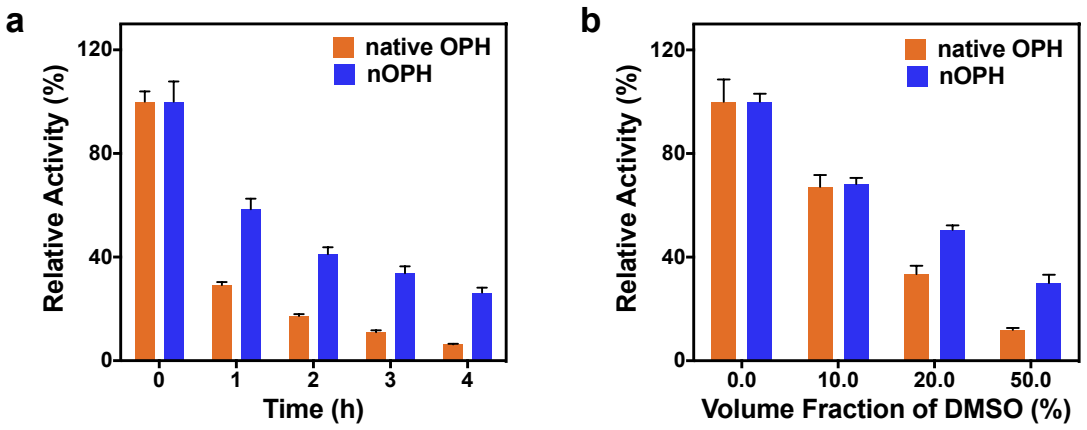

Figure 2.6 a) Relative activities of native OPH and nOPH incubated at 65 °C. b) Relative activities of native OPH and nOPH exposed to 50mM HEPES buffer (pH=8.5) solution containing different diffractions of DMSO.

2.3.4 Decontamination capability

The use of nOPH as an effective OP decontamination agent was demonstrated using paraoxon-containing agarose gels as model OP-contaminated media (e.g. soil). Briefly, agarose solution (0.25 wt %) was mixed with different amounts of paraoxon to form

contaminated gels in 24-well plates. Native OPH or nOPH were then applied onto the gel surface; hydrolysis kinetics of paraoxon was evaluated by their K_m and k_{cat} parameters. It was found that the native OPH and nOPH exhibit a K_m of 1.06 mM and 2.43 mM and k_{cat} of 688 s^{-1} and 1389.3 s^{-1}, respectively. The doubled k_{cat} observed in nOPH clearly suggests the great potential of using nOPH as an effective decontamination agent. When comparing K_m and k_{cat} of native OPH and nOPH in solution, the higher K_m observed in the gel media can be attributed to the increased substrate-diffusion resistance. The observed increase in k_{cat} for native OPH and nOPH might be due to the uneven distribution of enzyme in the solution/gel system. Nevertheless, in the gel system, k_{cat}/K_m still retains at a high level (5.71×10^5 $mol^{-1}\cdot L\cdot s^{-1}$), sufficient for decontamination purposes. Combined with the enhanced stability, such highly active nOPH can be a great interest for OP decontamination to various military and civilian applications.

2.3.5 Biocompatibility and *in vivo* detoxification

The capability to fabricate nOPH with significantly enhanced activity and stability provides a novel platform for OP detoxification, decontamination and further fabrication of active OPH nanocomposites. To explore the detoxification capability, nOPH cytotoxicity was first examined. Figure 2.6a and2.6b compares the viability of HeLa cells and NIH 3T3 cells after exposure to native OPH and nOPH under different concentrations. Clearly, both native OPH and nOPH exhibit similar cytotoxicity; even at a high concentration of 800 nM, cell viability still maintains around 90%. These *in-vitro* studies clearly suggest that nOPH exhibits low cytotoxicity.

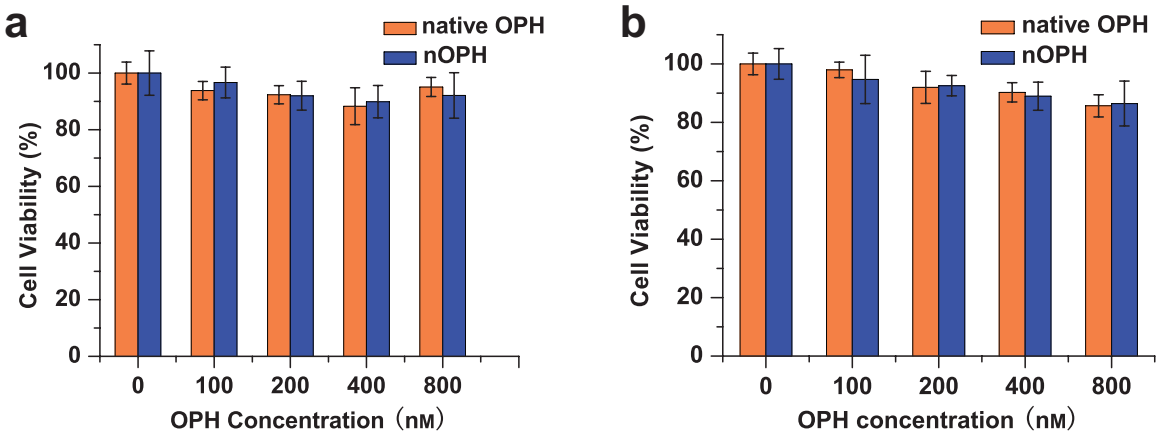

Figure 2.7 Cell viability of a) HeLa cells and b) 3T3 cells after exposure to different concentrations of native OPH and nOPH and incubation for 3h showing low cytotoxicity of nOPH.

A preliminary *in-vivo* study was conducted to examine the potential of using nOPH as prophylactics against acute OP poisoning. The native OPH or nOPH was tail-injected into mice as prophylactics; and paraoxon was then injected 5 min after the administration of native OPH and nOPH. It was found that the mice without the injection of native OPH or nOPH died within 5 min after the paraoxon injection. The mice injected with nOPH survived from OP poisoning without any gross toxic symptoms through the first 24 hour observation; two out of three mice injected with native OPH survived, but with gross toxic effects in the first 2 hours after paraoxon administration. This preliminary study clearly demonstrates that nOPH exhibits better prophylactic effect against acute OP poisoning, which is consistent with their better stability and activity discussed above. This study clearly demonstrates the great potentials of using highly robust and active nOPH as therapeutic and prophylactic agents against OP intoxication.

2.3.6 Fabrication of nOPH based protection device

Besides the use as detoxification and decontamination agents, the highly stable and active nOPHs also possess nanoscale size (tunable at tens of nanometers) and controllable

surface with functional chemical structure, which enables them to be ideal building blocks for the fabrication of active OPH composites for protective purpose. To demonstrate this concept, active OPH-cellulose composites were constructed by covalently attaching nOPHs to bacterial cellulose (a model cellulose fiber). As illustrated in Figure 2.8a, the cellulose pad was first treated using $KMnO_4$ to generate surface carboxylic (-COOH) groups; nOPHs were then conjugated to the cellulose through the reactions between the -COOH groups and the amine groups on the nOPHs. Figure 2.8b presents a photograph of nOPH-cellulose composite gel prepared from fluorescein-isothiocyanate (FITC)-labeled nOPH. After extensively washing and dialysis, the FITC-labeled composite still exhibits intensive fluorescence, confirming the strong linkage nOPHs onto the cellulose matrix. On contrast, the fluorescence of the composite prepared by physical entrapment of FITC-labeled nOPH within the cellulose networks rapidly disappears after subsequent washing and dialysis process, indicating the importance of covalent linkage. After conjugated to cellulose, nOPHs possess high stability during catalyst recycling and storage. As shown in Figure 2.8c, the nOPH composites retain high activity (> 90% original activity) even after seven recycles. Additionally, during the 10-day storage at room temperature, the nOPH-cellulose composites retained more than 90% of its original activity (Figure 2.8d). Since cotton, consisting mostly of cellulose, is commonly used in fabricating protection devices (e.g. mask, cloth, glove), this work reveals a bright future of using nOPHs for OP protection.

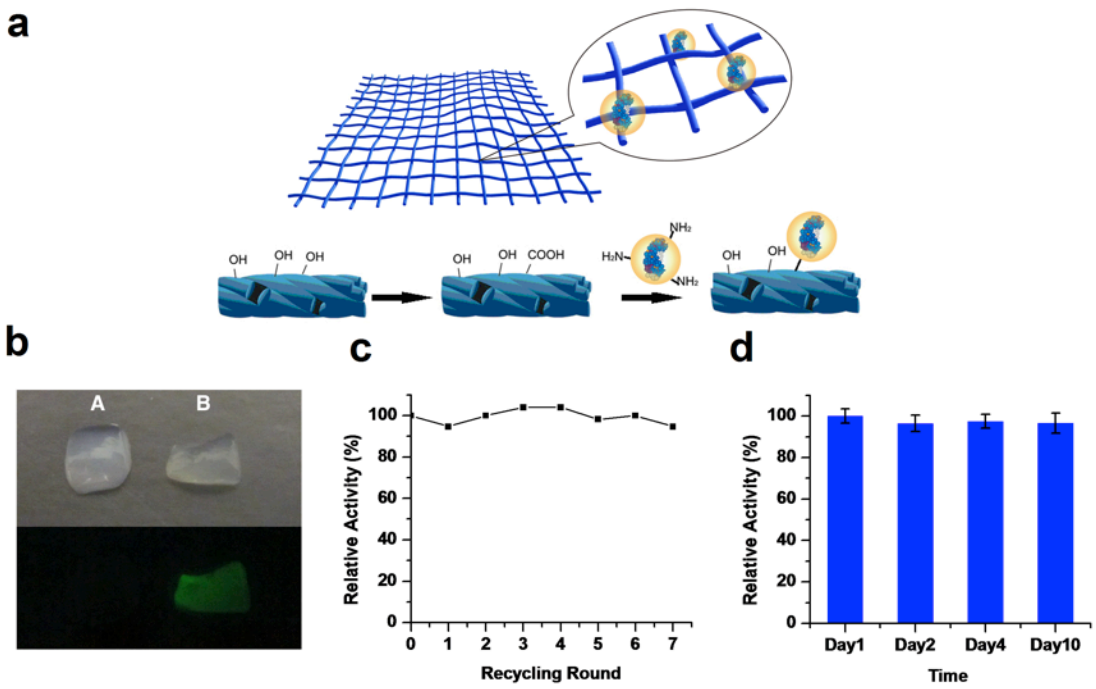

Figure 2.8 Synthesis of Active OPH-Cellulose Nanocomposites. a) Schematic illustration of the immobilization of nOPH on carboxylated bacterial cellulose. b) Bright field and fluorescent image comparison of A) physical absorption and B) covalent linkage of FITC-labeled nOPH onto the bacterial cellulose after extensively wash and dialysis process. c) Relative activity of the OPH-cellulose composite during seven catalyst recycles. d) Relative activity of the enzyme nanocomposites stored at room temperature for 10 days.

2.4 Summary

In conclusion, we have demonstrated a novel approach to prepare robust and highly active OPH nanocapsules. The intrinsic OPH activity may be enhanced by manipulating the local chemical environment while the stability of nanocapsules is significantly improved compared with native OPH. The OPH nanocapsules can be applied for environmental decontamination and further be made into cellulose composite for personnel protection purpose. The nanocapsule are also highly biocompatible and can be used as prophylactics or antidotes for OP intoxication. This novel class of OPH nanocapsules shows great promise for broad military and civilian application.

Chapter 3 Robust enzyme-silica composite made from enzyme nanocapsules

3.1 Introduction

The synthesis of materials with bioactive functions has been of great interest for a broad range of applications. To date, various biomolecules (e.g., proteins and DNAs) have been integrated with synthetic materials (e.g., small molecules, clusters, quantum dots, polymers and inorganic frameworks), creating a new class of bioactive composites.[217-222] Compared with other biomolecules, enzyme plays the most dynamic and diverse roles in living organisms; the synthesis of enzyme-based composites is therefore of particular interest. However, the synthesis of enzyme-based composites has been limited by poor stability of enzymes in non-physiological environment, which results in significant loss of the protein activity. Although immobilization yields a great extent of stability improvement, significant decrease of k_{cat} and sharp increase of K_m were usually observed[223-225] due to damaged microenvironment and substrate diffusion resistance, resulting comprised overall activity. To endow the enzyme with both improved stability and high activity, it's crucial to create highly stable and permeable layer around the enzymes that could optimizing the microenvironment of enzymes. We have recently developed a nano-encapsulation platform, which enables the synthesis of enzyme nanocapsules with highly retained activity, improved stability, tunable surface chemistry and uniform size (tens nanometers in diameter).[200] Using such nanocapsules as the building blocks, we report herein the synthesis of enzyme-silica nanocomposites with highly retained activity. Furthermore, by tuning the microenvironment around the

enzyme molecules, such highly robust composites may exhibit enzyme activity higher than the native enzyme counterparts.

3.2 Experimental

3.2.1 Materials

N-acryloxysuccinimide, acrylamide (AAM), N,N'-methylenebisacrylamide (BIS), ammonium persulfate (APS), tetramethylethylenediamine (TEMED), HEPES, sodium acetate, acetic acid, sodium phosphate monobasic monohydrate, sodium phosphate dibasic, Pluronic®P123, tetramethyl orthosilicate (TMOS), 1,4-bis(triethoxysilyl)benzene (BES), (3-aminopropyl) trimethoxysilane (AMS), paraoxon, 4-nitrophenyl laurate, glucose, 3,3',5,5'-tetramethylbenzidine (TMB), bicinchoninic acid (BCA), tartaric acid, $CuSO_4$, dimethyl sulfoxide (DMSO), sodium dodecyl sulfate (SDS), lipase from thermomyces lanuginosus, horseradish peroxidase (HRP) and glucose oxidase (GOX) from Aspergillus niger were purchased from Sigma-Aldrich and were used as received. N-(3-aminopropyl) methacrylamide was purchased from Polymer Science, Inc.

3.2.2 Instruments

Fourier Transformed Infrared Spectroscopy (FT-IR) was acquired with JASCO FT/IR-420 spectrometer. TEM images were obtained on a Philips EM-120 TEM instrument. Particle size and zeta potential were measured with Zetasizer Nano-ZS (Malvern Instruments Ltd., UK). UV-Visible adsorption was acquired with a Beckman Coulter DU®730 UV/Vis Spectrophotometer. Fluorescence intensities were measured with a Tecan GENios Multifunction microplate reader. ASAP 2020 pore analyzer was used for Brunauer-Emmett-Teller (BET) test.

3.2.3 Protein expression and purification

OPH from *Pseudomonas diminuta* was expressed by E. coli strain BL21 carrying pET28-derived expression vector. Bacterial cells were grown in a LB and $CoCl_2$ were added at the induction step to a final concentration of 1 mM. Subsequent enzyme extraction were purified by gel filtration with Sepharose® 6B (Sigma Aldrich) and ion exchange with DEAE–Sephadex® (Sigma Aldrich) at 4 °C in 50 mM HEPES buffer (pH 8.5) according to the method described by Omburo [212].

EGFP was expressed by E. coli strain BL21 carrying pET28-derived expression vector with His-tag on C-terminal. Bacterial cells were grown in a LB and EGFP extraction were purified by Hispur™ Ni-NTA column (Thermo Scientific) and further desalted on a G25 desalting column (GE Healthcare).

3.2.4 Preparation of nanocapsules

OPH was modified by N-acryloxysuccinimide at a molar ratio of 1 : 5 in 50 mM HEPES buffer at pH 8.5. The acryloylation reaction took place at 4 °C for 2 hours. Acryloylated OPH was further reacted for 4 hours at 4 °C with monomers acrylamide (AAM) and N-(3-aminopropyl) methacrylamide hydrochloride (APM), crosslinker N,N'-methylenebisacrylamide (BIS), initiated by ammonium persulfate (APS) and tetramethylethylenediamine (TEMED). The molar ratio of acryloylated OPH : AAM : APM : BIS was 1 : 2500 : 500 : 200. The resulted nanocapsules were dialyzed against 50 mM HEPES buffer at pH 8.5 and further purified with Sephadex G-75 to remove the unreacted monomers, initiators and enzymes. Lipase, EGFP and GOX nanocapsules were synthesized in similar method. Briefly, lipase, EGFP and GOX were dialyzed against 10mM phosphate buffer at pH 7.0 and acryloylated by N-acryloxysuccinimide at molar ratio of 1 : 5. Subsequently, AAM, APM and BIS were introduced and initiated by APS

and TEMED at the same molar ratio as preparation of nOPH. The resulted nLipase, nEGFP and nGOX were purified by dialysis and Sephadex G-75.

3.2.5 Synthesis of enzyme-silica composites

P123 with amount of 0.2g was dissolved in 10 ml of phosphate buffer (pH = 4.7) at room temperature until the solution became transparent, and then nanocapsules were added. After stirring for 0.5 h, 0.278 mL tetramethyl orthosilicate (TMOS) was added and stirred for 24 h. The resulted precipitates were centrifuged and washed with 50mM pH 8.5 HEPES buffer. The products were then extracted in ethanol/buffer solution for 24 h to remove the P123. The synthesis of the nanocomposites from other silica precursors, 1,4-bis(triethoxysilyl)benzene (BES) and (3-aminopropyl) trimethoxysilane (AMS), was conducted in the same approach by replacing 20% molar ratio of TMOS to BES or AMS. nLipase-silica, nEGFP-silica and nGOX-silica nanocomposites were prepared by same method with the same amount of P123 and precursors. The resulted precipitates were centrifuged, washed with 10mM pH 7.0 phosphate buffer. The products were then extracted in ethanol/buffer solution for 24 h to remove the P123.

3.2.6 DLS measurement

DLS experiments were performed with a Zetasizer Nano-ZS (Malvern Instruments Ltd., UK) equipped with a 10-mW helium-neon laser (λ = 632.8 nm) and thermoelectric temperature controller. Measurements were taken at 173° scattering angle. The samples are in a pH 8.5 50 mM HEPES buffer with a protein concentration of 0.5 mg/mL at 25 °C.

3.2.7 TEM measurement

TEM images were obtained on a Philips EM-120 transmission electro microscopy. For nanocapsules imaging, 10 μL 0.5 mg/mL nOPH is dropped on a copper grid. After 2 min,

the solution is drawn off from the edge of the grid with filter paper. 5 μL of 1% pH=7.0 phosphotungstic acid (PTA) solution was immediately added on top of the grid. After another 5 min, the grid is washed 3 times with DI-water and allowed to dry in air. The grid is then stored for TEM observation. For enzyme-silica composite imaging, nOPH-silica suspension was dried on a copper grid and directly used for TEM observation without further staining. TEM images are acquired with an acceleration voltage of 120 kV.

3.2.8 N_2 adsorption–desorption and BET test

N_2 adsorption–desorption isotherms were obtained on an ASAP 2020 pore analyzer at 77 K under continuous adsorption condition. Brunauer-Emmett-Teller (BET) and Barrett-Joyner-Halenda (BJH) methods were used to determine the surface area, pore size distribution.

3.2.9 BCA protein content quantification

All the protein content in solution was determined by bicinchoninic acid (BCA) colorimetric protein assay. Briefly, a tartrate buffer (pH 11.25) containing 25 mM BCA, 3.2 nM $CuSO_4$, and appropriately diluted protein/nanocapsules was incubated at 60 °C for 30min. After the solution was cooled to room temperature, absorbance reading at 562 nm was determined with a UV-Vis spectrometer. OPH, lipase, EGFP and GOX solutions with known concentration were used as standards. For the protein content in the enzyme-silica nanocomposites, the difference between the total amount of protein/nanocapsules added and the amount of protein/nanocapsules remained in the supernatant after precipitation was used as the protein content in the composites.

3.2.10 Enzyme activity assay

OPH: 10 μL of paraoxon (75 mM) solution in DMSO was added to 1.0 mL of HEPES buffer solutions (50 mM, pH 8.5) containing the native enzyme, nanocapsule and enzyme-silica composites with same amount of OPH respectively. The mixture was placed in a quartz cuvette and the absorbance change was monitored at 405 nm under room temperature. One unit is defined as hydrolysis reaction to release 1.0 μmol 4-nitrophenol per minute.

Lipase: 100 μL of 4-nitrophenyl laurate (10 mM) solution in DMSO was added to 1.0 ml of phosphate buffer solutions containing the native lipase, the nanocapsule and enzyme-silica composites with the same amount of lipase respectively. The mixture was placed in a quartz cuvette and the absorbance change was monitored at 405 nm under room temperature. One unit is defined as hydrolysis reaction to release 1.0 μmol 4-nitrophenol per minute.

EGFP: All fluorescence spectra were recorded on Tecan GENios Multifunction microplate reader at room temperature. 488 nm and 535nm were chosen as the excitation and emission wavelength respectively.

GOX: Glucose, TMB and HRP were dissolved in sodium acetate buffer (50mM, pH 5.1) at a final concentration of 1.72%, 0.5 mM and 0.01mg/ml respectively. The native enzyme, the nanocapsules and enzyme-silica composites with the same amount of GOX were added to the assay solution respectively. The mixture was placed in a quartz cuvette and the absorbance change was monitored at 655 nm under room temperature. One unit is defined as oxidation of 1.0 μmol of β-D-glucose to D-gluconolactone and H_2O_2 per minute.

3.2.11 Stability assay

Thermal and organic solvent stability assay for OPH: For thermal stability, activities of native OPH, OPH nanocapsules and nOPH-silica were measured after incubation at 60 °C for 1-4 h. For organic solvent stability, activities of native OPH, nOPH and nOPH-silica incubated in the solutions with different volume fractions of DMSO were measured. The activity was expressed in the percentage relative to the initial activities.

Thermal stability activity assay for lipase: Activities of native lipase, lipase nanocapsules and nLipase-silica at different temperatures were measured in buffer solutions at pH 7.0 from 30 to 90 °C. The activity was expressed in the percentage relative to the maximal activity value at 40 °C.

Thermal and SDS stability assay for EGFP: For thermal stability, fluorescence of native EGFP, EGFP nanocapsules and nEGFP-silica were measured after incubation at 75 °C for 1-4 h. For surfactant stability, activities of native EGFP, nEGFP and nEGFP-silica incubated in the solutions with 0.5% SDS at 55 °C were measured. The fluorescence intensity was expressed in the percentage relative to the initial fluorescence intensity.

Recycle stability assay and long-term storage stability assay: For recycle stability, enzyme-silica composites were centrifuged and precipitated from assay buffer and suspended for activity assay again in next cycle. For long-term stability, the enzyme-silica composites were suspended in storage buffer and keep at room temperature for certain days before activity assay.

3.3 Result and discussion

3.3.1 Synthesis of nanocapsule and enzyme-silica composite

Herein, we use OPH as a model enzyme. Figure 3.1 illustrates our synthesis strategy. The nanocapsules of OPH, denoted as nOPH, were synthesized by an *in-situ* free-radical

polymerization technique.[200] Briefly, OPH was firstly conjugated with polymerizable acrylate groups (Step I). As-modified OPH was then dispersed in an aqueous solution containing monomers, crosslinker and initiator. Driven by hydrogen bonding and electrostatic interactions, the monomers N-(3-aminopropyl) methacrylamide (APM) and acrylamide (AAM) and the crosslinker N,N'-methylenebisacrylamide (BIS) were enriched around the OPH molecules[176, 226]. Subsequent polymerization led to the formation of nOPH that contains an OPH core and a thin polymer shell; such shell structure stabilizes the OPH while allow effective substrate transport (Step II). The nanocapsules were then co-assembled with P123 and silicate clusters made through hydrolysis and condensation reactions of tetramethyl orthosilicate, where P123 is an amphiphilic block copolymer $EO_{20}PO_{70}EO_{20}$ (EO and PO represent ethylene oxide and propylene oxide, respectively). This self-assembling process leads to the formation of silicate/P123/nOPH composites; subsequent removal of the P123 affords the formation of mesoporous nOPH composites (Step III). The mesoporous silica further stabilizes the enzymes while allows effective transport of the substrates throughout the composites (Figure 3.1 IV), affording such composites with enhanced enzyme stability and high activity.

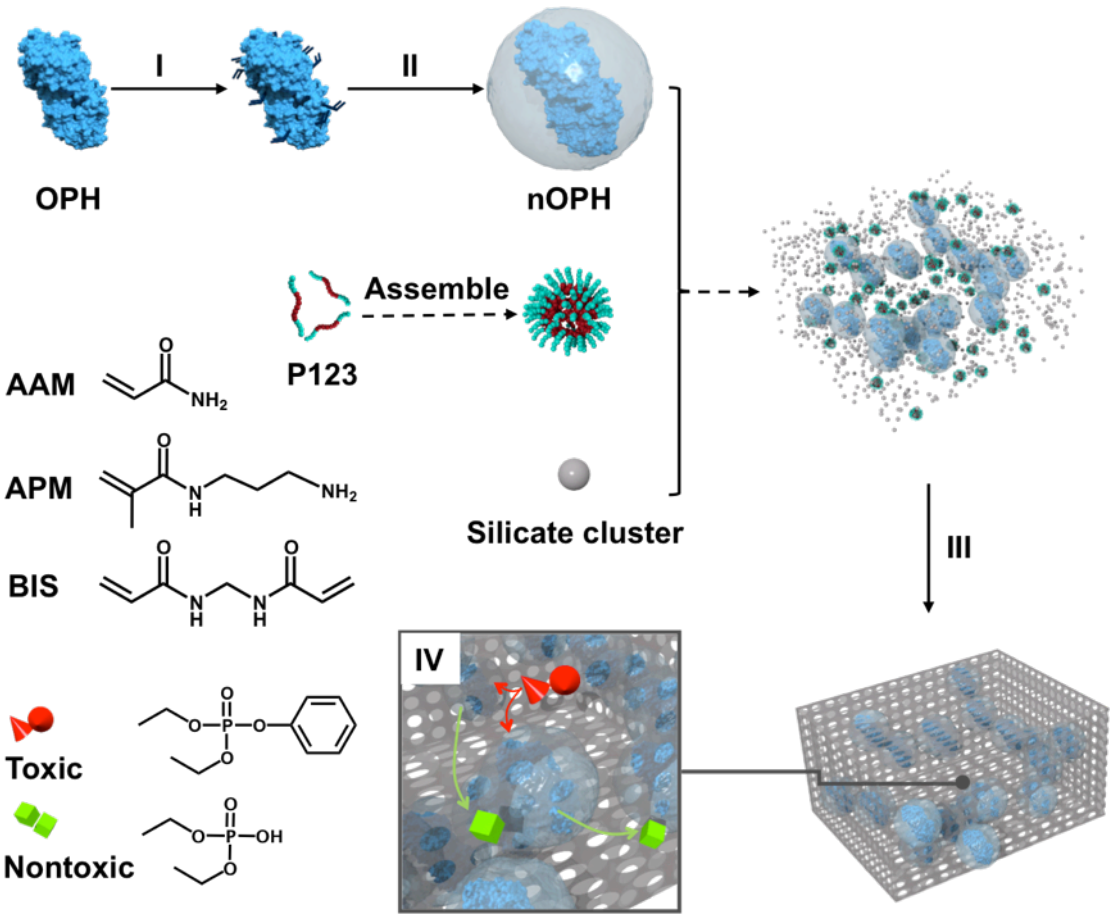

Figure 3.1 Schematic illustration of forming mesoporous OPH-silica composite from enzyme nanocapsules.

3.3.2 Characterization of nanocapsule and enzyme-silica composite

Figure 3.2a presents the transmission electron microscopic (TEM) image of nOPH, which shows a spherical structure with diameter ranging from 15 to 25 nm and is consistent with the dynamic light scattering (DLS) study (Figure 3.3a). Since APM is an amine-containing monomer, nOPH shows a positive zeta potential of 3 mV, which is significantly different from that of the native OPH (-6 mV) (Figure 3.3b). This observation confirms the formation of nOPH with cationic polymer shells. The polymer shells were further examined by Fourier transform infrared spectroscopy (FTIR) study, which exhibits the characteristic absorptions of poly(acrylamide) at 1670, and 1460 cm^{-1}

[227] (Figure 3.2c). Figure 3.2b presents a TEM image of a nOPH-silica composite, showing a mesoporous structure templated by P123. FTIR spectrum of the composite consistently shows the characteristic absorption of amide and Si-O bonds at 1670 cm^{-1} and 1051 cm^{-1}, respectively, confirming the incorporation of nOPH within the silica composite (Figure 3.2c) [215]. Figure 3.2d shows the nitrogen sorption isotherms and the pore size distribution of the composite, indicating a mesoporous structure with pore diameter centered at 7.5 nm, which is similar to those of P123-templated mesoporous silica [228].

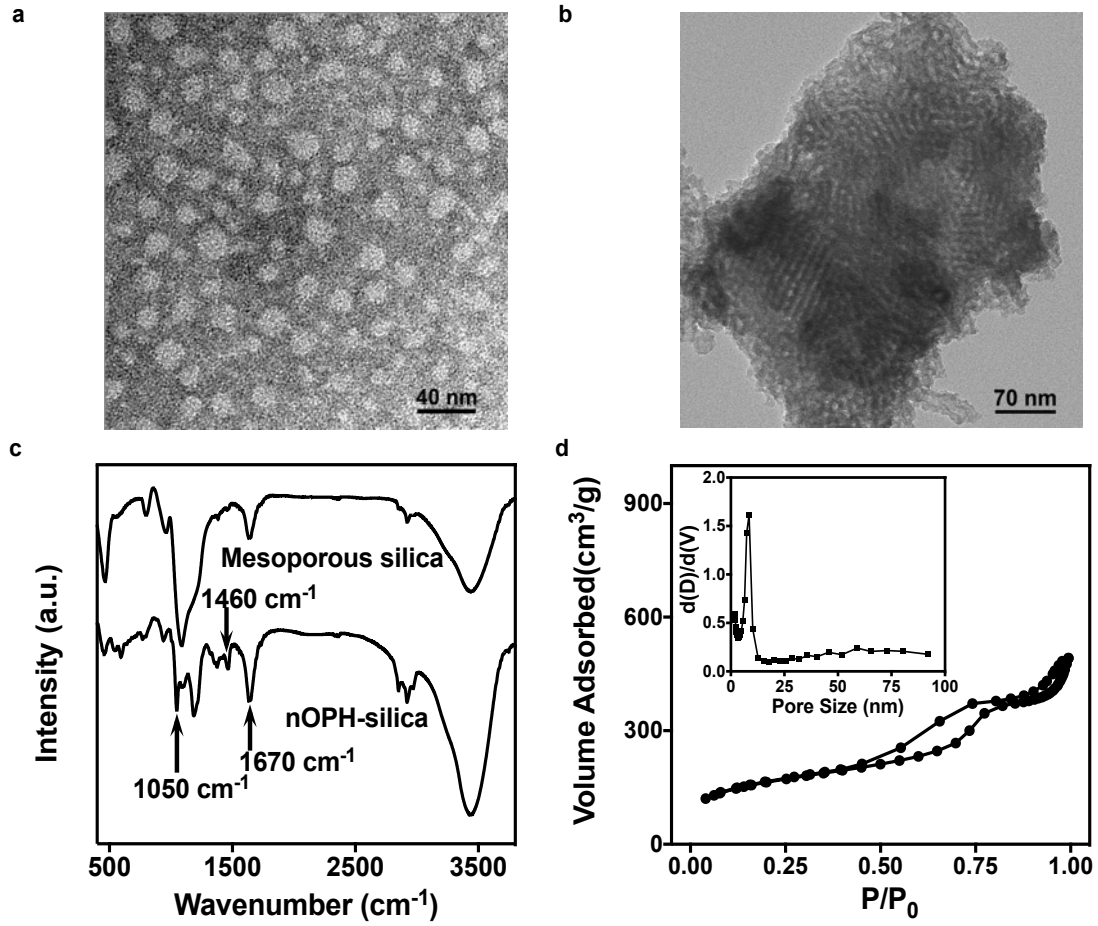

Figure 3.2 a) TEM of OPH nanocapsules nOPH, b) TEM of nOPH-silica composites, c) FTIR of mesoporous silica with and without incorporating nOPH, d) N_2 sorption isotherms and pore size distribution (inset) of the nOPH-silica composite.

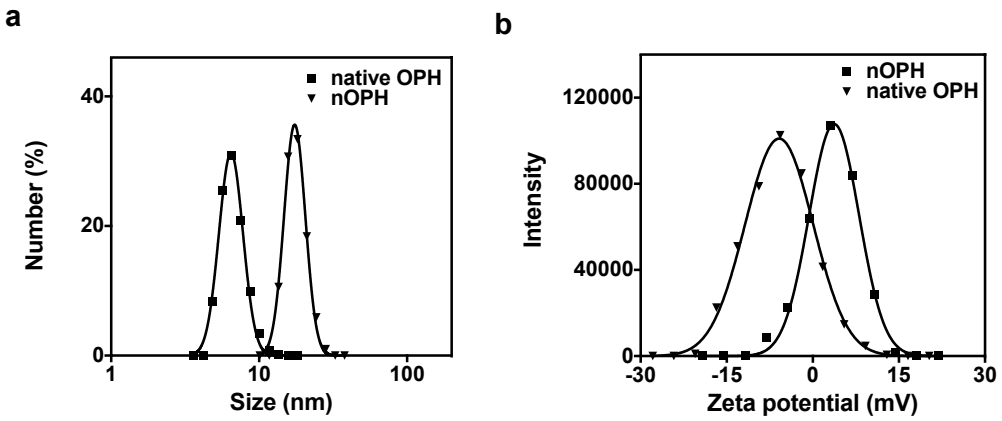

Figure 3.3 a) DLS for native OPH and OPH nanocapsule. b) Zeta potential for native OPH and OPH nanocapsule.

3.3.3 Activity enhancement and enzyme microenvironment manipulation

Currently, enzyme-silica composites are synthesized either by a sol-gel process in which the enzymes were mixed with silicate clusters and trapped within the silicate networks [229], or by adsorbing or covalently attaching enzymes to preformed silica scaffolds.[230, 231] Such processes often result in significant lose of the enzyme activity.[230, 232, 233] Consistently, sol-gel process by direct mixing of native OPH with silicate clusters results in composites (denote as OPH-silica) with significantly reduced enzyme activity. As shown in Figure 3.4, native OPH exhibits an activity of 371 Units/mg, while the OPH-silica composite shows a dramatically reduced activity of 8 Units/mg. The significant loss of the activity is associated with the non-physiological conditions during the synthesis of the composites, such as ethanol or methanol produced during the sol-gel process. This could be overcome by using enzyme nanocapsules as building blocks that offer significantly enhanced stability. As expected, the composite made from nOPH (denoted as nOPH-silica) exhibits a much higher activity of 686 Units/mg, similar to that of the nOPH (706 Units/mg). This indicates that the activity of nOPH is fully retained during

the composite synthesis, in comparison with the native OPH that lost near 98% of the activity.

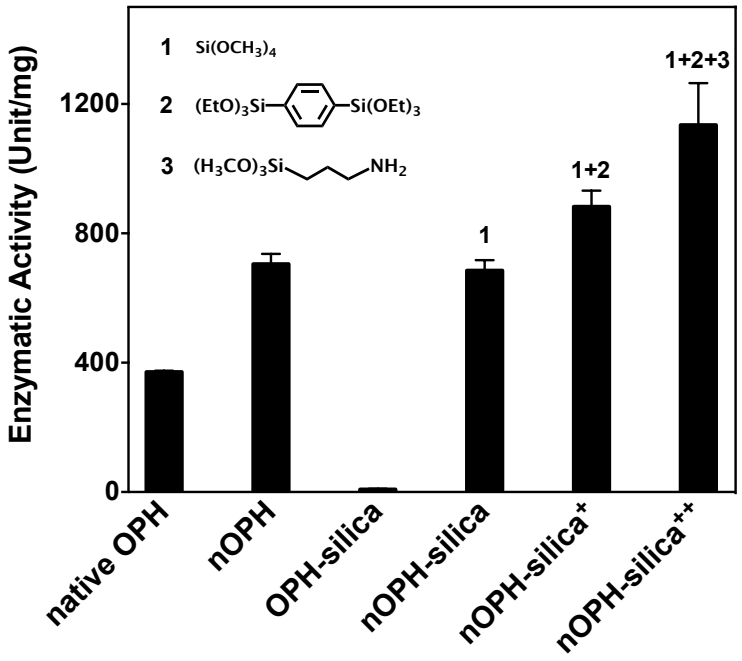

Figure 3.4 Enzymatic activity of native OPH, nanocapsule nOPH, and the composites made from native OPH and precursor *1* (OPH-silica), nOPH and precursor *1* (nOPH-silica), nOPH and precursor *1* and *2* (nOPH-silica^{+}), or nOPH and precursor *1*, *2*, and *3* (nOPH-silica^{++}).

Beyond the capability of retaining high enzyme activity within the composites using enzyme nanocapsules as the building component, the enzyme activity could be further improved by constructing suitable microenvironment with both polymer and silica shell. OPH effectively decomposes hydrophobic organophosphates with the optimum pH of 9.0 [234, 235]. Constructing a hydrophobic microenvironment helps to enrich the hydrophobic substrates around the enzyme leading to improved enzymatic kinetics. Furthermore, constructing a local alkaline environment, such as by introducing amine groups near the OPH molecules, facilitates the enzymatic decomposition. As expected,

introducing amines groups within the nOPH shells by using the amine-containing APM molecules as the co-monomer (see Figure 3.1) affords the nOPH with high activity of 706 Units/mg (Figure 3.4 nOPH vs native OPH), which outperforms that of the native OPH (371 Units/mg) and is consistent with our previous finding [201].

To further construct hydrophobic and alkaline microenvironments within the composites, three different silanes were used, including tetramethyl orthosilicate (*1*), 1,4 bis(triethoxysilyl)benzene (*2*), and 3-aminopropyl trimethoxysilane (*3*). Precursor *2* contains non-hydrolyzable and hydrophobic benzene moiety; while precursor *3* contains non-hydrolyzable and alkaline aminopropyl moiety. Sol-gel process using *1* and *2* as the co-precursors affords the formation of silica matrix with hydrophobic microenvironment; while the use of *1*, *2*, and *3* as the co-precursors affords the formation of silica matrix with both hydrophobic and alkaline microenvironment. Compared with the nOPH-silica composite made from *1* with activity 686 Units/mg, the composite made from precursor *1* and *2* (denoted as nOPH-silica^{+}) shows an increased activity of 883 Unit/mg owning to the hydrophobic microenvironment (Figure 3.4). The composite made from *1*, *2*, and *3* (denoted nOPH-silica^{++}) shows further increased activity of 1135 Units/mg (Fig. 4). The activity of nOPH-silica^{++} composite is ~2 folds higher than that of nOPH-silica composite, 141 folds higher than OPH-silica composite, or 3 folds higher than that of the native OPH. Consistently, nanocomposites made from precursors *1* and *2* and glucose oxidase (GOX), a model enzyme that catalyzes the oxidation of hydrophilic substrate glucose, resulted in lower activity than those made from precursor *1* only (Figure 3.5b). This result further confirms the important role of enzyme microenvironment in the overall activity. Considering that a large library of organosilanes with various non-

hydrolyzable groups are commercially available, this approach offers feasibility to construct various microenvironments for various enzyme composites, such as silica composites made from lipase nanocapsules (Figure 3.5a).

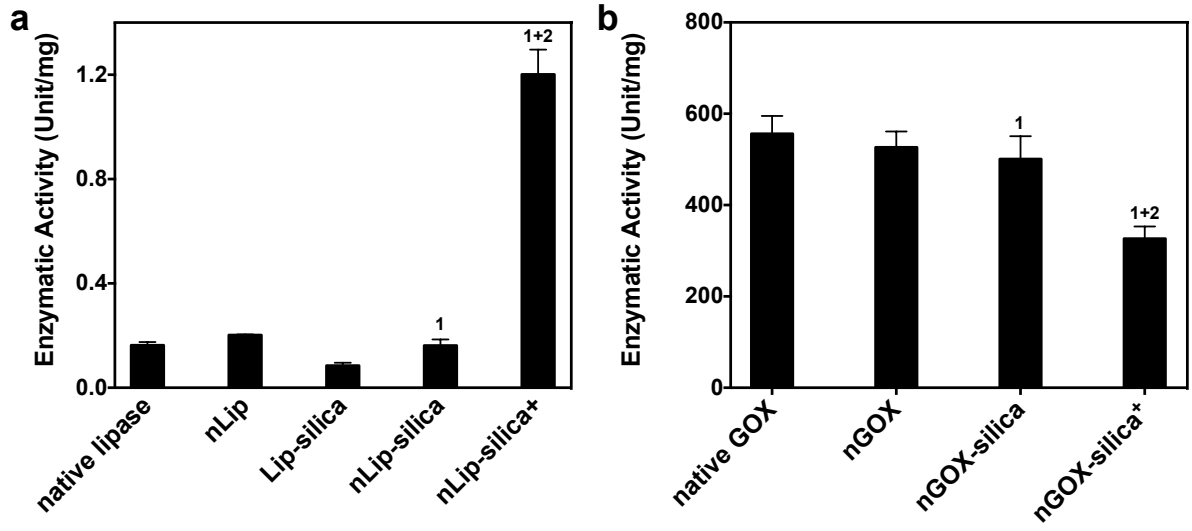

Figure 3.5 a) Enzymatic activity of lipase, lipase nanocapsule and the composites made from native lipase and precursor *1* (Lip-silica), nLipase and precursor *1* (nLip-silica), nLipase and precursor *1* and *2* (nLip-silica^{+}). b) Enzymatic activity of GOX, GOX nanocapsule and the composites made from nGOX and precursor *1* (nGOX-silica), nGOX and precursor *1* and *2* (nGOX-silica^{+})

3.3.4 Kinetics study of enzyme-silica composite

Table 3.1 further shows the Michaelis-Menten kinetics parameters, K_m and k_{cat}, of the native OPH, nOPH and the composites. The native OPH exhibits a similar K_m (0.061 mM) as that of nOPH (0.071 mM), suggesting that thin polymer shells around the OPH cores do not cause any significant resistance for substrate transport. Incorporating nOPH into the silica composites, as expected, increases the transport resistance of the substrates evidenced from the increased K_m (0.181 mM). Nevertheless, when hydrophobic moiety was incorporated (nOPH-silica^{+} and nOPH-silica^{++}), the K_m shows obvious decrease in both cases (0.111 mM and 0.116 mM). This result further indicates the importance of hydrophobic microenvironment for hydrophobic substrate transport. Comparing with the

native OPH with k_{cat} of 594 s^{-1}, nOPH exhibits a significantly higher k_{cat} (1322 s^{-1}), confirming the role of the local alkaline environment in enhancing the catalytic effect. The value of k_{cat} further increases when nOPH is incorporated within the silica composites, reaching the highest value of 2854 s^{-1} for nOPH-silica^{++}. The increased k_{cat} within the silica matrix may due to the concentrating effect, where nOPH are highly concentrated within the silica matrix and provides a microenvironment with basic pH.

Table 3.1 The enzymatic kinetic parameters K_m and k_{cat} of the native OPH, nOPH, and OPH-silica composites.

	K_m (mM)	k_{cat} (s^{-1})
Native OPH	0.061±0.009	594±22
nOPH	0.071±0.017	1322±85
nOPH-silica	0.181±0.032	2324±156
nOPH-silica^{+}	0.111±0.017	2456±130
nOPH-silica^{++}	0.116±0.022	2854±175

3.3.5 Enhanced stability of enzyme-silica composite

Besides the greatly enhanced activity, these composites also exhibit outstanding stability against denaturation from high temperature, organic solvent, surfactant and enzyme leaching from the composites. Figure 3.6a compares the relative activity of native OPH, nOPH and nOPH-silica composite after incubation at 60 °C for 4 hours. Distinct from the fast denaturation of the native OPH and nOPH, which retains respectively 6% and 26% of the activity, nOPH-silica composite retains a 73% of initial activity. The significantly

enhanced activity observed in the nOPH-silica composite can be attributed to the covalent attachments between the OPH and the polymer shells, as well as the silica matrix that hinders the denature process.[236] Similar results were also observed in the silica composites of lipase and enhanced green fluorescent protein (EGFP) (Figure 3.7a and 3.7b), which offers a general enzyme-stabilization approach.

Organic solvents such as DMSO, methanol and ethanol are commonly used as co-solvent to increase the solubility of hydrophobic substrates.[237-239] Developing enzyme systems that tolerate organic solvents is therefore importance for industry applications.[240, 241] Protein engineering is the current strategy to improve solvent-tolerance of enzymes, which is time-consuming and usually results in reduced activity [242]. Nevertheless, our approach offers significantly improved organic-solvent tolerance without compromising activity. As shown in Figure 3.6b, after incubating with a series of DMSO/buffer solutions, the nOPH-silica composite retains more than 80% of its initial activity even in the presence of 50% DMSO. In contrast, native OPH and nOPH only retain 10% and 30% of their initial activity, respectively. Such improvement can be attributed to the synergic effect from the soft polymer shells and the hard silicate matrix, which protects the essential water from being stripped off by polar organic solvent [237, 241].

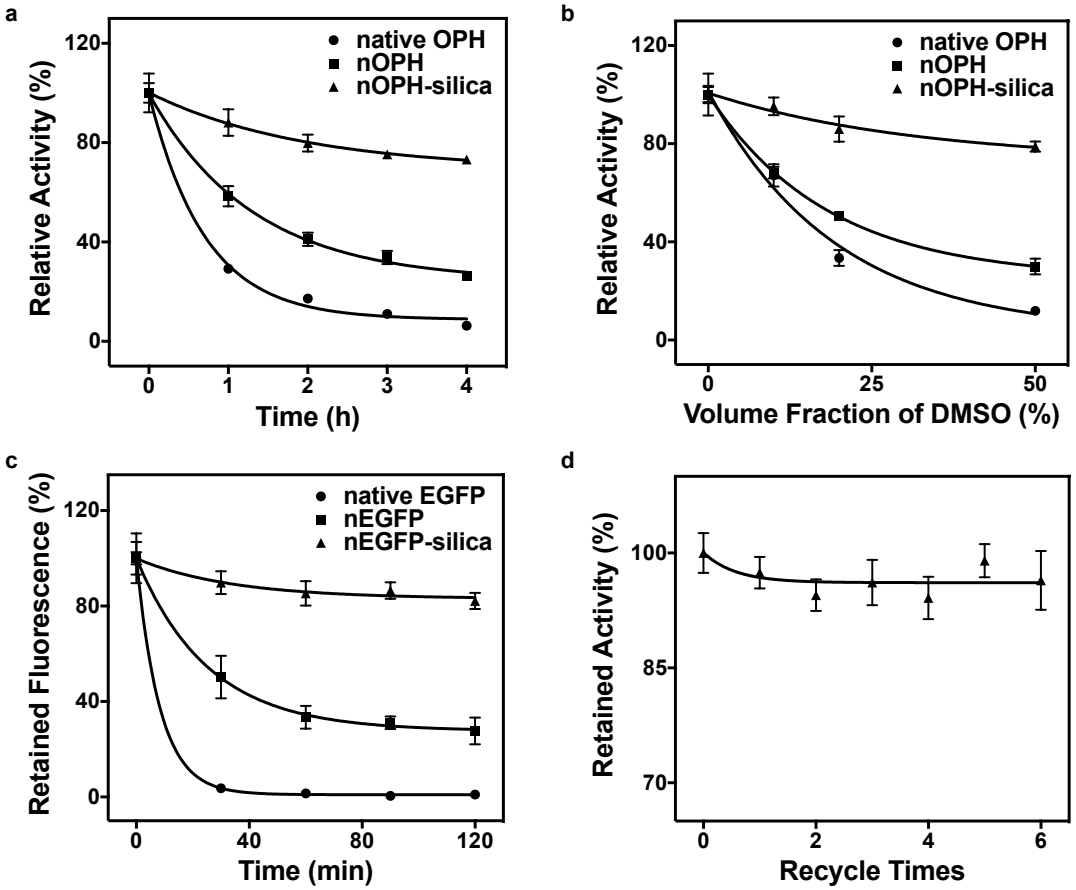

Figure 3.6 a) Relative enzyme activity of native OPH, nOPH and nOPH-silica composite after incubation at 60 °C for 4 hour; b) Relative enzyme activity of native OPH, nOPH and the nOPH-silica composite after incubation with DMSO/buffer solutions at different volumetric ratios; c) Relative fluorescence intensity of native EGFP, EGFP nanocapsules (nEGFP) and nEGFP-silica composite incubated in 0.5% SDS solution at 55 °C; d) Relative enzyme activity of nOPH-silica composite during six catalyst recycles.

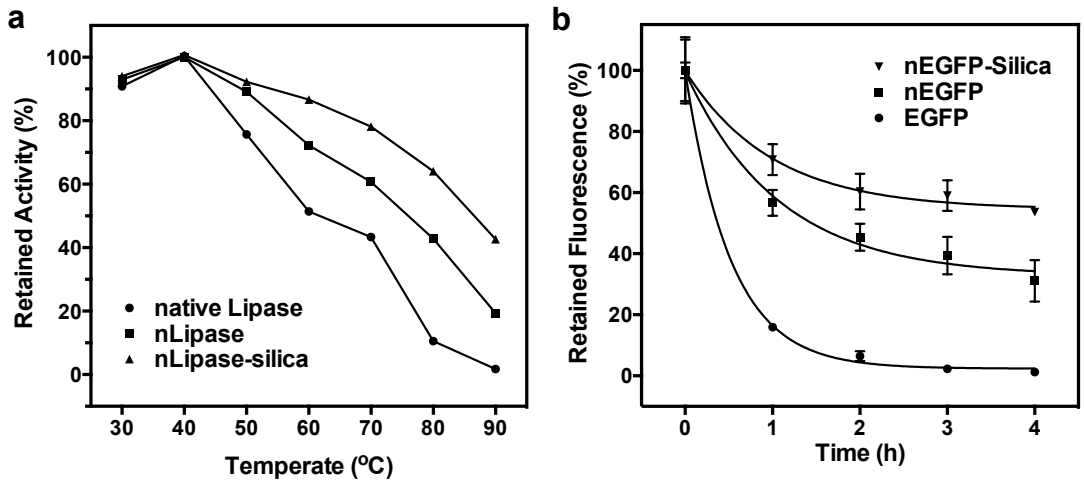

Figure 3.7 a) Relative activity of native lipase, nLipase and nLipase-silica at different temperature. b) Relative activity of native EGFP, nEGFP and nEGFP-silica at 75 °C.

In the aspect of enzyme stability against surfactant denaturation, Figure 3.6c shows the relative fluorescence intensity of native EGFP, EGFP nanocapsules (nEGFP), and nEGFP-silica composite made from nEGFP and silica precursor *1* (Figure 3.4) after 2 hrs incubation with 0.5% sodium dodecyl sulphate (SDS) at 55 °C. The native EGFP rapidly loses its fluorescence and nEGFP retains 27% of its initial fluorescence. For comparison, the nEGFP-silica composite still retains 85% of its initial fluorescence. The enhanced tolerance to surfactant is an important feature that could broaden the applications of enzymes in industrial manufactures where surfactants are commonly used to increase the solubility of substrates.

In the aspect of enzyme leaching from the composites, our enzyme-silica composite structure prevents the enzymes from leaching completely, distinct from traditional immobilization methods [243-245]. Figure 3.6d shows the relative enzyme activity of the nOPH-silica composites after repeated recycling from their assay buffer containing paraoxon. The leaching of enzyme was not observed even after 6 times recycling. The

silica composites made from lipase nanocapsules also show no leaching after repeated recycling from the assay buffer containing 4-nitrophenyl laurate (Figure 3.8a). Moreover, long-term storage stability of enzymes immobilized by calcium carbonate [246] and calcium phosphate [247] has been reported. Consistently, the composites made using this approach also exhibit good long-terms stability. For example, the nLipase-silica composites retained more than 90% of the initial activity at room temperature for 10 days (Figure 3.8b). The excellent durability endows the composites with great potentials for industrial applications.

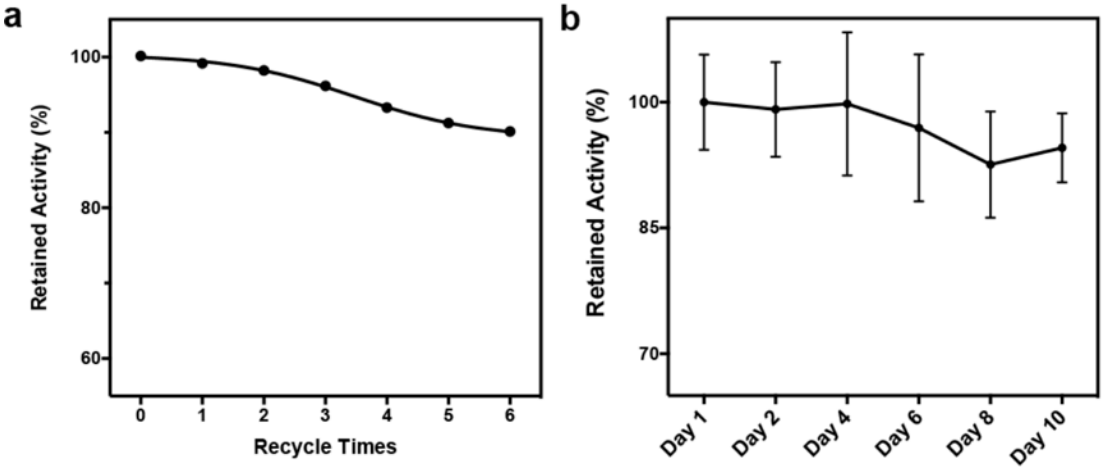

Figure 3.8 a) The recycling durability and b) long-term storage stability of nLipase-silica composite.

3.4 Summary

In conclusion, we have demonstrated the synthesis of robust enzyme-silica composites using enzyme nanocapsules and silica precursors with desired functional moieties. Judicious design of the microenvironment within the silica matrix can further improve the enzyme activity, leading to the formation of enzyme composites with activity and stability far excess that of the native counterparts. This approach leads to the formation of a novel class of enzyme composites with significantly enhanced activity, stability and

resistance against leaching from the composites. This novel class of enzyme-silica composite has great promise to broaden the application of various enzymes in industry.

Chapter 4. Self-crosslinking cell-penetrating nanocapsules for redox responsive intracellular protein delivery

4.1 Introduction

Modern biotechnology has led to the development of a large family of potential therapeutic proteins [1]. These proteins exhibit higher specificity and superior efficiency comparing to traditional small molecule drugs and also prevent the potential genetic change risk compared to gene therapy [1, 248]. Particularly, the intracellular use of therapeutic proteins is of great importance in the treatment of cancer and protein deficiency diseases; however, the effectiveness of protein therapy has been limited by its low delivery efficiency and poor stability against proteases digestion and thermal denaturing. Developing a simple and robust approach to deliver and stabilize targeted functional proteins is therefore necessary and crucial.

Physical methods like microinjection or electroporation has been used for the delivery of membrane-impermeable molecules in cell experiments. However, they are invasive in nature and could damage cellular membrane. Thus noninvasive protein delivery methods are desired. To date, protein encapsulation and conjugation methods have been widely explored for intracellular delivery by developing delivery vectors such as liposomes [249], polymeric [250, 251] and mesoporous materials [252] carbon nanotubes [253] which provide certain controlled release and improved transmembrane properties. Another popular method relies on protein conjugation or fusion to cell penetration

peptides [254] to improve intracellular delivery efficiency. Although showing certain merit, these methods still have problems like limited transduction efficiency [67], low stability at physiological pH values and temperatures [255], high toxicity [254], tedious preparation process [256] and potential bioactivity loss during these process [251, 256]. Recently, Yan *et al.* reported novel intercellular protein delivery platform based on single-protein nanocapsule by *in-situ* polymerization which shows great promise.[200] However, the acrylation and free radical polymerization may cause damage to fragile proteins. Developing an effective and protein friendly approach for intracellular deliver of functional proteins with effective cargo release is still challenging.

4.2 Experimental

4.2.1 Materials

Polyallylamine hydrochloride (PAH, M_w 17500), poly(ethylene glycol) 2000 methyl ether (MPEG2000), succinic anhydride, N-hydroxysuccinimide, triethylamine, boric acid, sodium tetraborate, Sephadex G-75, Trizma® base, sodium phosphate monobasic monohydrate, sodium phosphate dibasic, Dulbecco's modified Eagle's medium (DMEM), resazurin, bicinchoninic acid (BCA), tartaric acid, $CuSO_4$, 3,3',5,5'-tetramethylbenzidine, glucose, ethanol, uric acid, 30% hydrogen peroxide solution, glucose oxidase (GOX) from Aspergillus niger, Catalase (Cat) from bovine liver, horseradish peroxidase (HRP), alcohol oxidase (AOX) from Pichia Pastoris were purchased from Sigma-Aldrich and were used as received. Traut's reagent (2-thiolanimine hydrochloride), was purchased from MP Biomedicals™, fatal bovine serum (FBS) were purchased from Corning™. Active recombinant human Caspase 3 was purchased from BDBiosciences. Urate oxidase (UOX) is a kind gift from Dr. Jianmin Li from Beijing Institute of Biotechnology.

4.2.2 Instruments

TEM images were obtained on a Philips EM-120 TEM instrument. Particle size and zeta potential were measured with Zetasizer Nano-ZS (Malvern Instruments Ltd., UK). NMR spectrum was conducted on AV400 NMR spectrometer from Bruke Corporation. UV-Visible adsorption was acquired with a Beckman Coulter DU®730 UV/Vis Spectrophotometer. Fluorescence intensities were measured with a Tecan GENios Multifunction microplate reader. Carl Zeiss Axio Observer inverted fluorescence microscope. Flow cytometry analysis was achieved using a BD LSRFortessa cell analyzer.

4.2.3 Synthesis of SCP:

Poly(ethylene glycol) 2000 methyl ether (MPEG-2000) was used without further purification. The activation of MPEG-2000 was done by first converting it to PEG-succinate and then to N-hydroxysuccinimide ester as described elsewhere.[257] The resulted active PEG-succinate NHS ester was further reacted with polyallylamine hydrochloride in methanol use triethylamine as acid binding reagent. The resulted PEGylated polyallylamine was dialyzed in deionized water and lyophilized. For synthesis of SCP, the lyophilized PEGylated polyallylamine was dissolved in pH 8.0 borate buffer with 10 mM EDTA and reacted with Traut's reagent to get about 37% modification of amine groups on PAH. The amount of thiol groups modified on the PAH backbone is quantified by Ellament's assay.

4.2.4 Preparation of nanocapsules:

BSA was dialysized against 10mM pH 7.0 phosphate buffer. Subsequently BSA was mixed with aqueous solution of SCP at a molar ratio of 1:20 followed by dialysis and air-

bubbling into the solution to ensure the crosslinking of nanocapsules by forming disulfide bond. The resulted nanocapsules were dialyzed against 10 mM phosphate buffer at pH 7.0 and further purified with Sephadex G-75 to remove the unreacted monomers, initiators and enzymes. GOX, HRP, Cat, AOX and UOX nanocapsules were synthesized in similar method.

4.2.5 BCA protein content quantification

All the protein content in solution was determined by bicinchoninic acid (BCA) colorimetric protein assay. Briefly, a tartrate buffer (pH 11.25) containing 25 mM BCA, 3.2 nM $CuSO_4$, and appropriately diluted protein/nanocapsules was incubated at 60 °C for 30min. After the solution was cooled to room temperature, absorbance reading at 562 nm was determined with a UV-Vis spectrometer. GOX, HRP, Cat, UOX and AOX solutions with known concentration were used as standards.

4.2.6 Protein activity assay

HRP activity assay: H_2O_2 and 3,3',5,5'-tetramethylbenzidine were dissolved in sodium acetate buffer (50mM, pH 5.1) at a final concentration of 0.3 % and 0.5 mM respectively. The native HRP and nHRP were added to the assay solution respectively. The mixture was placed in a quartz cuvette and the absorbance change was monitored at 655 nm under room temperature.

GOX activity assay: Glucose, 3,3',5,5'-tetramethylbenzidine and HRP were dissolved in sodium acetate buffer (50mM, pH 5.1) at a final concentration of 1.72 %, 0.5 mM and 0.01mg/ml respectively. The native GOX and nGOX were added to the assay solution respectively. The mixture was placed in a quartz cuvette and the absorbance change was monitored at 655 nm under room temperature.

Cat activity assay: H_2O_2 was dissolved in phosphate buffer (20mM, pH 7.0) at a final concentration of 0.03 %. The native Cat and nCat were added to the assay solution respectively. The mixture was placed in a quartz cuvette and the absorbance change was monitored at 240 nm under room temperature.

UOX activity assay: Uric acid was dissolved in borate buffer (100mM, pH 8.5) at a final concentration of 0.12 mM. The native UOX and nUOX were added to the assay solution respectively. The mixture was placed in a quartz cuvette and the absorbance change was monitored at 290 nm under room temperature.

AOX activity assay: Ethanol, 3,3',5,5'-tetramethylbenzidine and HRP were dissolved in phosphate buffer (20mM, pH 6.0) at a final concentration of 0.1 %, 0.5 mM and 0.01mg/ml respectively. The native AOX and nAOX were added to the assay solution respectively. The mixture was placed in a quartz cuvette and the absorbance change was monitored at 655 nm under room temperature.

4.2.7 Stability test

Cat nanocapsules stability: Stability of nCat was measured in the presence of 0.5 mg/mL trypsin at 37 °C in Tris-HCl buffer with 10 mM $CaCl_2$. The activity of native Cat and nCat were measured every 20 min and compared with original activity.

GOX nanocapsules stability: Stability of nGOX was measured in the presence of 0.5 mg/mL pepsin at 37 °C in pH 2.7 glycine-HCl buffer. The activity of native GOX and nGOX were measured every 30 min and compared with original activity.

4.2.8 Cell proliferation assay

The toxicity of the BSA nanocapsules was assessed by the resazurin assay using native BSA as control. HeLa cells (5000 cells/well) were seeded on a 96-well plate in 100 ul

DMEM the day before exposure to BSA nanocapsules. After incubation with nanocapsules at different concentrations for 24 hrs, the cells were washed with PBS and incubated with 100 ul frest medium containing resazurin (10 μL 0.1mg/mL in PBS) for 3 h. The cell viability was then determined by measuring the fluorescence of each well (λ_{ex} = 550 nm, λ_{em} = 595 nm) by microplate reader. Untreated cells and fresh medium were used as the 100% and 0% cell proliferation control, respectively.

4.2.9 *In vitro* cellular internalization

Cellular internalization studies were assessed via fluorescence microscopic technique and fluorescence-activated cell sorting (FACS). HeLa cells were cultured in Dulbecco's modified Eagle's medium (DMEM) supplemented with 10% fatal bovine serum (FBS) and 1% penicillin/streptomycin. Cells (20000 cells/well, 24-well plate) were seeded the day before adding the nanocapsules. Nanocapsules or native proteins with different concentrations were added into the cell medium. After incubation at 37 °C for 4 hrs, the cells were washed three times with PBS and either visualized with a fluorescent microscope or trypsinized, centrifuged, and re-suspended in PBS and analyzed via flow cytometry.

4.3 Result and discussion

4.3.1 Synthesis of redox responsive self-crosslinked cell-penetrating nanocapsules

We synthesized the protein nanocapsule, which consist of a protein core and redox responsive self-crosslinking cell-penetrating polymer (SCP) shell. As illustrated in Figure 4.1b, polyallylamine hydrochloride (PAH) was used as SCP backbone which allowed cell penetration through cationic amine groups. PEGylation of polyallylamine hydrochloride (PAH) was achieved by PEG 2000 N-hydroxysuccinimide ester reaction to increase

stability and reduce toxicity of PAH. The successful synthesis of PEGylated PAH was verified by H^1NMR spectrum (Figure 4.2). The resulted PEGylated PAH was further modified with self-crosslinking thiol groups on the side chain by 2-iminothiolane hydrochloride (Traut's Reagent). Subsequently, self-assembly of negative charged protein and positively charged SCP lead to the formation of protein nanocapsules which were self-crosslinked by air-bubbling to allow disulfide bond formation.

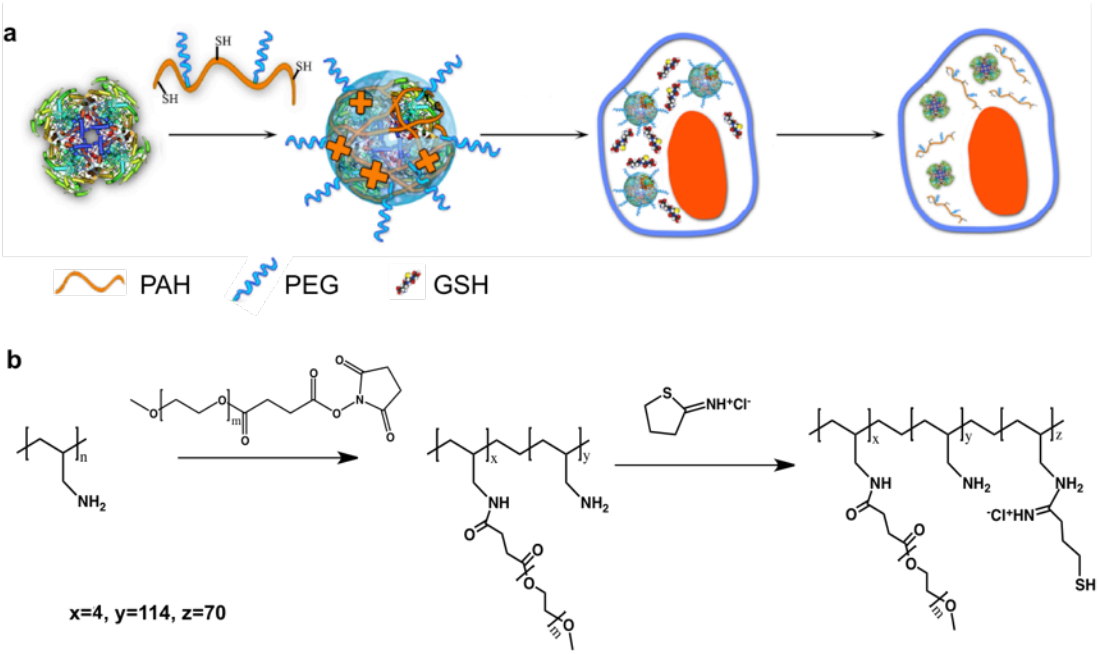

Figure 4.1 Construction of self-crosslinking cell-penetrating nanocapsules. a) Schematic showing the synthesis and cellular uptake and release of targeted protein through SCP based protein nanocapsules. b) Chemical structure of self-crosslinking cell-penetrating polymers.

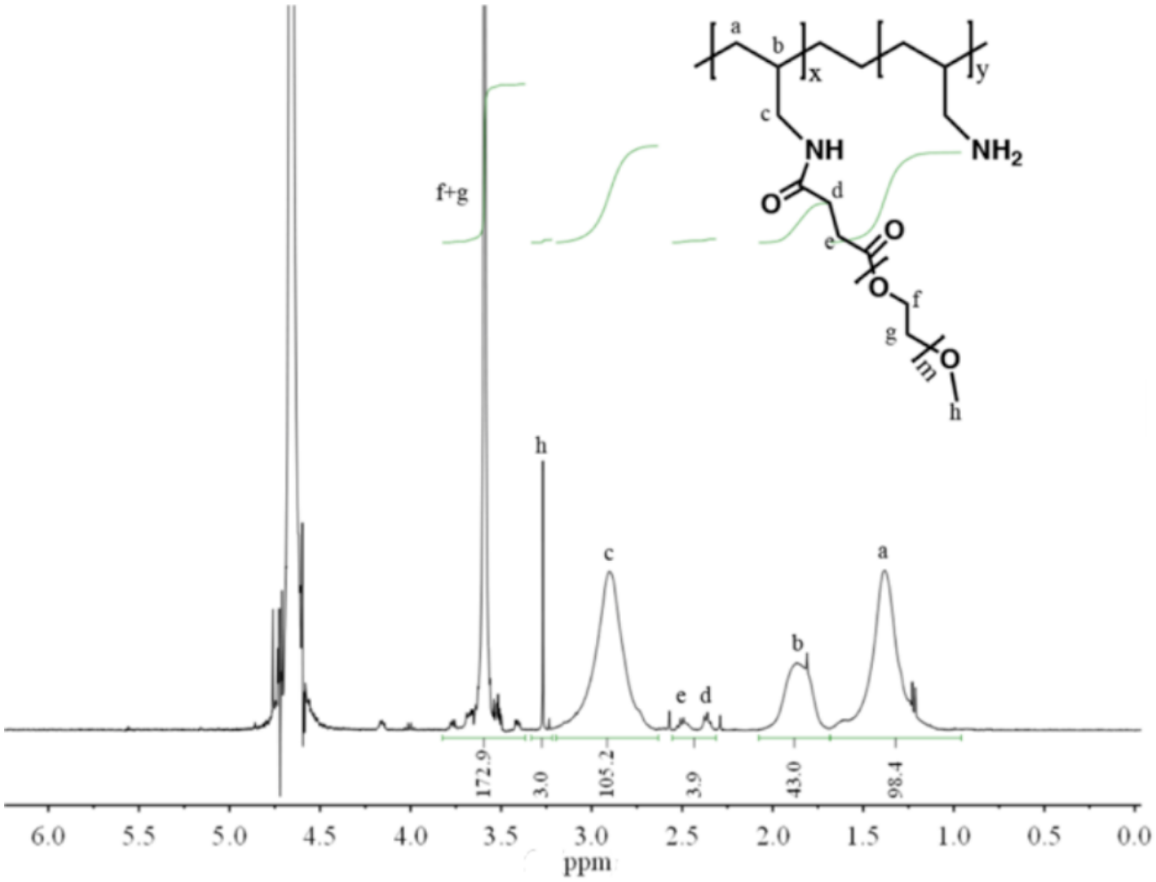

Figure 4.2 H[1]NMR spectrum of PEGylated PAH.

4.3.2 Characterization of SCP nanocapsules

Figure 4.3a present the size distribution of bovine serum albumin nanocapsules (denoted as nBSA) by dynamic light scattering (DLS). The diameter of the nBSA centered around 20 nm, significantly different from the native BSA (5 nm). Consistent with DLS, the transmission electron microscopy (TEM) image (Figure 4.3c) also confirms the uniform size of nBSA around 20-30 nm. Since PAH is a positively charged polymer, nBSA shows a positive zeta potential of 14 mV, which is significantly different from that of the native BSA (-7 mV) (Figure 4.3b). The formation of redox responsive nanocapsules is further demonstrated by agarose gel analysis. As illustrated in Figure 4.3d, both uncrosslinked and crosslinked nanocapsules (2 and 4) bearing positive charges moved towards the

negative electrode. However, after heparin was added, the FITC labeled BSA released from the uncrosslinked nanocapsule, while crosslinked nBSA remained stable (3 and 5). Moreover, the encapsulated BSA can be released after incubated in 10 mM glutathione (GSH). The FITC labeled BSA was dissociated from nanocapsules by adding heparin after the disulfide bond was degraded by GSH (6 and 7). The degradation of SCP nanocapsules under 10 mM glutathione is of great promise to delivery and release bioactive therapeutic proteins intracellularly since the cytosol contains 2 to 3 orders higher level of glutathione (GSH) (approximately 2–10 mM) than the extracellular fluids (approximately 2–20 μM)[169].

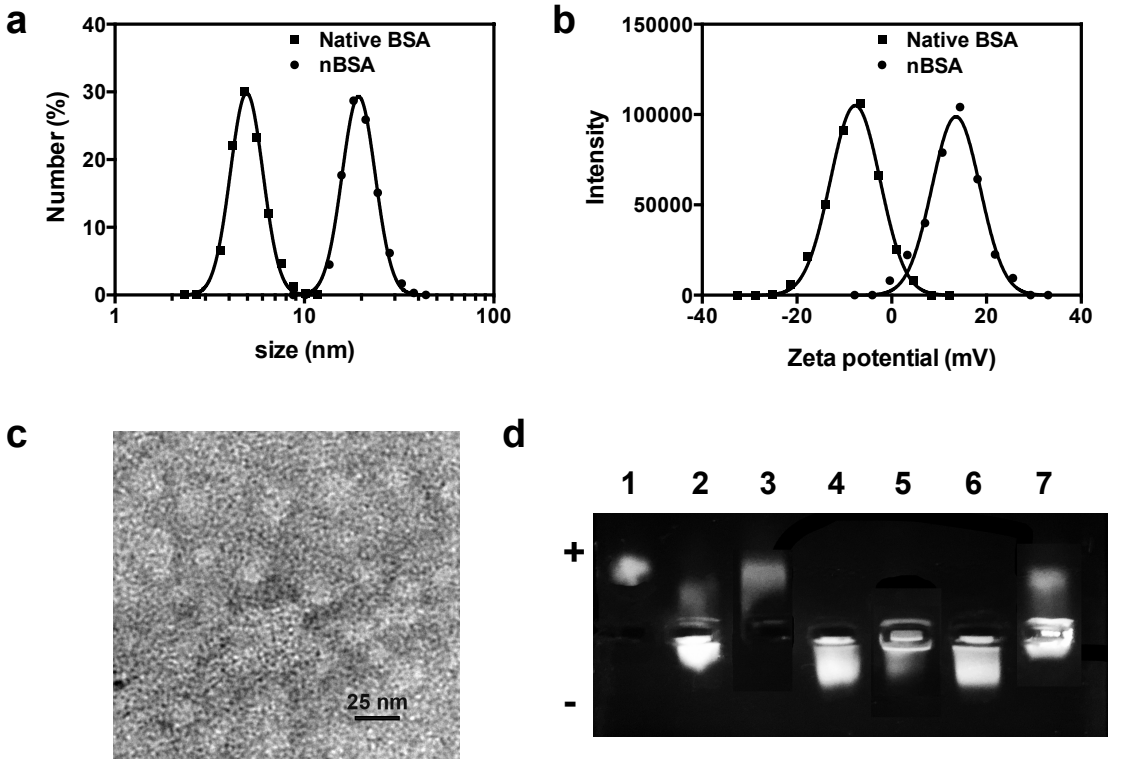

Figure 4.3 a) Particle size distribution of native BSA and nBSA. b) Zeta potential distribution of native BSA and nBSA. c) Representative TEM images of nBSA. d) Agarose gel analysis of (1) native BSA, (2 and 3) uncrosslinked nBSA, (4 and 5) crosslinked nBSA, (6 and 7) GSH degraded nBSA with or without heparin treatment.

4.3.3 Activity and stability of SCP nanocapsules

Currently, the use of common protein delivery vectors often results in reduced protein active and proteins may still vulnerable to protease degradation. The nanocapsules fabricated with SCP greatly enhanced the protein stability while minimize the activity loss. Figure 4.4 shows the relative activity remaining of various proteins nanocapsules compared with their native forms. Glucose oxidase (GOX), horseradish peroxidase (HRP), catalase (Cat) (denoted as nGOX, nHRP and nCat) retained almost 100% of their original activity after nanocapsules are made, while nanocapsules made from urate oxidase (UOX), alcohol oxidase (AOX) (denoted as nUOX and nAOX) also retained 90% and 86% of their original activity, respectively. The larger activity reduction of nUOX and nAOX may be attributed to the conformation change by disulfide exchange of cysteine on proteins with SCP. Nevertheless, it is still a favorable result compared with protein conjugation and encapsulation methods [258-262]. Besides the well-retained activity, nanocapsules show elevated proteolytic stability against protease digestion, which is a significant hindrance for protein therapy. Figure 4.5a compares the relative activity of nCat and native Cat in the present of 0.5 mg/ml trypsin at 37 °C. Distinct from the fast deactivation of the native Cat, which lost more than 95% of its original activity after 100 min, nCat underwent a much slower decrease with 84% activity retained. Even under much harsher challenge when incubated with 0.5 mg/ml pepsin at a pH of 2.7 at 37 °C, the GOX nanocapsule could still keep 53% of original activity after 120 min while native GOX lost all its activity (Figure 4.5b).

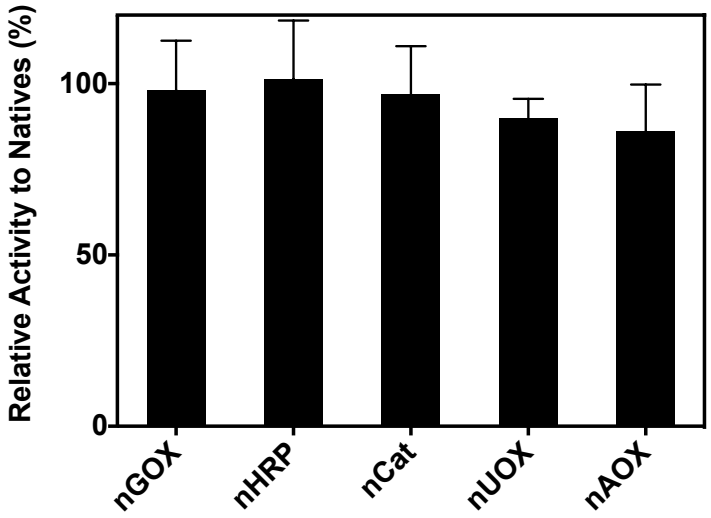

Figure 4.4 Activity of self-crosslinked nanocapsules.

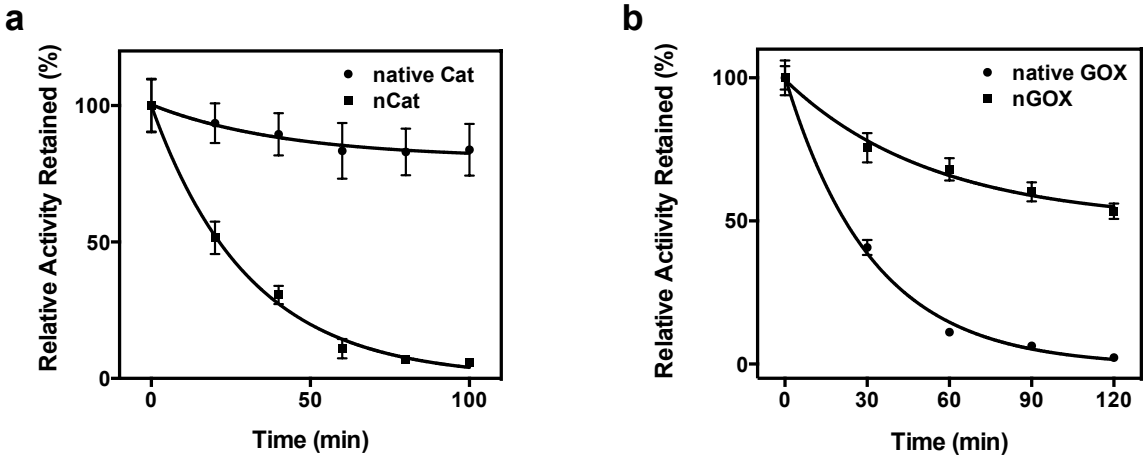

Figure 4.5 a) Relative Activities of native Cat and nCat after exposure to 0.5 mg/ml trypsin at 37°C. b) Relative Activities of native GOX and nGOX after exposure to 0.5 mg/ml pepsin at pH 2.7 at 37°C.

4.3.4 Biocompatibility of SCP nanocapsule

One of the concerns for intracellular protein delivery vectors is their biocompatibility. By adjusting the PEGylation degree on the SCP backbone, the cytotoxicity of our nanocapsules can be minimized. Herein, nBSA and HeLa cells were applied as a representative example for cytotoxicity assay. Briefly, nBSA with different PEG/PAH molar ratio in SCP was incubated with HeLa cells for 12 hours at 37 °C. As shown in

Figure 4.6a, cell viability gradually increases with the increment of poly (ethylene glycol) ratio grafted on SCP side chain with highest cell viability reached at PEG/PAH ratio of 4. Figure 4.6b also compares the viability of HeLa cells after exposure to different nBSA concentrations and suggests similar cytotoxicity for both nBSA (PEG/PAH ratio of 4) and native BSA. Following exposure to nanocapsules at a maximum concentration of 100 μg/ml, cell viability decreased by only 6%. The excellent biocompatibility renders the nanocapsule with great potential for in vivo application.

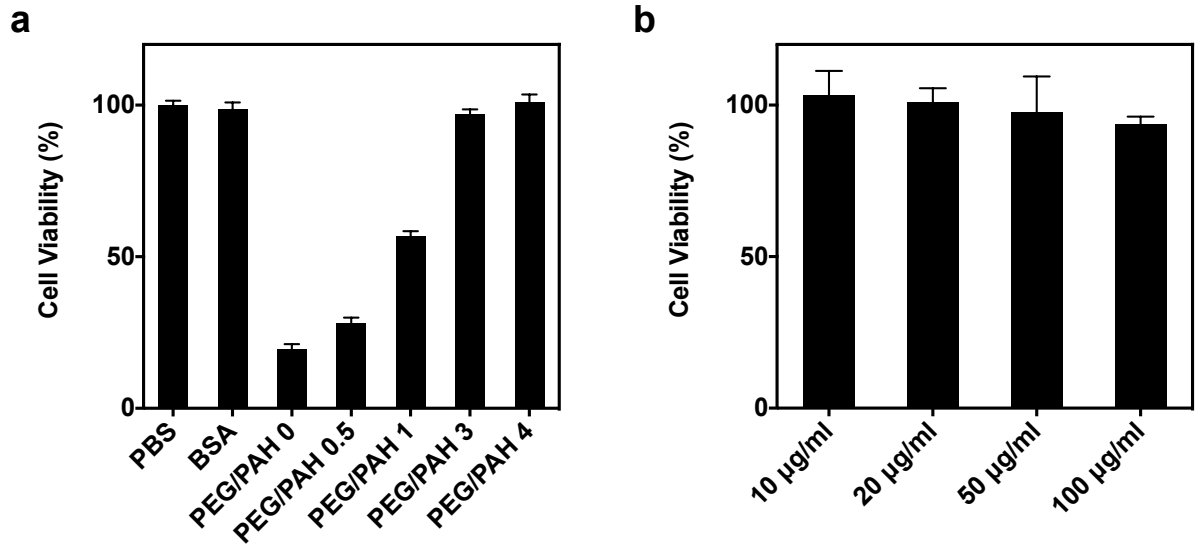

Figure 4.6 a) HeLa cell viability after incubation with nBSA with different PEG/PAH ratios. B) HeLa cell viability after incubation with nBSA of different concentrations.

4.3.5 Intracellular delivery of SCP nanocapsules

To verify the intracellular delivery efficacy, cellular uptake of nanocapsules was studied using FITC and Rhodamine labeled nBSA (F-nBSA and R-nBSA). After incubated with both F-nBSA and R-nBSA for 4 hours, the HeLa cells exhibited significant internalization of both nanocapsules, as both fluorescence of FITC and Rhodamine is clearly overlapped with cell phase image (Figure 4.7a). Such a multiple protein delivery

method has great potential for therapies in which proteins act synergistically or in tandem.[263] Nevertheless, native BSA didn't show any uptake by HeLa cells. Further quantification measurement of cellular uptake was conducted with flow cytometry. Cells incubated with F-nBSA show three to four orders higher fluorescence intensities than those with native BSA at a concentration dependent manner (Figure 4.7b). Moreover, active proteins were able to be delivered intracellularly. Exemplified with HRP, nHRP was incubated with HeLa cells, and were then exposed to a chromogenic substrate after thorough wash with PBS containing heparin. The blue color in the cell medium intensified with increasing nanocapsule concentration, indicating successful delivery of active HRP (Figure 4.7c). The successful internalization of active proteins shows great promise for future medical application of SCP nanocapsules, such as bioluminescence imaging, cancer treatment and regulation of cell behavior.

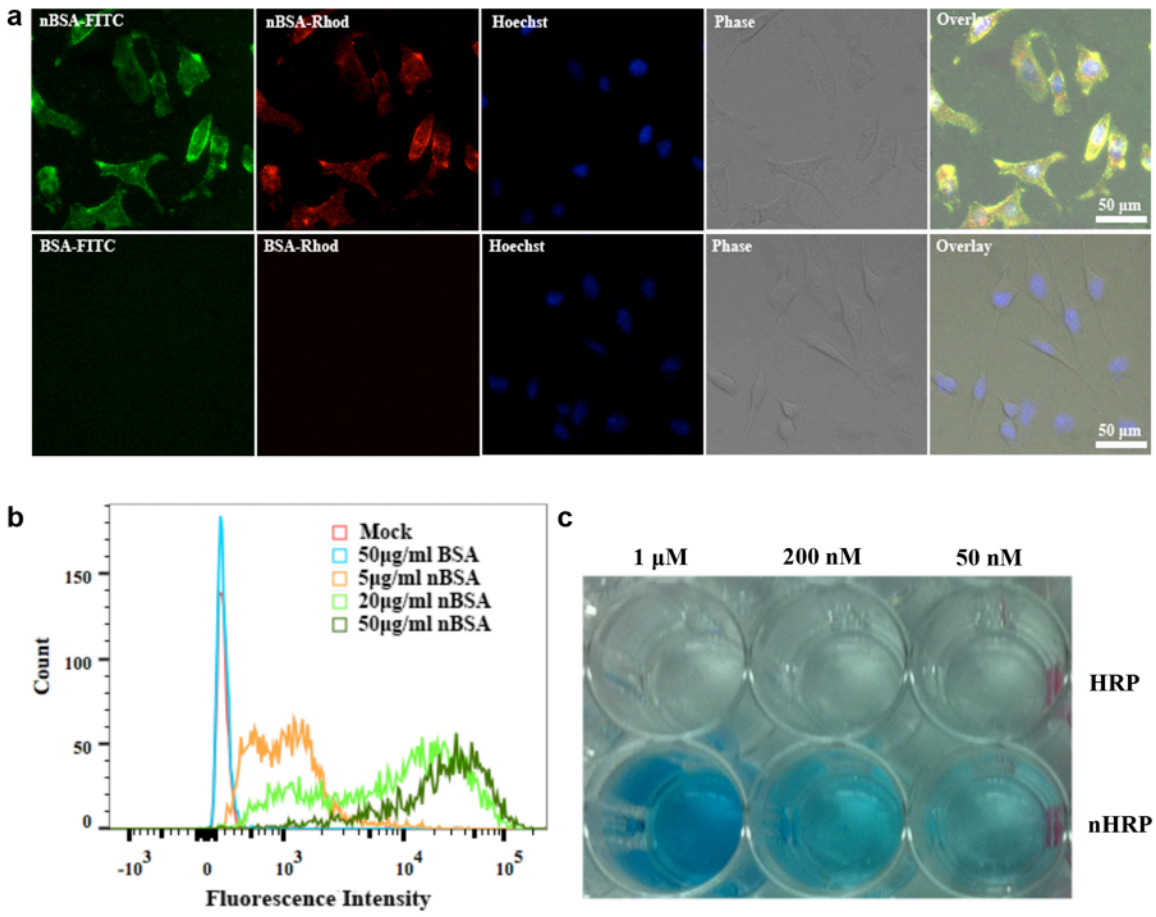

Figure 4.7 Transduction efficiency of protein nanocapsules in HeLa cells. a) Fluorescent images show the uptake of FITC and Rhodamine labeled nBSA but not FITC and Rhodamine labeled native BSA. b) Fluorescence activated cell sorting of HeLa cells incubated with different concentrations of FITC labeled nBSA and native BSA. c) HeLa cells after incubation with native HRP or nHRP at different concentrations for 3 h, followed by phosphate buffered saline washes and incubation with 3,3',5,5'-tetramethylbenzidine (TMB) and H_2O_2.

4.4 Summary

To conclude, we have demonstrated a novel protein delivery platform, based on self-crosslinked protein/polymer assemblies. The yielded protein nanocapsules gain enhanced stability against proteolysis and efficient cell internalization without sacrifice of bioactivity. Moreover, the SCP based protein nanocapsules are highly biocompatible and the potential of release cargos under high GSH level in cytosol holds great promise for

active proteins delivery to activate cell signaling pathway, which greatly expand our ability to manipulate cell behavior. Future work will be focus on delivery of active proteins that interact with biomacromolecules inside cells, which can guide cell signal and be potentially applied for cancer therapies, and tissue engineering. We believe that this strategy is a big step forward towards wider applications of protein therapy.

Chapter 5 pH sensitive zwitterionic polymer grafted nanocapsules for tumor site targeting

5.1 Introduction

Amongst various cancer therapies, chemotherapy is one of major treatment modalities along with debulking surgery. Major challenges in chemotherapy are linked to toxicity on healthy proliferating cells.[264] The life threatening side effects caused by non-specific tissue distribution of the drugs have restricted the systemic high dose strategy.[265] Tumor-targeting vectors have been developed for improved efficacy and reduced toxicity by altering biodistribution of cancer drugs and by using specific cell surface interactions.[266, 267] However, most of the vectors are often cleared out rapidly with undesired accumulation commonly in the liver, spleen or kidney [202, 268], before they can reach the target site. Particularly in case of protein therapeutics, modifying the proteins with poly(ethylene glycol) (PEG) remains as the golden standard, which leads to improved protein stability, prolonged circulation time, and reduced immune response.[269-271] It has been found that, however, ~25% of the patients have developed the anti-PEG antibodies. Protein therapeutics injected are subsequently opsonized by the

circulating antibodies and cleared rapidly, resulting in an accelerated blood clearance and reduced efficacy.[272-274]

It has been known that zwitterionic polymer exhibiting outstanding biocompatibility and protein-adsorption-resistant ability;[275, 276] such neutral polymers have been clinically explored as antifouling coatings for blood-contacting devices.[277] Thus, zwitterionic grafted protein nanocapsules have great potential to escape opsonization, increasing accumulation in the tumor site by enhanced permeability and retention (EPR) effect and reducing undesired accumulation in liver and spleen.

Recently, pH-sensitive polymeric carriers have been used in targeted antitumor drug delivery[278-281] based on intrinsic differences between various solid tumors and the surrounding normal tissues in terms of their relative acidity[282]. The extracellular pH (pH_e) in most tumors is more acidic (pH 6.5–7.2) than in normal tissues.[283-285] Hydrazone and acetal bonds between the drug and the micelles can be cleaved by acidic pH [87, 278, 281] therefore are of particular interest for creating such pH-sensitive carriers.

5.2 Experimental

5.2.1 Materials

Polyallylamine hydrochloride (PAH, M_w 17500), 2-methacryloyloxyethyl phosphorylcholine (MPC), 4-cyano-4-(phenylcarbonothioylthio) pentanoic acid (PTPA), 4,4′-azobis(4-cyanovaleric acid) (ACVA), 2,2-bis(aminoethoxy)propane, 1-ethyl-3-(3-dimethylaminopropyl)carbodiimide hydrochloride (EDC), N-hydroxysuccinimide (NHS), dithiobis(succinimidyl propionate) (DTSP), triethylamine, boric acid, sodium tetraborate, Sephadex G-75, Trizma® base, sodium phosphate monobasic monohydrate, sodium

phosphate dibasic, Dulbecco's modified Eagle's medium (DMEM), resazurin, bicinchoninic acid (BCA), tartaric acid, $CuSO_4$ were purchased from Sigma-Aldrich and were used as received. Fatal bovine serum (FBS) was purchased from Corning™. Murine macrophage cell line J774A.1 was purchased from ATCC.

5.2.2 Instruments

Particle size and zeta potential were measured with Zetasizer Nano-ZS (Malvern Instruments Ltd., UK). NMR spectrum was conducted on AV400 NMR spectrometer from Bruke Corporation. UV-Visible adsorption was acquired with a Beckman Coulter DU®730 UV/Vis Spectrophotometer. Fluorescence intensities were measured with a Tecan GENios Multifunction microplate reader. Carl Zeiss Axio Observer inverted fluorescence microscope.

5.2.3 Synthesis of PMPC by reversible addition fragmentation chain transfer (RAFT) polymerization

A mixed solution with monomer/CTA/initiator molar at a ratio of 20:1:0.2 was prepared by dissolving 0.148 g MPC, 7 mg PTPA and 1.4 mg ACVA in a mixture of 0.2 mL dimethylformamide (DMF) and 0.4 mL methanol. The solution was degassed by three freeze-pump-thaw cycle and purged with nitrogen to remove oxygen. The degassed solution was set at 60 °C for 6 hours and the resulted PMPC was diluted with 1 mL methanol and precipitated and washed with tetrahydrofuran (THF). The resulted PMPC has about 20 units per polymer chain as determined by H^1NMR spectrum.

5.2.4 Synthesis of PMPC conjugated PAH with acid liable linker (PAH-*de*-PMPC)

The activation of PMPC was done by EDC/NHS activation. Briefly, 0.1 g PMPC was dissolved in 1 mL methanol followed by adding 33 mg EDC (10x molar excess) and 2

mg NHS. The active PMPC-NHS ester was further reacted with 5x molar excess of ketal linker, 2,2-bis(aminoethoxy)propane (13mg). The resulted ketal-PMPC was purified by precipitation in THF to remove the excess 2,2-bis(aminoethoxy)propane, EDC and NHS. The purified ketal-PMPC was reacted with 5x molar excess of dithiobis(succinimidyl propionate) (DTSP) in methanol with triethylamine as acid binding agent. The resulted NHS ester of ketal-PMPC was further purified by precipitation in THF. Subsequent reaction with PAH resulted PMPC conjugated PAH (PAH-*de*-PMPC) which is detachable under acidic environment. The nondetachable PMPC conjugated PAH (PAH-*non*-PMPC) was also synthesized by direct reaction between PAH and PMPC-NHS.

5.2.5 Synthesis of PMPC grafting nanocapsules

BSA was dialyzed against 10 mM pH 8.0 phosphate buffer. Subsequently BSA was mixed with aqueous solution of PAH-*de*-PMPC at a molar ratio of 1:15 and self assembled to nanocomplexes. The nanocomplexes were further crosslinked by reaction with DTSP at a BSA/DTSP ratio of 1:100 to form *de*-nBSA. The nondetachable PAH-*non*-PMPC was also self-assembled with BSA and further crosslinked by DTSP to make *non*-nBSA.

5.2.6 BCA protein content quantification

Protein content in solution was determined by bicinchoninic acid (BCA) colorimetric protein assay. Briefly, a tartrate buffer (pH 11.25) containing 25 mM BCA, 3.2 nM $CuSO_4$, and appropriately diluted protein/nanocapsules was incubated at 60 °C for 30min. After the solution was cooled to room temperature, absorbance reading at 562 nm was determined with a UV-Vis spectrometer. BSA solutions with known concentration were used as standards.

5.2.7 DLS measurement

DLS experiments were performed with a Zetasizer Nano-ZS (Malvern Instruments Ltd., UK) equipped with a 10-mW helium-neon laser (λ = 632.8 nm) and thermoelectric temperature controller. Measurements were taken at 173° scattering angle. The *de*-nBSA was incubated both at pH 7.5 and pH 6.5 phosphate buffer respectively for 2 hours and zeta potential and size distribution were further measured at pH 7.5 at protein concentration of 0.5 mg/mL at 25 °C.

5.2.8 In vitro macrophage uptake

Cellular internalization studies were assessed via fluorescence microscopic technique. Murine macrophage J774A.1 were cultured in Dulbecco's modified Eagle's medium (DMEM) supplemented with 10% fatal bovine serum (FBS) and 1% penicillin/streptomycin. Cells (5000 cells/well, 96-well plate) were seeded the day before adding the nanocapsules. Native BSA, *de*-nBSA and *non*-nBSA were added into the cell medium with different pH at a final BSA concentration of 0.05 mg/ml. After incubation at 37 °C for 4 hours, the cells were washed three times with PBS and visualized with Carl Zeiss Axio Observer inverted fluorescence microscope.

5.3 Result and discussion

5.3.1 Synthesis of pH sensitive zwitterionic grafting nanocapsules

We synthesized the protein nanocapsule, which consist of a protein core and polymer shell with PMPC conjugated polyallylamine hydrochloride (PAH) through acid liable ketal linker (PAH-*de*-PMPC). As illustrated in Figure 5.1a, PMPC zwitterionic polymer was synthesized by reversal addition fragmentation transfer (RAFT) polymerization (Step I) using 2-methacryloyloxyethyl phosphorylcholine (MPC) as monomer, 4-cyano-4-

(phenylcarbonothioylthio) pentanoic acid as CTA and 4,4′-azobis(4-cyanovaleric acid) (ACVA) as initiator and the successful synthesis of PMPC with 20 units per polymer chain was verified by H^1NMR spectrum (Figure 5.2). The carboxyl group on the polymer end was further conjugated with 2,2-bis(aminoethoxy)propane through EDC/NHS reaction (Step II), and subsequently conjugated with PAH through dithiobis(succinimidyl propionate) (DTSP) (Step III and IV). Self-assembly of negative charged protein and positively charged SCP lead to the formation of protein nanocapsules (denoted as *de*-nProtein) (Step V) and further crosslinked by DTSP (Step VI). At physiological pH, the PMPC will form hydration layer to shield nanocapsule from opsonization and macrophage uptake. However, when pH drops to pH 6.5 or lower, the PMPC will be detached from the PAH backbone. The resulted positively charged nanocapsules could be internalized by cells. The nondetachable PAH-PMPC based nanocapsules were also synthesized and denoted as *non*-nProtein.

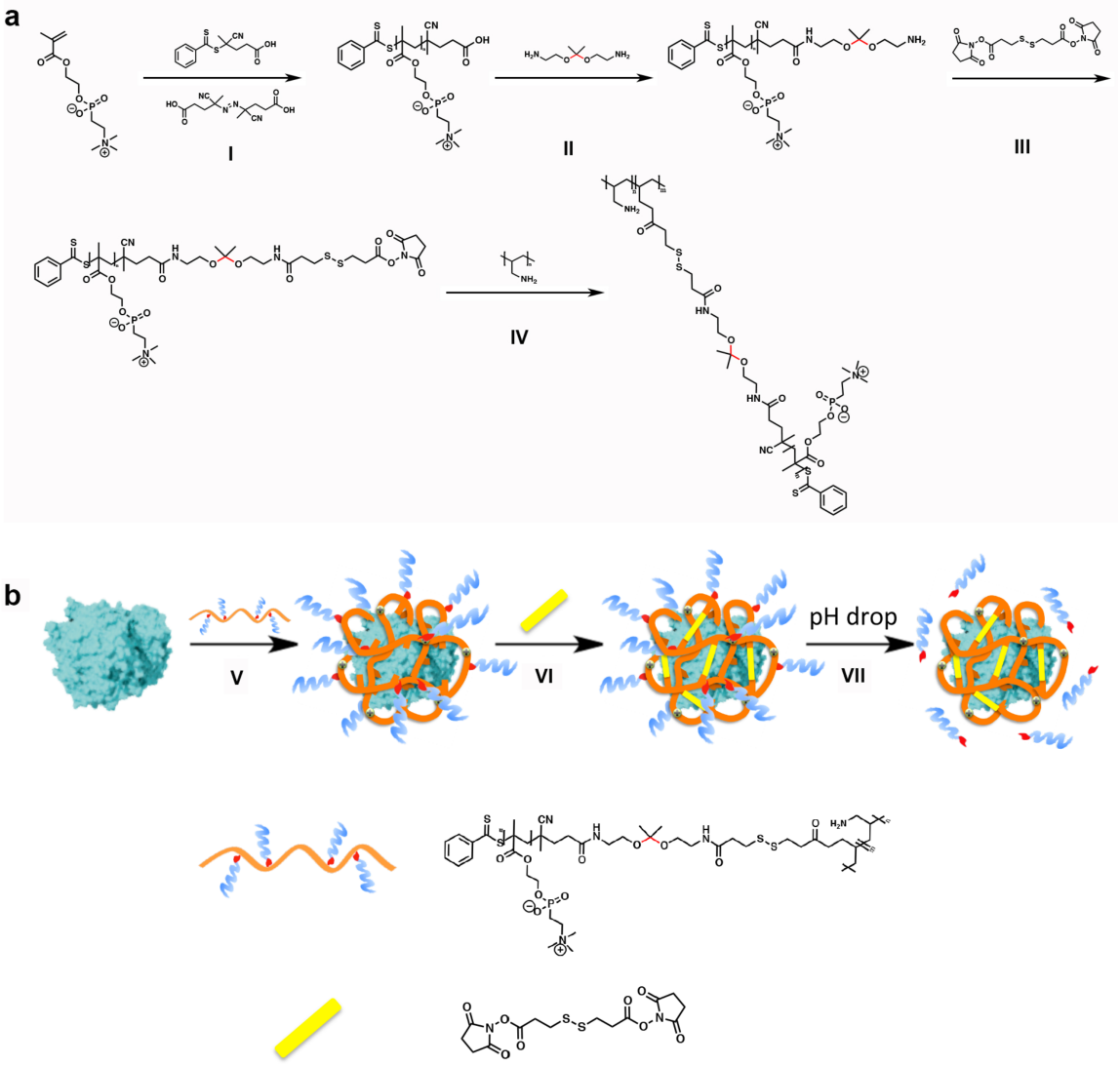

Figure 5.1 Scheme of synthesis of PAH-*de*-PMPC and subsequent synthesis of *de*-nProtein.

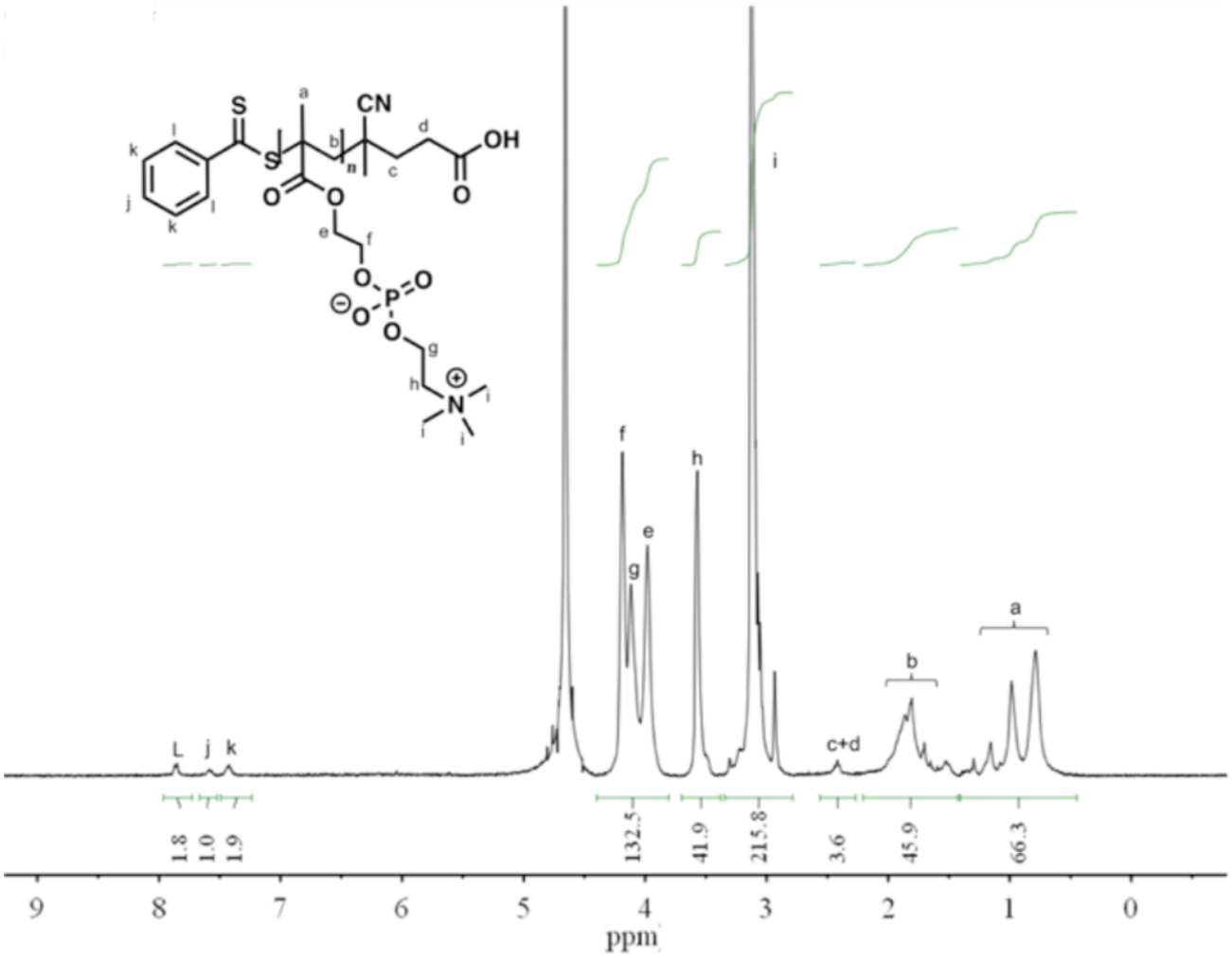

Figure 5.2 H[1]NMR spectrum of PMPC

5.3.2 Characterization of zwitterionic polymer grafted nanocapsules

Using bovine serum albumin (BSA) as a model protein, the successful synthesis of *de*-nBSA was characterized by zeta potential and DLS measurement. Figure 5.3 present the zeta potential distribution of *de*-nBSA. The zeta potential of the *de*-nBSA centered at 0 mV, significantly different from the native BSA (-7 mV), indicating that the successful shielding of charges on the nanocapsules due to PMPC attachment. However, after the *de*-nBSA was incubated at pH 6.5 for 2 hrs, the zeta potential shift to +7 mV, suggesting that the positive charge on the PAH backbone was exposed after the detachment of

PMPC. Consistent with zeta potential analysis, the size distribution measured by DLS (Figure 5.4) also confirms the uniform size of *de*-nBSA around 14 nm at pH 7.4, significantly different from that of the native BSA (5 nm). And after incubation at pH 6.5 for 2 hours, the size deceased to 12 nm, which can be attributed to the smaller hydraulic radius after the detachment of hydrophilic PMPC with large hydration layer. The formation of *de*-nBSA is further demonstrated by agarose gel analysis. As illustrated in Figure 5.5, both FITC labeled *non*-nBSA (2 and 3) and *de*-nBSA (4 and 5) shows retention in the well, which is significantly different from the FITC labeled native BSA bearing negative charge moving towards the positive electrode. After incubation at pH 6.5 for two hours (2 and 4), the *non*-nBSA didn't show charge change (2 and 3). Nevertheless, *de*-nBSA obviously gained positive charged, as significant movement towards negative electrode was shown. This further confirms the results of zeta potential analysis that PMPC shielding layer is detached from the nanocapsules. This pH sensitive property makes *de*-nProtein promising for targeted protein delivery towards more acidic tumor site.

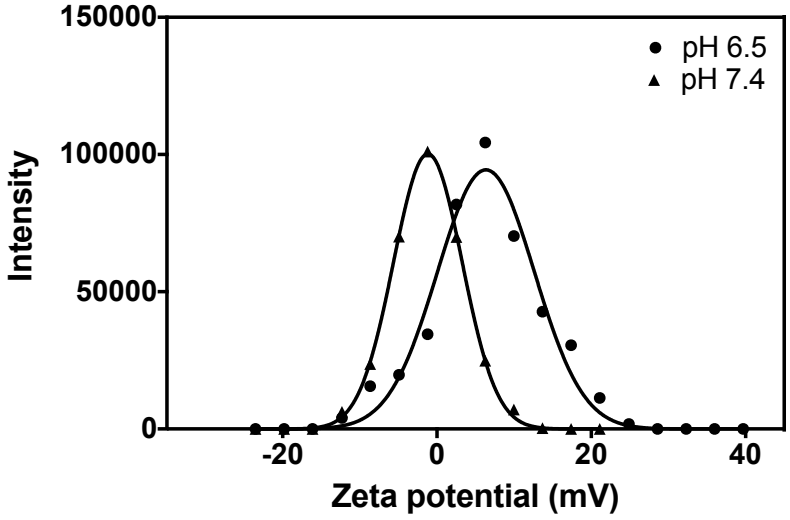

Figure 5.3 Zeta potential distribution of *de*-nBSA before and after incubation at pH

6.5 for 2 hours.

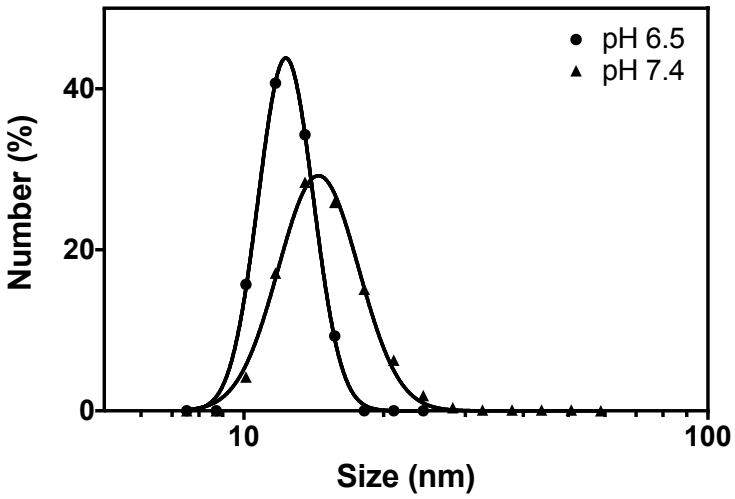

Figure 5.4 Size distribution of *de*-nBSA before and after incubation at pH 6.5 for 2 hours.

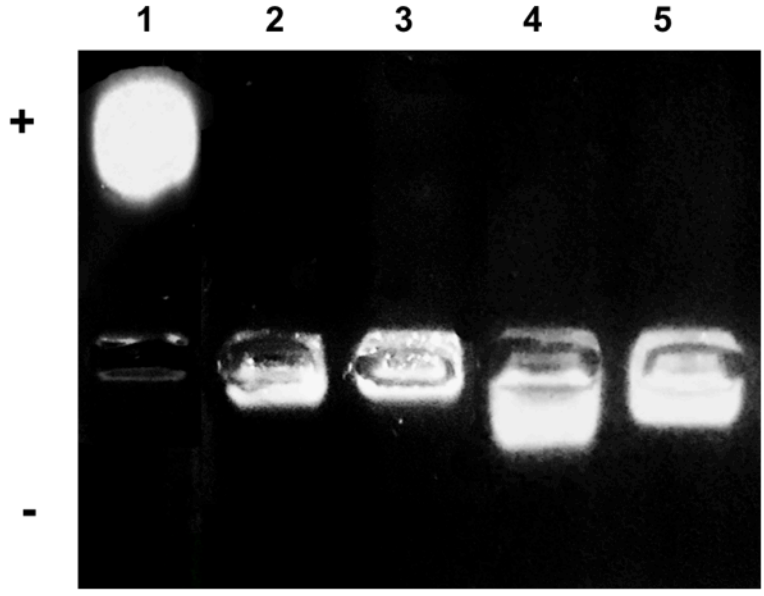

Figure 5.5 Agarose gel analysis of native BSA (1), *non*-nBSA after incubation at pH 6.5 (2), at pH 7.4 (3), *de*-nBSA after incubation at pH 6.5 (4) and at pH 7.4 (5).

5.2.3 Macrophage uptake

Nanoparticles can easily be opsonized in the blood circulation and uptake by macrophages in the liver and spleen before they can ever reach the targeted site. Thus, escape from opsonization and macrophage uptake is the most important issue for targeted delivery of proteins. Herein, we tested the macrophage escape capability using J774A.1 cell line, which is reticulum macrophage cell from ascites of BALB/cN mice. As is shown in Figure 5.6, FITC labeled native BSA shows similar moderate uptake by J774A.1 both under pH 6.5 and pH 7.4 after incubation with mouse serum (Figure 5.6 a and b). Nevertheless, macrophage uptake is significantly reduced when *non*-nBSA was incubated with macrophage and mouse serum both at pH 6.5 and pH 7.4 (Figure 5.6 e and f). This indicates the great shielding ability of PMPC hydration layer on the nanocapsule surface and the *non*-nProtein can be potentially applied for delivery of proteins which need long circulation, such as remove of uric acid or alcohol in the case of gout treatment or alcohol intoxication. On the other hand, *de*-nBSA also shows reduced macrophage uptake at pH 7.4 (Figure 5.6 d), but after incubated at pH 6.5 (Figure 5.6 c), significant macrophage uptake can be observed. This result further demonstrates the successful detachment of the PMPC side chains from the PAH backbones by acid liable ketal linker. The successful escape of macrophage uptake at physiological condition and detaching of PMPC upon exposed to acid environment can be very promising for protein delivery towards acidic tumor site.

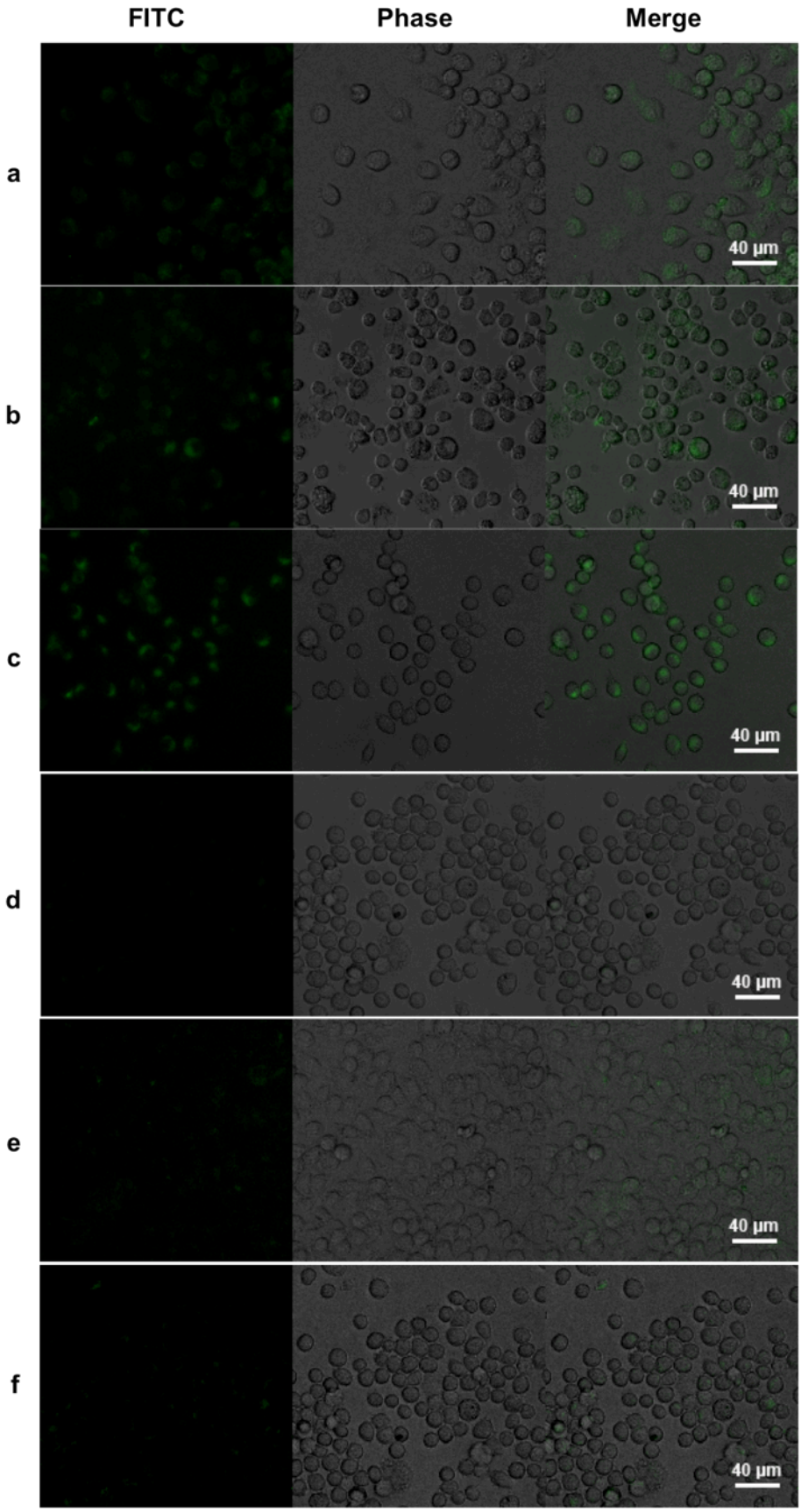
FITC
Phase
Merge
a
b
c
d
e
f
40 µm
40 µm
40 µm
40 µm
40 µm
40 µm

Figure 5.6 Native BSA incubated in a) pH 6.5 and b) pH 7.4 medium; *de*-nBSA incubated in c) pH 6.5 and d) pH 7.4 medium; *non*-nBSA incubated in e) pH 6.5 and d) pH 7.4 medium.

5.4 Summary

In conclusion, we have successfully synthesized the pH sensitive PMPC grafted polymer PMPC-*de*-PAH and nondetachable PMPC grafted polymer PMPC-*non*-PAH. We then made *de*-nBSA and *non*-nBSA by self assembly of BSA with PMPC-*de*-PAH and PMPC-*non*-PAH respectively and further crosslinked with DTSP. The *de*-nBSA shows pH-sensitive detachment of PMPC and was verified by DLS and agarose gel analysis. The detachment at acid environment was also demonstrated by macrophage uptake experiment, in which the *de*-nBSA can escape macrophage uptake at physiological condition but significantly internalized by macrophage at acid environment. This makes *de*-nProtein very promising for targeted protein delivery at tumor site by EPR effect with higher selectivity due to increased accumulation by prolonged circulation time at physiological pH. On the other hand, the *non*-nBSA can escape macrophage uptake at both physiological and low pH, which makes *non*-nProtein very promising to delivery proteins that require long circulation in the body, such as modulating metabolic disorder by eliminating harmful small molecule. Further research need to be conducted on active proteins for pH responsive delivery and both cancer cell lines and normal cell lines need to be tested to verify the effectiveness.

Chapter 6 Conclusions

As a summary, I have developed novel strategies for engineering protein carries for wide range of applications based on protein nanocapsules. This dissertation mainly explore the

design of nanocapsules both by *in-situ* polymerization and protein-polymer self-assembly and crosslinking. The nanocapsules by *in-situ* polymerization were further used as building blocks for novel enzyme composite design.

Nanocapsules by *in-situ* polymerization were applied to OPH for organophosphorus detoxification. This approach can enhance the activity of OPH by creating alkaline enzyme microenvironment preferred by OPH. The stability of native OPH can also be enhanced by the hydrophilic polymer shell. The OPH nanocapsules show excellent capability for decontamination in the environment and also as antidote for *in vivo* prophylactic.

This nanocapsule can be used as nanocomposite building block. The nOPH have been covalently conjugated with cellulose and show both excellent recycling stability and long-term storage stability. The nanocapsules can be further incorporated into mesoporous silica by direct sol-gel process. The activity of enzyme-silica composite can be manipulated by optimizing enzyme microenvironment via careful choosing both silica precursors and monomers. The activity of OPH and lipase composite can be several times higher than their native counterparts while the stability can be significantly increased not only compared with native proteins but also with their nanocapsule building blocks. This technique provides us new tools for engineering high performance enzyme composites.

Protein nanocapsules by *in-situ* polymerization many exhibit significant activity loss due to the first step acrylation on lysine of active site or second step free radicals. By designing self-assembling driven self-crosslinking polymer-protein nanocapsules, the activity of large amount of proteins including GOX, HRP, Cat, AOX and UOX can be retained to a great extent and the stability against proteases degradation is also improved.

More importantly, the nanocapsules were able to enhance cellular uptake and cargos can be release in the cytosol triggered by high GSH level. This technique provides us new potentials for engineering delicate proteins for protein therapeutics.

PEG dilemma is an important issue for targeted delivery. Since PEGylation can decrease the clearance of nanocarriers by the reticuloendothelial system (RES) but significantly comprise the cellular uptake at the target sites. Also, the PEG can cause undesired immunoresponse after repeated injection, resulting quick clearance. Using pH liable ketal linker, the zwitterionic polymer PMPC can be grafted onto the protein nanocapsules and exhibit pH sensitive detachment once exposed to acidic environment. This pH sensitive detachment has been verified by DLS and agarose gel analysis. This novel protein nanocapsules can escape macrophage uptake at physiological pH, but significantly internalized by macrophage at a lower pH of 6.5, which can be very for targeting acidic tumor microenvironment.

Overall, my research establishes several novel strategies for engineering protein carries for wide range of applications from enzyme composite synthesis to protein therapeutics development. Nanocapsules both by *in-situ* polymerization and polymer-protein self assembly and crosslinking serve as robust platforms to build protein carriers, which opens new doors to broaden the *in vitro* and *in vivo* application of proteins.

References

[1] B. Leader, Q.J. Baca, D.E. Golan, Protein therapeutics: a summary and pharmacological classification, Nat Rev Drug Discov, 7 (2008) 21-39.

[2] J. James, B.K. Simpson, M.R. Marshall, Application of enzymes in food processing, Critical Reviews in Food Science and Nutrition, 36 (1996) 437-463.

[3] J.B.v. Beilen, Z. Li, Enzyme technology: an overview, Curr. Opin. Biotechnol., 13 (2002) 338-344.

[4] L.R. Lynd, M.S. Laser, D. Bransby, B.E. Dale, B. Davison, R. Hamilton, M. Himmel, M. Keller, J.D. McMillan, J. Sheehan, C.E. Wyman, How biotech can transform biofuels, Nat Biotech, 26 (2008) 169-172.

[5] S.K. Ahuja, G.M. Ferreira, A.R. Moreira, Utilization of Enzymes for Environmental Applications, Critical Reviews in Biotechnology, 24 (2004) 125-154.

[6] K.E. LeJeune, A.J. Russell, Covalent binding of a nerve agent hydrolyzing enzyme within polyurethane foams, Biotechnol. Bioeng., 51 (1996) 450-457.

[7] F.M. Andreopoulos, M.J. Roberts, M.D. Bentley, J.M. Harris, E.J. Beckman, A.J. Russell, Photoimmobilization of organophosphorus hydrolase within a PEG-based hydrogel, Biotechnol. Bioeng., 65 (1999) 579-588.

[8] Y. Lee, I. Stanish, V. Rastogi, T.-c. Cheng, A. Singh, Sustained Enzyme Activity of Organophosphorus Hydrolase in Polymer Encased Multilayer Assemblies, Langmuir, 19 (2003) 1330-1336.

[9] M. Ramanathan, H.R. Luckarift, A. Sarsenova, J.R. Wild, E.K. Ramanculov, E.V. Olsen, A.L. Simonian, Lysozyme-mediated formation of protein‚Äìsilica nano-composites for biosensing applications, Colloids Surf., B, 73 (2009) 58-64.

[10] A. Mulchandani, W. Chen, P. Mulchandani, J. Wang, K.R. Rogers, Biosensors for direct determination of organophosphate pesticides, Biosens. Bioelectron., 16 (2001) 225-230.

[11] A.J. Patil, E. Muthusamy, S. Mann, Synthesis and Self-Assembly of Organoclay-Wrapped Biomolecules, Angewandte Chemie International Edition, 43 (2004) 4928-4933.

[12] V.A. Pedrosa, S. Paliwal, S. Balasubramanian, D. Nepal, V. Davis, J. Wild, E. Ramanculov, A. Simonian, Enhanced stability of enzyme organophosphate hydrolase interfaced on the carbon nanotubes, Colloids Surf., B, 77 (2010) 69-74.

[13] C. Krejsa, M. Rogge, W. Sadee, Protein therapeutics: new applications for pharmacogenetics, Nature Reviews Drug Discovery, 5 (2006) 507-521.

[14] A.L. Clark, G. Knight, P. Wiles, H. Keen, J. Ward, J. Cauldwell, R. Adeniyi-Jones, J. Leiper, R. Jones, A. Maccuish, Biosynthetic human insulin in the treatment of diabetes: a double-blind crossover trial in established diabetic patients, The Lancet, 320 (1982) 354-357.

[15] I.B. Hirsch, Insulin analogues, New England Journal of Medicine, 352 (2005) 174-183.

[16] A. Abuchowski, D. Karp, F.F. Davis, Reduction of plasma urate levels in the cockerel with polyethylene glycol-uricase, Journal of Pharmacology and Experimental Therapeutics, 219 (1981) 352-354.

[17] J.S. Bomalaski, M.A. Clark, Serum uric acid-lowering therapies: where are we heading in management of hyperuricemia and the potential role of uricase, Current rheumatology reports, 6 (2004) 240-247.

[18] J.S. Bomalaski, F.W. Holtsberg, C.M. Ensor, M.A. Clark, Uricase formulated with polyethylene glycol (uricase-PEG 20): biochemical rationale and preclinical studies, The Journal of rheumatology, 29 (2002) 1942-1949.

[19] P. Caliceti, F.M. Veronese, Pharmacokinetic and biodistribution properties of poly (ethylene glycol)–protein conjugates, Advanced drug delivery reviews, 55 (2003) 1261-1277.

[20] F. Fuertges, A. Abuchowski, The clinical efficacy of poly (ethylene glycol)-modified proteins, Journal of controlled release, 11 (1990) 139-148.

[21] K. Savoca, F. Davis, N. Palczuk, Induction of tolerance in mice by uricase and monomethoxypolyethylene glycol-modified uricase, International Archives of Allergy and Immunology, 75 (1984) 58-67.

[22] M.R. Sherman, M.G. Saifer, F. Perez-Ruiz, PEG-uricase in the management of treatment-resistant gout and hyperuricemia, Advanced drug delivery reviews, 60 (2008) 59-68.

[23] C.M. Ensor, M.A. Clark, F.W. Holtsberg, PEG-modified uricase, Google Patents, 2005.

[24] S. Davis, Y. Park, A. Abuchowski, F. Davis, Hypouricaemic effect of polyethyleneglycol modified urate oxidase, The Lancet, 318 (1981) 281-283.

[25] H. Nishimura, Y. Ashihara, A. Matsushima, Y. Inada, Modification of yeast uricase with polyethylene glycol: disappearance of binding ability towards anti-uricase serum, Enzyme, 24 (1978) 261-264.

[26] F.F. Davis, T. Van Es, N.C. Palczuk, Non-immunogenic polypeptides, Google Patents, 1979.

[27] S.J. Kelly, M. Delnomdedieu, M.I. Oliverio, L.D. WILLIAMS, M.G. SAIFER, M.R. SHERMAN, T.M. COFFMAN, G.A. JOHNSON, M.S. HERSHFIELD, Diabetes insipidus in uricase-deficient mice: a model for evaluating therapy with poly (ethylene glycol)-modified uricase, Journal of the American Society of Nephrology, 12 (2001) 1001-1009.

[28] M.R. Sherman, M.G. Saifer, L.D. Williams, M.S. Hershfield, S.J. Kelly, Aggregate-Free Urate Oxidase for Preparation of Non-Immunogenic Polymer Conjugates, Google Patents, 2011.

[29] L.D. Williams, M.S. Hershfield, S.J. Kelly, M.G. Saifer, M.R. Sherman, PEG-urate oxidase conjugates and use thereof, Google Patents, 2003.

[30] M.S. Hershfield, R.H. Buckley, M.L. Greenberg, A.L. Melton, R. Schiff, C. Hatem, J. Kurtzberg, M.L. Markert, R.H. Kobayashi, A.L. Kobayashi, Treatment of adenosine deaminase deficiency with polyethylene glycol–modified adenosine deaminase, New England Journal of Medicine, 316 (1987) 589-596.

[31] E.R. Stiehm, Immunologic disorders in infants and children, WB Saunders Co1989.

[32] M.S. Hershfield, PEG-ADA replacement therapy for adenosine deaminase deficiency: an update after 8.5 years, Clinical immunology and immunopathology, 76 (1995) S228-S232.

[33] S. Cohen, L. Moreland, J. Cush, M. Greenwald, S. Block, W. Shergy, P. Hanrahan, M. Khraishi, A. Patel, G. Sun, A multicenter double-blind randomized placebo-controlled trial of Kineret (R)(anakinra), a recombinant interleukin 1 receptor antagonist, in patients with rheumatoid arthritis treated with background methotrexate therapy, Ann Rheum Dis [Epub ahead of print], (2004).

[34] G. Heil, D. Hoelzer, M.A. Sanz, K. Lechner, J.A.L. Yin, G. Papa, L. Noens, J. Szer, A. Ganser, C. O'Brien, A randomized, double-blind, placebo-controlled, phase III study of filgrastim in remission induction and consolidation therapy for adults with de novo acute myeloid leukemia, Blood, 90 (1997) 4710-4718.

[35] H. Hurwitz, L. Fehrenbacher, W. Novotny, T. Cartwright, J. Hainsworth, W. Heim, J. Berlin, A. Baron, S. Griffing, E. Holmgren, Bevacizumab plus irinotecan, fluorouracil, and leucovorin for metastatic colorectal cancer, New England journal of medicine, 350 (2004) 2335-2342.

[36] M.P. Manns, J.G. McHutchison, S.C. Gordon, V.K. Rustgi, M. Shiffman, R. Reindollar, Z.D. Goodman, K. Koury, M.-H. Ling, J.K. Albrecht, Peginterferon alfa-2b plus ribavirin compared with interferon alfa-2b plus ribavirin for initial treatment of chronic hepatitis C: a randomised trial, The Lancet, 358 (2001) 958-965.

[37] Z. Wainberg, J.R. Hecht, A phase III randomized, open-label, controlled trial of chemotherapy and bevacizumab with or without panitumumab in the first-line treatment of patients with metastatic colorectal cancer, Clinical colorectal cancer, 5 (2006) 363-367.

[38] N. Sakuragawa, K. Shimizu, K. Kondo, S. Kondo, M. Niwa, Studies on the effect of PEG-modified urokinase on coagulation-fibrinolysis using beagles, Thrombosis research, 41 (1986) 627-635.

[39] J.-i. Kajihara, K. Shibata, Y. Nakano, S. Nishimuro, K. Kato, Physicochemical characterization of PEG-PPG conjugated human urokinase, Biochimica et Biophysica Acta (BBA)-General Subjects, 1199 (1994) 202-208.

[40] H. Tan, H. Jin, H. Mei, L. Zhu, W. Wei, Q. Wang, F. Liang, C. Zhang, J. Li, X. Qu, PEG-urokinase nanogels with enhanced stability and controllable bioactivity, Soft Matter, 8 (2012) 2644-2650.

[41] S. Pizzo, Preparation, in vivo properties and proposed clinical use of polyoxyethylene-modified tissue plasminogen activator and streptokinase, Advanced Drug Delivery Reviews, 6 (1991) 153-166.

[42] A. Koide, S. Suzuki, S. Kobayashi, Preparation of polyethylene glycol-modified streptokinase with disappearance of binding ability towards anti-serum and retention of activity, FEBS letters, 143 (1982) 73-76.

[43] F. Brucato, S. Pizzo, Catabolism of streptokinase and polyethylene glycol-streptokinase: evidence for transport of intact forms through the biliary system in the mouse, Blood, 76 (1990) 73-79.

[44] S. Rajagopalan, S.L. Gonias, S.V. Pizzo, A nonantigenic covalent streptokinase-polyethylene glycol complex with plasminogen activator function, Journal of Clinical Investigation, 75 (1985) 413.

[45] A. Gámez, C.N. Sarkissian, L. Wang, W. Kim, M. Straub, M.G. Patch, L. Chen, S. Striepeke, P. Fitzpatrick, J.F. Lemontt, Development of pegylated forms of recombinant Rhodosporidium toruloides phenylalanine ammonia-lyase for the treatment of classical phenylketonuria, Molecular Therapy, 11 (2005) 986-989.

[46] N. Longo, C.O. Harding, B.K. Burton, D.K. Grange, J. Vockley, M. Wasserstein, G.M. Rice, A. Dorenbaum, J.K. Neuenburg, D.G. Musson, Single-dose, subcutaneous recombinant phenylalanine ammonia lyase conjugated with polyethylene glycol in adult

patients with phenylketonuria: an open-label, multicentre, phase 1 dose-escalation trial, The Lancet, 384 (2014) 37-44.

[47] I. Petrikovics, M. Budai, S. Baskin, G. Rockwood, J. Childress, L. Budai, P. Grof, I. Klebovich, M. Szilasi, Characterization of liposomal vesicles encapsulating rhodanese for cyanide antagonism, Drug delivery, 16 (2009) 312-319.

[48] I. Petrikovics, P. Jayanna, J. Childress, M. Budai, S. Martin, G. Kuzmitcheva, G. Rockwood, Optimization of Liposomal Lipid Composition for a New, Reactive Sulfur Donor, and In Vivo Efficacy Studies on Mice to Antagonize Cyanide Intoxication, Journal of drug delivery, 2011 (2011).

[49] I. Petrikovics, T.-C. Cheng, D. Papahadjopoulos, K. Hong, R. Yin, J. DeFrank, J. Jaing, Z. Song, W. McGuinn, D. Sylvester, Long circulating liposomes encapsulating organophosphorus acid anhydrolase in diisopropylfluorophosphate antagonism, Toxicological Sciences, 57 (2000) 16-21.

[50] I. Petrikovics, W. McGuinn, D. Sylvester, P. Yuzapavik, J. Jiang, J. Way, D. Papahadjopoulos, K. Hong, R. Yin, T.-C. Cheng, In vitro studies on sterically stabilized liposomes (SL) as enzyme carriers in organophosphorus (OP) antagonism, Drug delivery, 7 (2000) 83-89.

[51] I. Petrikovics, K. Hong, G. Omburo, Q. Hu, L. Pei, W. McGuinn, D. Sylvester, C. Tamulinas, D. Papahadjopoulos, J. Jaszberenyi, Antagonism of paraoxon intoxication by recombinant phosphotriesterase encapsulated within sterically stabilized liposomes, Toxicology and applied pharmacology, 156 (1999) 56-63.

[52] M. Budai, P. Chapela, P. Gróf, A. Zimmer, M.E. Wales, J.R. Wild, I. Klebovich, I. Petrikovics, M. Szilasi, Physicochemical characterization of stealth liposomes encapsulating an organophosphate hydrolyzing enzyme, Journal of liposome research, 19 (2009) 163-168.

[53] Z.K. Han, Z.N. Liu, L. Yuan, P.S. Zhang, M. Zhao, Preparation of paraoxonase‐1 liposomes and studies on their in vivo pharmacokinetics in rats, Clinical and Experimental Pharmacology and Physiology, 41 (2014) 825-829.

[54] Y. Liu, J. Du, M. Yan, M.Y. Lau, J. Hu, H. Han, O.O. Yang, S. Liang, W. Wei, H. Wang, J. Li, X. Zhu, L. Shi, W. Chen, C. Ji, Y. Lu, Biomimetic enzyme nanocomplexes and their use as antidotes and preventive measures for alcohol intoxication, Nat Nano, 8 (2013) 187-192.

[55] J. Crosnier, P. Jungers, A.-M. Couroucé, A. Laplanche, E. Benhamou, F. Degos, B. Lacour, P. Prunet, Y. Cerisier, P. Guesry, Randomised placebo-controlled trial of hepatitis B surface antigen vaccine in French haemodialysis units: I, Medical staff, The Lancet, 317 (1981) 455-459.

[56] L.H. Sigal, J.M. Zahradnik, P. Lavin, S.J. Patella, G. Bryant, R. Haselby, E. Hilton, M. Kunkel, D. Adler-Klein, T. Doherty, A vaccine consisting of recombinant Borrelia burgdorferi outer-surface protein A to prevent Lyme disease, New England Journal of Medicine, 339 (1998) 216-222.

[57] I.Z. MacKenzie, J. Bichler, G.C. Mason, C.B. Lunan, P. Stewart, F. Al-Azzawi, M. De Bono, N. Watson, I. Andresen, Efficacy and safety of a new, chromatographically purified rhesus (D) immunoglobulin, European Journal of Obstetrics & Gynecology and Reproductive Biology, 117 (2004) 154-161.

[58] A. Campos-Neto, V. Rodrigues-Junior, D. Pedral-Sampaio, E. Netto, P. Ovendale, R. Coler, Y. Skeiky, R. Badaro, S. Reed, Evaluation of DPPD, a single recombinant Mycobacterium tuberculosis protein as an alternative antigen for the Mantoux test, Tuberculosis, 81 (2001) 353-358.

[59] R.T. Maguire, V.L. Pascucci, A.N. Maroli, J.V. Gulfo, Immunoscintigraphy in patients with colorectal, ovarian, and prostate cancer. Results with site‐specific immunoconjugates, Cancer, 72 (1993) 3453-3462.

[60] H.B. Urnovitz, J.C. Sturge, T.D. Gottfried, Increased sensitivity of HIV-1 antibody detection, Nature medicine, 3 (1997) 1258-1258.

[61] I.M. Verma, N. Somia, Gene therapy-promises, problems and prospects, Nature, 389 (1997) 239-242.

[62] M. Roberts, M. Bentley, J. Harris, Chemistry for peptide and protein PEGylation, Advanced drug delivery reviews, 64 (2012) 116-127.

[63] L.M. Graham, T.M. Nguyen, S.B. Lee, Nanodetoxification: emerging role of nanomaterials in drug intoxication treatment, Nanomedicine, 6 (2011) 921-928.

[64] V.P. Torchilin, Recent advances with liposomes as pharmaceutical carriers, Nature reviews Drug discovery, 4 (2005) 145-160.

[65] F. Schuber, A. Kichler, C. Boeckler, B. Frisch, Liposomes: from membrane models to gene therapy, Pure and applied chemistry, 70 (1998) 89-96.

[66] G.L. Scherphof, J. Dijkstra, H.H. Spanjer, J.T. Derksen, F.H. Roerdink, Uptake and Intracellular Processing of Targeted and Nontargeted Liposomes by Rat Kupffer Cells In Vivo and In Vitroa, Annals of the New York Academy of Sciences, 446 (1985) 368-384.

[67] V.P. Torchilin, Recent advances with liposomes as pharmaceutical carriers, Nat Rev Drug Discov, 4 (2005) 145-160.

[68] A.L. Klibanov, K. Maruyama, V.P. Torchilin, L. Huang, Amphipathic polyethyleneglycols effectively prolong the circulation time of liposomes, FEBS letters, 268 (1990) 235-237.

[69] Z.E. Suntres, Liposomal antioxidants for protection against oxidant-induced damage, Journal of toxicology, 2011 (2011).

[70] K. Whiteman, V. Subr, K. Ulbrich, V. Torchilin, Poly (HPMA)-coated liposomes demonstrate prolonged circulation in mice, Journal of Liposome Research, 11 (2001) 153-164.

[71] V. Torchilin, T. Levchenko, K. Whiteman, A. Yaroslavov, A. Tsatsakis, A. Rizos, E. Michailova, M. Shtilman, Amphiphilic poly-N-vinylpyrrolidones:: synthesis, properties and liposome surface modification, Biomaterials, 22 (2001) 3035-3044.

[72] J.M. Metselaar, P. Bruin, L.W. de Boer, T. de Vringer, C. Snel, C. Oussoren, M.H. Wauben, D.J. Crommelin, G. Storm, W.E. Hennink, A novel family of L-amino acid-based biodegradable polymer-lipid conjugates for the development of long-circulating liposomes with effective drug-targeting capacity, Bioconjugate chemistry, 14 (2003) 1156-1164.

[73] H. Takeuchi, H. Kojima, H. Yamamoto, Y. Kawashima, Evaluation of circulation profiles of liposomes coated with hydrophilic polymers having different molecular weights in rats, J. Controlled Release, 75 (2001) 83-91.

[74] O. Zelphati, Y. Wang, S. Kitada, J.C. Reed, P.L. Felgner, J. Corbeil, Intracellular Delivery of Proteins with a New Lipid-mediated Delivery System, Journal of Biological Chemistry, 276 (2001) 35103-35110.

[75] D. Dalkara, G. Zuber, J.-P. Behr, Intracytoplasmic Delivery of Anionic Proteins[ast], Mol Ther, 9 (2004) 964-969.

[76] Q. Tan, N. Wang, H. Yang, L. Chen, H. Xiong, L. Zhang, J. Liu, C. Zhao, J. Zhang, Preparation and characterization of lipid vesicles containing uricase, Drug delivery, 17 (2010) 28-37.

[77] Q. Tan, N. Wang, H. Yang, L. Zhang, S. Liu, L. Chen, J. Liu, L. Zhang, N. Hu, C. Zhao, Characterization, stabilization and activity of uricase loaded in lipid vesicles, International journal of pharmaceutics, 384 (2010) 165-172.

[78] M. Gaspar, R. Perez-Soler, M. Cruz, Biological characterization of L-asparaginase liposomal formulations, Cancer chemotherapy and pharmacology, 38 (1996) 373-377.

[79] J.C. Jorge, R. Perez-Soler, J.G. Morais, M.E.M. Cruz, Liposomal palmitoyl-L-asparaginase: characterization and biological activity, Cancer chemotherapy and pharmacology, 34 (1994) 230-234.

[80] V.P. Torchilin, R. Rammohan, V. Weissig, T.S. Levchenko, TAT peptide on the surface of liposomes affords their efficient intracellular delivery even at low temperature and in the presence of metabolic inhibitors, Proceedings of the National Academy of Sciences, 98 (2001) 8786-8791.

[81] M. Furuhata, H. Kawakami, K. Toma, Y. Hattori, Y. Maitani, Intracellular delivery of proteins in complexes with oligoarginine-modified liposomes and the effect of oligoarginine length, Bioconjugate chemistry, 17 (2006) 935-942.

[82] J. Park, D. Kirpotin, K. Hong, R. Shalaby, Y. Shao, U. Nielsen, J. Marks, D. Papahadjopoulos, C. Benz, Tumor targeting using anti-her2 immunoliposomes, Journal of Controlled Release, 74 (2001) 95-113.

[83] K.F. Pirollo, A. Rait, Q. Zhou, X.-q. Zhang, J. Zhou, C.-S. Kim, W.F. Benedict, E.H. Chang, Tumor-targeting nanocomplex delivery of novel tumor suppressor RB94 chemosensitizes bladder carcinoma cells in vitro and in vivo, Clinical Cancer Research, 14 (2008) 2190-2198.

[84] P. Sapra, T.M. Allen, Internalizing antibodies are necessary for improved therapeutic efficacy of antibody-targeted liposomal drugs, Cancer Research, 62 (2002) 7190-7194.

[85] R.J. Lee, P.S. Low, Delivery of liposomes into cultured KB cells via folate receptor-mediated endocytosis, Journal of Biological Chemistry, 269 (1994) 3198-3204.

[86] C.C. Visser, S. Stevanović, L.H. Voorwinden, L. van Bloois, P.J. Gaillard, M. Danhof, D.J. Crommelin, A.G. de Boer, Targeting liposomes with protein drugs to the blood–brain barrier in vitro, European journal of pharmaceutical sciences, 25 (2005) 299-305.

[87] R.M. Sawant, J.P. Hurley, S. Salmaso, A. Kale, E. Tolcheva, T.S. Levchenko, V.P. Torchilin, "SMART" Drug Delivery Systems: Double-Targeted pH-Responsive Pharmaceutical Nanocarriers, Bioconjugate Chemistry, 17 (2006) 943-949.

[88] M.A. Gauthier, H.-A. Klok, Polymer–protein conjugates: an enzymatic activity perspective, Polymer Chemistry, 1 (2010) 1352-1373.

[89] F.M. Veronese, G. Pasut, PEGylation, successful approach to drug delivery, Drug discovery today, 10 (2005) 1451-1458.

[90] S. Jevševar, M. Kunstelj, V.G. Porekar, PEGylation of therapeutic proteins, Biotechnology journal, 5 (2010) 113-128.

[91] D.P. Humphreys, S.P. Heywood, A. Henry, L. Ait-Lhadj, P. Antoniw, R. Palframan, K.J. Greenslade, B. Carrington, D.G. Reeks, L.C. Bowering, Alternative antibody Fab′ fragment PEGylation strategies: combination of strong reducing agents, disruption of the

interchain disulphide bond and disulphide engineering, Protein Engineering Design and Selection, 20 (2007) 227-234.

[92] O. Kinstler, G. Molineux, M. Treuheit, D. Ladd, C. Gegg, Mono-N-terminal poly (ethylene glycol)–protein conjugates, Advanced drug delivery reviews, 54 (2002) 477-485.

[93] F.M. Veronese, A. Mero, F. Caboi, M. Sergi, C. Marongiu, G. Pasut, Site-specific pegylation of G-CSF by reversible denaturation, Bioconjugate chemistry, 18 (2007) 1824-1830.

[94] S. DeFrees, Z.-G. Wang, R. Xing, A.E. Scott, J. Wang, D. Zopf, D.L. Gouty, E.R. Sjoberg, K. Panneerselvam, E.C. Brinkman-Van der Linden, GlycoPEGylation of recombinant therapeutic proteins produced in Escherichia coli, Glycobiology, 16 (2006) 833-843.

[95] B. Mojtaba, K. Maryam, D.U. Larry, Poly(ethylene glycol) and Poly(carboxy betaine) Based Nonfouling Architectures: Review and Current Efforts, Proteins at Interfaces III State of the Art, American Chemical Society2012, pp. 621-643.

[96] F.M. Veronese, P. Caliceti, O. Schiavon, Branched and linear poly (ethylene glycol): influence of the polymer structure on enzymological, pharmacokinetic, and immunological properties of protein conjugates, Journal of bioactive and compatible polymers, 12 (1997) 196-207.

[97] C.S. Fishburn, The pharmacology of PEGylation: balancing PD with PK to generate novel therapeutics, Journal of pharmaceutical sciences, 97 (2008) 4167-4183.

[98] M. Hamidi, P. Rafiei, A. Azadi, Designing PEGylated therapeutic molecules: advantages in ADMET properties, (2008).

[99] M. Vellard, The enzyme as drug: application of enzymes as pharmaceuticals, Curr. Opin. Biotechnol., 14 (2003) 444-450.

[100] A. Aiuti, Advances in gene therapy for ADA-deficient SCID, Current opinion in molecular therapeutics, 4 (2002) 515-522.

[101] P.A. Dinndorf, J. Gootenberg, M.H. Cohen, P. Keegan, R. Pazdur, FDA drug approval summary: pegaspargase (Oncaspar®) for the first-line treatment of children with acute lymphoblastic leukemia (ALL), The oncologist, 12 (2007) 991-998.

[102] N. Schlesinger, U. Yasothan, P. Kirkpatrick, Pegloticase, Nature Reviews Drug Discovery, 10 (2011) 17-18.

[103] C.M. Ensor, F.W. Holtsberg, J.S. Bomalaski, M.A. Clark, Pegylated arginine deiminase (ADI-SS PEG20, 000 mw) inhibits human melanomas and hepatocellular carcinomas in vitro and in vivo, Cancer research, 62 (2002) 5443-5450.

[104] N.J. Ganson, S.J. Kelly, E. Scarlett, J.S. Sundy, M.S. Hershfield, Control of hyperuricemia in subjects with refractory gout, and induction of antibody against poly (ethylene glycol)(PEG), in a phase I trial of subcutaneous PEGylated urate oxidase, Arthritis research & therapy, 8 (2005) R12.

[105] D. Nevozhay, R. Budzynska, U. Kanska, M. Jagiello, M.S. Omar, J. Boratynski, A. Opolski, Antitumor properties and toxicity of dextran-methotrexate conjugates are dependent on the molecular weight of the carrier, Anticancer Res., 26 (2006) 1135-1143.

[106] F. Haaf, A. Sanner, F. Straub, Polymers of N-vinylpyrrolidone: synthesis, characterization and uses, Polymer Journal, 17 (1985) 143-152.

[107] H.A. Ravin, A.M. Seligman, J. Fine, Polyvinyl pyrrolidone as a plasma expander: Studies on its excretion, distribution and metabolism, New England Journal of Medicine, 247 (1952) 921-929.

[108] C. Monfardini, F.M. Veronese, Stabilization of Substances in Circulation, Bioconjugate Chem., 9 (1998) 418-450.

[109] R. Mehvar, Dextrans for targeted and sustained delivery of therapeutic and imaging agents, J. Controlled Release, 69 (2000) 1-25.

[110] T.E. Wileman, R.L. Foster, P.N. Elliott, Soluble asparaginase‐dextran conjugates show increased circulatory persistence and lowered antigen reactivity, Journal of pharmacy and pharmacology, 38 (1986) 264-271.

[111] Y. Yasuda, T. Fujita, Y. Takakura, M. Hashida, H. Sezaki, Biochemical and biopharmaceutical properties of macromolecular conjugates of uricase with dextran and polyethylene glycol, Chem. Pharm. Bull, 38 (1990) 2053-2056.

[112] R. Melton, C. Wiblin, R. Foster, R. Sherwood, Covalent linkage of carboxypeptidase G 2 to soluble dextrans—I: Properties of conjugates and effects on plasma persistence in mice, Biochemical pharmacology, 36 (1987) 105-112.

[113] C.E. Zinderman, L. Landow, R.P. Wise, Anaphylactoid reactions to Dextran 40 and 70: reports to the United States Food and Drug Administration, 1969 to 2004, Journal of vascular surgery, 43 (2006) 1004-1009.

[114] P. Caliceti, O. Schiavon, M. Morpurgo, F.M. Veronese, L. Sartore, E. Ranucci, P. Ferruti, Physico-chemical and biological properties of monofunctional hydroxy

teriminating poly (N-vinylpyrrolidone) conjugated superoxide dismutase, Journal of bioactive and compatible polymers, 10 (1995) 103-120.

[115] P. Caliceti, O. Schiavon, F.M. Veronese, Immunological properties of uricase conjugated to neutral soluble polymers, Bioconjugate Chem., 12 (2001) 515-522.

[116] Z. Ahmad, A. Shah, M. Siddiq, H.-B. Kraatz, Polymeric micelles as drug delivery vehicles, RSC Advances, 4 (2014) 17028-17038.

[117] R. Savić, L. Luo, A. Eisenberg, D. Maysinger, Micellar Nanocontainers Distribute to Defined Cytoplasmic Organelles, Science, 300 (2003) 615-618.

[118] N. Suthiwangcharoen, R. Nagarajan, Enhancing Enzyme Stability by Construction of Polymer–Enzyme Conjugate Micelles for Decontamination of Organophosphate Agents, Biomacromolecules, 15 (2014) 1142-1152.

[119] X. Yi, M.C. Zimmerman, R. Yang, J. Tong, S. Vinogradov, A.V. Kabanov, Pluronic-modified superoxide dismutase 1 attenuates angiotensin II-induced increase in intracellular superoxide in neurons, Free Radical Biology and Medicine, 49 (2010) 548-558.

[120] R. Scavenging, Superoxide Dismutase/Catalase Mimetics by the Use of an Oxidation-Sensitive Nanocarrier/Enzyme Conjugate Hu, Ping; Tirelli, Nicola, Bioconjugate Chemistry, 23 (2012) 438-449.

[121] J. Futami, M. Kitazoe, T. Maeda, E. Nukui, M. Sakaguchi, J. Kosaka, M. Miyazaki, M. Kosaka, H. Tada, M. Seno, J. Sasaki, N.-H. Huh, M. Namba, H. Yamada, Intracellular delivery of proteins into mammalian living cells by polyethylenimine-cationization, Journal of Bioscience and Bioengineering, 99 (2005) 95-103.

[122] M. Kitazoe, J. Futami, M. Nishikawa, H. Yamada, Y. Maeda, Polyethylenimine-cationized β-catenin protein transduction activates the Wnt canonical signaling pathway more effectively than cationic lipid-based transduction, Biotechnology Journal, 5 (2010) 385-392.

[123] J. Du, J. Jin, M. Yan, Y. Lu, Synthetic nanocarriers for intracellular protein delivery, Current drug metabolism, 13 (2012) 82-92.

[124] H. Murata, M. Sakaguchi, J. Futami, M. Kitazoe, T. Maeda, H. Doura, M. Kosaka, H. Tada, M. Seno, N.-h. Huh, H. Yamada, Denatured and Reversibly Cationized p53 Readily Enters Cells and Simultaneously Folds to the Functional Protein in the Cells†, Biochemistry, 45 (2006) 6124-6132.

[125] S.H. Kim, J.H. Jeong, C.O. Joe, T.G. Park, Folate receptor mediated intracellular protein delivery using PLL–PEG–FOL conjugate, Journal of controlled release, 103 (2005) 625-634.

[126] Y. Lee, S. Fukushima, Y. Bae, S. Hiki, T. Ishii, K. Kataoka, A Protein Nanocarrier from Charge-Conversion Polymer in Response to Endosomal pH, Journal of the American Chemical Society, 129 (2007) 5362-5363.

[127] Y. Lee, T. Ishii, H. Cabral, H.J. Kim, J.H. Seo, N. Nishiyama, H. Oshima, K. Osada, K. Kataoka, Charge‐Conversional Polyionic Complex Micelles—Efficient Nanocarriers for Protein Delivery into Cytoplasm, Angewandte Chemie, 121 (2009) 5413-5416.

[128] H. Ayame, N. Morimoto, K. Akiyoshi, Self-Assembled Cationic Nanogels for Intracellular Protein Delivery, Bioconjugate Chemistry, 19 (2008) 882-890.

[129] H. Murata, J. Futami, M. Kitazoe, T. Yonehara, H. Nakanishi, M. Kosaka, H. Tada, M. Sakaguchi, Y. Yagi, M. Seno, N.-h. Huh, H. Yamada, Intracellular Delivery of Glutathione S-transferase-fused Proteins into Mammalian Cells by Polyethylenimine–Glutathione Conjugates, Journal of Biochemistry, 144 (2008) 447-455.

[130] D. Dalkara, C. Chandrashekhar, G. Zuber, Intracellular protein delivery with a dimerizable amphiphile for improved complex stability and prolonged protein release in the cytoplasm of adherent cell lines, Journal of Controlled Release, 116 (2006) 353-359.

[131] J. Mandeville, H. Tajmir-Riahi, Complexes of dendrimers with bovine serum albumin, Biomacromolecules, 11 (2010) 465-472.

[132] M. De, P.S. Ghosh, V.M. Rotello, Applications of nanoparticles in biology, Advanced Materials, 20 (2008) 4225-4241.

[133] P. Nativo, I.A. Prior, M. Brust, Uptake and intracellular fate of surface-modified gold nanoparticles, ACS nano, 2 (2008) 1639-1644.

[134] A. Verma, O. Uzun, Y. Hu, Y. Hu, H.-S. Han, N. Watson, S. Chen, D.J. Irvine, F. Stellacci, Surface-structure-regulated cell-membrane penetration by monolayer-protected nanoparticles, Nature materials, 7 (2008) 588-595.

[135] S. Pujals, N.G. Bastús, E. Pereiro, C. López‐Iglesias, V.F. Puntes, M.J. Kogan, E. Giralt, Shuttling Gold Nanoparticles into Tumoral Cells with an Amphipathic Proline‐Rich Peptide, Chembiochem, 10 (2009) 1025-1031.

[136] P. Ghosh, G. Han, M. De, C.K. Kim, V.M. Rotello, Gold nanoparticles in delivery applications, Advanced drug delivery reviews, 60 (2008) 1307-1315.

[137] A.C. Templeton, W.P. Wuelfing, R.W. Murray, Monolayer-protected cluster molecules, Accounts of Chemical Research, 33 (2000) 27-36.

[138] G. Schmid, Large clusters and colloids. Metals in the embryonic state, Chemical Reviews, 92 (1992) 1709-1727.

[139] A.G. Tkachenko, H. Xie, Y. Liu, D. Coleman, J. Ryan, W.R. Glomm, M.K. Shipton, S. Franzen, D.L. Feldheim, Cellular trajectories of peptide-modified gold particle complexes: comparison of nuclear localization signals and peptide transduction domains, Bioconjugate chemistry, 15 (2004) 482-490.

[140] P. Ghosh, X. Yang, R. Arvizo, Z.-J. Zhu, S.S. Agasti, Z. Mo, V.M. Rotello, Intracellular delivery of a membrane-impermeable enzyme in active form using functionalized gold nanoparticles, Journal of the American Chemical Society, 132 (2010) 2642-2645.

[141] P. Yang, Z. Quan, L. Lu, S. Huang, J. Lin, Luminescence functionalization of mesoporous silica with different morphologies and applications as drug delivery systems, Biomaterials, 29 (2008) 692-702.

[142] Y. Zhu, J. Shi, W. Shen, X. Dong, J. Feng, M. Ruan, Y. Li, Stimuli‐Responsive Controlled Drug Release from a Hollow Mesoporous Silica Sphere/Polyelectrolyte Multilayer Core‐Shell Structure, Angewandte Chemie, 117 (2005) 5213-5217.

[143] I. Slowing, B.G. Trewyn, V.S.-Y. Lin, Effect of surface functionalization of MCM-41-type mesoporous silica nanoparticles on the endocytosis by human cancer cells, Journal of the American Chemical Society, 128 (2006) 14792-14793.

[144] J.L. Vivero-Escoto, I.I. Slowing, C.-W. Wu, V.S.-Y. Lin, Photoinduced intracellular controlled release drug delivery in human cells by gold-capped mesoporous silica nanosphere, Journal of the American Chemical Society, 131 (2009) 3462-3463.

[145] I.I. Slowing, B.G. Trewyn, V.S.-Y. Lin, Mesoporous silica nanoparticles for intracellular delivery of membrane-impermeable proteins, Journal of the American Chemical Society, 129 (2007) 8845-8849.

[146] C.R. Martin, P. Kohli, The emerging field of nanotube biotechnology, Nature Reviews Drug Discovery, 2 (2003) 29-37.

[147] N.W. Shi Kam, T.C. Jessop, P.A. Wender, H. Dai, Nanotube molecular transporters: internalization of carbon nanotube-protein conjugates into mammalian cells, Journal of the American Chemical Society, 126 (2004) 6850-6851.

[148] N.W.S. Kam, H. Dai, Carbon nanotubes as intracellular protein transporters: generality and biological functionality, Journal of the American Chemical Society, 127 (2005) 6021-6026.

[149] A. Bianco, J. Hoebeke, S. Godefroy, O. Chaloin, D. Pantarotto, J.-P. Briand, S. Muller, M. Prato, C.D. Partidos, Cationic carbon nanotubes bind to CpG oligodeoxynucleotides and enhance their immunostimulatory properties, Journal of the American Chemical Society, 127 (2005) 58-59.

[150] D. Pantarotto, J.-P. Briand, M. Prato, A. Bianco, Translocation of bioactive peptides across cell membranes by carbon nanotubes, Chemical Communications, (2004) 16-17.

[151] D. Pantarotto, R. Singh, D. McCarthy, M. Erhardt, J.P. Briand, M. Prato, K. Kostarelos, A. Bianco, Functionalized carbon nanotubes for plasmid DNA gene delivery, Angewandte Chemie, 116 (2004) 5354-5358.

[152] N.W.S. Kam, M. O'Connell, J.A. Wisdom, H. Dai, Carbon nanotubes as multifunctional biological transporters and near-infrared agents for selective cancer cell destruction, Proceedings of the National Academy of Sciences of the United States of America, 102 (2005) 11600-11605.

[153] Q. Lu, J.M. Moore, G. Huang, A.S. Mount, A.M. Rao, L.L. Larcom, P.C. Ke, RNA polymer translocation with single-walled carbon nanotubes, Nano Letters, 4 (2004) 2473-2477.

[154] N.W.S. Kam, Z. Liu, H. Dai, Functionalization of carbon nanotubes via cleavable disulfide bonds for efficient intracellular delivery of siRNA and potent gene silencing, Journal of the American Chemical Society, 127 (2005) 12492-12493.

[155] Y. Lu, W. Sun, Z. Gu, Stimuli-responsive nanomaterials for therapeutic protein delivery, Journal of Controlled Release, 194 (2014) 1-19.

[156] T. Jiang, R. Mo, A. Bellotti, J. Zhou, Z. Gu, Gel‐Liposome‐Mediated Co‐Delivery of Anticancer Membrane‐Associated Proteins and Small‐Molecule Drugs for Enhanced Therapeutic Efficacy, Advanced Functional Materials, 24 (2014) 2295-2304.

[157] S. Mura, J. Nicolas, P. Couvreur, Stimuli-responsive nanocarriers for drug delivery, Nat Mater, 12 (2013) 991-1003.

[158] Z. Deng, Z. Zhen, X. Hu, S. Wu, Z. Xu, P.K. Chu, Hollow chitosan–silica nanospheres as pH-sensitive targeted delivery carriers in breast cancer therapy, Biomaterials, 32 (2011) 4976-4986.

[159] G.H. Gao, M.J. Park, Y. Li, G.H. Im, J.-H. Kim, H.N. Kim, J.W. Lee, P. Jeon, O.Y. Bang, J.H. Lee, The use of pH-sensitive positively charged polymeric micelles for protein delivery, Biomaterials, 33 (2012) 9157-9164.

[160] J.-Z. Du, X.-J. Du, C.-Q. Mao, J. Wang, Tailor-made dual pH-sensitive polymer–doxorubicin nanoparticles for efficient anticancer drug delivery, Journal of the American Chemical Society, 133 (2011) 17560-17563.

[161] Y. Du, W. Chen, M. Zheng, F. Meng, Z. Zhong, pH-sensitive degradable chimaeric polymersomes for the intracellular release of doxorubicin hydrochloride, Biomaterials, 33 (2012) 7291-7299.

[162] Y. Jin, L. Song, Y. Su, L. Zhu, Y. Pang, F. Qiu, G. Tong, D. Yan, B. Zhu, X. Zhu, Oxime linkage: a robust tool for the design of pH-sensitive polymeric drug carriers, Biomacromolecules, 12 (2011) 3460-3468.

[163] S. Zhu, D.S. Lansakara-P, X. Li, Z. Cui, Lysosomal delivery of a lipophilic gemcitabine prodrug using novel acid-sensitive micelles improved its antitumor activity, Bioconjugate chemistry, 23 (2012) 966-980.

[164] J. Heller, A. Chang, G. Rood, G. Grodsky, Release of insulin from pH-sensitive poly (ortho esters), Journal of Controlled Release, 13 (1990) 295-302.

[165] Y. Lee, T. Ishii, H.J. Kim, N. Nishiyama, Y. Hayakawa, K. Itaka, K. Kataoka, Efficient delivery of bioactive antibodies into the cytoplasm of living cells by charge‐conversional polyion complex micelles, Angewandte Chemie, 122 (2010) 2606-2609.

[166] Y. Hu, P.U. Atukorale, J.J. Lu, J.J. Moon, S.H. Um, E.C. Cho, Y. Wang, J. Chen, D.J. Irvine, Cytosolic Delivery Mediated via Electrostatic Surface Binding of Protein, Virus, or siRNA Cargos to pH-Responsive Core− Shell Gel Particles, Biomacromolecules, 10 (2009) 756-765.

[167] X. Wu, S. Wu, L. Yang, J. Han, S. Han, Cytosolic delivery of proteins mediated by aldehyde-displaying silica nanoparticles with pH-responsive characteristics, Journal of Materials Chemistry, 22 (2012) 17121-17127.

[168] X. Gu, J. Wang, Y. Wang, Y. Wang, H. Gao, G. Wu, Layer-by-layer assembled polyaspartamide nanocapsules for pH-responsive protein delivery, Colloids and Surfaces B: Biointerfaces, 108 (2013) 205-211.

[169] R. Cheng, F. Feng, F. Meng, C. Deng, J. Feijen, Z. Zhong, Glutathione-responsive nano-vehicles as a promising platform for targeted intracellular drug and gene delivery, J. Controlled Release, 152 (2011) 2-12.

[170] D.H. Nguyen, J.H. Choi, Y.K. Joung, K.D. Park, Disulfide-crosslinked heparin-pluronic nanogels as a redox-sensitive nanocarrier for intracellular protein delivery, Journal of Bioactive and Compatible Polymers, 26 (2011) 287-300.

[171] M. Zhao, A. Biswas, B. Hu, K.I. Joo, P. Wang, Z. Gu, Y. Tang, Redox-responsive nanocapsules for intracellular protein delivery, Biomaterials, 32 (2011) 5223-5230.

[172] M. Zhao, B. Hu, Z. Gu, K.I. Joo, P. Wang, Y. Tang, Degradable polymeric nanocapsule for efficient intracellular delivery of a high molecular weight tumor-selective protein complex, Nano Today, 8 (2013) 11-20.

[173] C. Zheng, X.G. Zhang, L. Sun, Z.P. Zhang, C.X. Li, Biodegradable and redox-responsive chitosan/poly(l-aspartic acid) submicron capsules for transmucosal delivery of proteins and peptides, J Mater Sci: Mater Med, 24 (2013) 931-939.

[174] D.-S. Guo, K. Wang, Y.-X. Wang, Y. Liu, Cholinesterase-responsive supramolecular vesicle, Journal of the American Chemical Society, 134 (2012) 10244-10250.

[175] A. Biswas, K.-I. Joo, J. Liu, M. Zhao, G. Fan, P. Wang, Z. Gu, Y. Tang, Endoprotease-mediated intracellular protein delivery using nanocapsules, ACS nano, 5 (2011) 1385-1394.

[176] J. Wen, S.M. Anderson, J. Du, M. Yan, J. Wang, M. Shen, Y. Lu, T. Segura, Controlled Protein Delivery Based on Enzyme-Responsive Nanocapsules, Advanced Materials, 23 (2011) 4549-4553.

[177] T. Shiomi, V. Lemaître, J. D'Armiento, Y. Okada, Matrix metalloproteinases, a disintegrin and metalloproteinases, and a disintegrin and metalloproteinases with thrombospondin motifs in non‐neoplastic diseases, Pathology international, 60 (2010) 477-496.

[178] D. Roth, M. Piekarek, M. Paulsson, H. Christ, W. Bloch, T. Krieg, J.M. Davidson, S.A. Eming, Plasmin modulates vascular endothelial growth factor-A-mediated angiogenesis during wound repair, The American journal of pathology, 168 (2006) 670-684.

[179] T. Syrovets, T. Simmet, Novel aspects and new roles for the serine protease plasmin, Cellular and Molecular Life Sciences CMLS, 61 (2004) 873-885.

[180] P.D. Thornton, R.J. Mart, S.J. Webb, R.V. Ulijn, Enzyme-responsive hydrogel particles for the controlled release of proteins: designing peptide actuators to match payload, Soft Matter, 4 (2008) 821-827.

[181] N. Bhattarai, H.R. Ramay, J. Gunn, F.A. Matsen, M. Zhang, PEG-grafted chitosan as an injectable thermosensitive hydrogel for sustained protein release, Journal of Controlled Release, 103 (2005) 609-624.

[182] H. Schild, Poly (N-isopropylacrylamide): experiment, theory and application, Progress in polymer science, 17 (1992) 163-249.

[183] J.-Y. Wu, S.-Q. Liu, P.W.-S. Heng, Y.-Y. Yang, Evaluating proteins release from, and their interactions with, thermosensitive poly (N-isopropylacrylamide) hydrogels, Journal of Controlled Release, 102 (2005) 361-372.

[184] Y. Hu, N. Zhao, J. Li, W. Yang, F. Xu, Temperature-responsive porous polycaprolactone-based films via surface-initiated ATRP for protein delivery, Journal of Materials Chemistry, 22 (2012) 21257-21264.

[185] T. Paunesku, S. Vogt, B. Lai, J. Maser, N. Stojicevic, K.T. Thurn, C. Osipo, H. Liu, D. Legnini, Z. Wang, Intracellular distribution of TiO2-DNA oligonucleotide nanoconjugates directed to nucleolus and mitochondria indicates sequence specificity, Nano letters, 7 (2007) 596-601.

[186] H. Zhou, X. Gan, T. Liu, Q. Yang, G. Li, Electrochemical study of photovoltaic effect of nano titanium dioxide on hemoglobin, Bioelectrochemistry, 69 (2006) 34-40.

[187] Y.-Y. Song, F. Schmidt-Stein, S. Bauer, P. Schmuki, Amphiphilic TiO2 nanotube arrays: an actively controllable drug delivery system, Journal of the American Chemical Society, 131 (2009) 4230-4232.

[188] Y.S. Wei, S.Y. Lin, S.L. Wang, M.J. Li, W.T. Cheng, Fourier transform IR attenuated total reflectance spectroscopy studies of cysteine‐induced changes in secondary conformations of bovine serum albumin after UV‐B irradiation, Biopolymers, 72 (2003) 345-351.

[189] B.A. Kerwin, R.L. Remmele, Protect from light: photodegradation and protein biologics, Journal of pharmaceutical sciences, 96 (2007) 1468-1479.

[190] L. Luo, Y. Guo, J. Yang, Y. Liu, S. Chu, F. Kong, Y. Wang, Z. Zou, An efficient visible light controlled protein delivery system, Chem. Commun., 47 (2011) 11243-11245.

[191] H. Tang, H. Kobayashi, Y. Niidome, T. Mori, Y. Katayama, T. Niidome, CW/pulsed NIR irradiation of gold nanorods: Effect on transdermal protein delivery mediated by photothermal ablation, Journal of Controlled Release, 171 (2013) 178-183.

[192] H.-W. Yang, M.-Y. Hua, H.-L. Liu, C.-Y. Huang, R.-Y. Tsai, Y.-J. Lu, J.-Y. Chen, H.-J. Tang, H.-Y. Hsien, Y.-S. Chang, T.-C. Yen, P.-Y. Chen, K.-C. Wei, Self-protecting core-shell magnetic nanoparticles for targeted, traceable, long half-life delivery of BCNU to gliomas, Biomaterials, 32 (2011) 6523-6532.

[193] Z. Huang, F. Tang, Preparation, structure, and magnetic properties of mesoporous magnetite hollow spheres, Journal of colloid and interface science, 281 (2005) 432-436.

[194] M. Chorny, E. Hood, R.J. Levy, V.R. Muzykantov, Endothelial delivery of antioxidant enzymes loaded into non-polymeric magnetic nanoparticles, J. Controlled Release, 146 (2010) 144-151.

[195] E. Teodor, S.-C. Litescu, V. Lazar, R. Somoghi, Hydrogel-magnetic nanoparticles with immobilized L-asparaginase for biomedical applications, J. Mater. Sci.: Mater. Med., 20 (2009) 1307-1314.

[196] T. Yoshimoto, K. Ohwada, K. Takahashi, A. Matsushima, Y. Saito, Y. Inada, Magnetic urokinase: targeting of urokinase to fibrin clot, Biochem. Biophys. Res. Commun., 152 (1988) 739-743.

[197] M.H. Cho, E.J. Lee, M. Son, J.-H. Lee, D. Yoo, J.-w. Kim, S.W. Park, J.-S. Shin, J. Cheon, A magnetic switch for the control of cell death signalling in in vitro and in vivo systems, Nature materials, 11 (2012) 1038-1043.

[198] J. Di, J. Price, X. Gu, X. Jiang, Y. Jing, Z. Gu, Ultrasound‐Triggered Regulation of Blood Glucose Levels Using Injectable Nano‐Network, Advanced healthcare materials, 3 (2014) 811-816.

[199] Z. Liu, M. Yan, J. Ge, P.K. Ouyang, Encapsulation of single enzyme in nanogel with enhanced biocatalytic activity and stability, J. Am. Chem. Soc., 128 (2006) 11008-11009.

[200] M. Yan, J.J. Du, Z. Gu, M. Liang, Y.F. Hu, W.J. Zhang, S. Priceman, L.L. Wu, Z.H. Zhou, Z. Liu, T. Segura, Y. Tang, Y.F. Lu, A novel intracellular protein delivery platform based on single-protein nanocapsules, Nat. Nanotechnol., 5 (2010) 48-53.

[201] W. Wei, J. Du, J. Li, M. Yan, Q. Zhu, X. Jin, X. Zhu, Z. Hu, Y. Tang, Y. Lu, Construction of Robust Enzyme Nanocapsules for Effective Organophosphate Decontamination, Detoxification, and Protection, Adv. Mater., 25 (2013) 2212-2218.

[202] S.M. Moghimi, A.C. Hunter, J.C. Murray, Long-Circulating and Target-Specific Nanoparticles: Theory to Practice, Pharmacological Reviews, 53 (2001) 283-318.

[203] D.E. Owens Iii, N.A. Peppas, Opsonization, biodistribution, and pharmacokinetics of polymeric nanoparticles, International Journal of Pharmaceutics, 307 (2006) 93-102.

[204] H. Soo Choi, W. Liu, P. Misra, E. Tanaka, J.P. Zimmer, B. Itty Ipe, M.G. Bawendi, J.V. Frangioni, Renal clearance of quantum dots, Nat Biotech, 25 (2007) 1165-1170.

[205] Z. Gu, M. Yan, B. Hu, K.-I. Joo, A. Biswas, Y. Huang, Y. Lu, P. Wang, Y. Tang, Protein Nanocapsule Weaved with Enzymatically Degradable Polymeric Network, Nano Lett., 9 (2009) 4533-4538.

[206] D. Liska, The detoxification enzyme systems, Altern Med Rev, 3 (1998) 187-198.

[207] W.J. Donarski, D.P. Dumas, D.P. Heitmeyer, V.E. Lewis, F.M. Raushel, Structure-activity relationships in the hydrolysis of substrates by the phosphotriesterase from Pseudomonas diminuta, Biochemistry, 28 (1989) 4650-4655.

[208] D. Purves, Neuroscience, 4th ed., Sinauer, Sunderland, Mass., 2008.

[209] J.L.K. Alan J. Russell, Jason A. Berberich, Using Biotechnology to Detect and Counteract Chemical Weapons, The Bridge: Linking Engineering and Society, 33 (2003) 19-24.

[210] W.J. Donarski, D.P. Dumas, D.P. Heitmeyer, V.E. Lewis, F.M. Raushel, Structure-activity relationships in the hydrolysis of substrates by the phosphotriesterase from Pseudomonas diminuta, Biochemistry, 28 (1989) 4650-4655.

[211] D.P. Dumas, S.R. Caldwell, J.R. Wild, F.M. Raushel, Purification and properties of the phosphotriesterase from Pseudomonas diminuta, J Biol Chem, 264 (1989) 19659-19665.

[212] G.A. Omburo, J.M. Kuo, L.S. Mullins, F.M. Raushel, Characterization of the zinc binding site of bacterial phosphotriesterase, J. Biol. Chem., 267 (1992) 13278-13283.

[213] I. Petrikovics, D. Papahadjopoulos, K. Hong, T.-C. Cheng, S.I. Baskin, J. Jiang, J.C. Jaszberenyi, B.A. Logue, M. Szilasi, W.D. McGuinn, J.L. Way, Comparing Therapeutic and Prophylactic Protection against the Lethal Effect of Paraoxon, Toxicol. Sci., 77 (2004) 258-262.

[214] M.M. Benning, J.M. Kuo, F.M. Raushel, H.M. Holden, Three-Dimensional Structure of Phosphotriesterase: An Enzyme Capable of Detoxifying Organophosphate Nerve Agents, Biochemistry, 33 (1994) 15001-15007.

[215] J. Jang, H. Park, Formation and structure of polyacrylamide–silica nanocomposites by sol–gel process, J. Appl. Polym. Sci., 83 (2002) 1817-1823.

[216] R.K. Sharma, S. Das, A. Maitra, Enzymes in the cavity of hollow silica nanoparticles, J. Colloid Interface Sci., 284 (2005) 358-361.

[217] W.C.W. Chan, S. Nie, Quantum Dot Bioconjugates for Ultrasensitive Nonisotopic Detection, Science, 281 (1998) 2016-2018.

[218] Y. Lu, S. Bangsaruntip, X. Wang, L. Zhang, Y. Nishi, H. Dai, DNA Functionalization of Carbon Nanotubes for Ultrathin Atomic Layer Deposition of High κ Dielectrics for Nanotube Transistors with 60 mV/Decade Switching, J. Am. Chem. Soc., 128 (2006) 3518-3519.

[219] H.K. Baca, C. Ashley, E. Carnes, D. Lopez, J. Flemming, D. Dunphy, S. Singh, Z. Chen, N. Liu, H. Fan, G.P. López, S.M. Brozik, M. Werner-Washburne, C.J. Brinker, Cell-Directed Assembly of Lipid-Silica Nanostructures Providing Extended Cell Viability, Science, 313 (2006) 337-341.

[220] A. Bhambhani, C.V. Kumar, Protein/DNA/Inorganic Materials: DNA Binding to Layered α-Zirconium Phosphate Enhances Bound Protein Structure and Activity, Adv. Mater., 18 (2006) 939-942.

[221] Y. Xia, Nanomaterials at work in biomedical research, Nat. Mater., 7 (2008) 758-760.

[222] P. Kohli, C.C. Harrell, Z. Cao, R. Gasparac, W. Tan, C.R. Martin, DNA-Functionalized Nanotube Membranes with Single-Base Mismatch Selectivity, Science, 305 (2004) 984-986.

[223] H. Ping, G. Gillian, J.H. Stephen, The on-line synthesis of enzyme functionalized silica nanoparticles in a microfluidic reactor using polyethylenimine polymer and R5 peptide, Nanotechnology, 19 (2008) 315603.

[224] G. Irazoqui, A. Villarino, F. Batista-Viera, B. Brena, Activity and stability of Escherichia coli Œ≤-galactosidase in cosolvent systems, Biotechnol. Tech., 12 (1998) 885-888.

[225] E. Tellechea, K.J. Wilson, E. Bravo, K. Hamad-Schifferli, Engineering the Interface between Glucose Oxidase and Nanoparticles, Langmuir, 28 (2012) 5190-5200.

[226] J. Ge, D. Lu, J. Wang, M. Yan, Y. Lu, Z. Liu, Molecular Fundamentals of Enzyme Nanogels, J. Phys. Chem. B, 112 (2008) 14319-14324.

[227] C. Baldock, L. Rintoul, S.F. Keevil, J.M. Pope, G.A. George, Fourier transform Raman spectroscopy of polyacrylamide gels (PAGs) for radiation dosimetry, Phys. Med. Biol., 43 (1998) 3617.

[228] D. Zhao, J. Feng, Q. Huo, N. Melosh, G.H. Fredrickson, B.F. Chmelka, G.D. Stucky, Triblock copolymer syntheses of mesoporous silica with periodic 50 to 300 angstrom pores, science, 279 (1998) 548-552.

[229] H.R. Luckarift, R. Greenwald, M.H. Bergin, J.C. Spain, G.R. Johnson, Biosensor system for continuous monitoring of organophosphate aerosols, Biosens. Bioelectron., 23 (2007) 400-406.

[230] C.H. Lei, Y.S. Shin, J. Liu, E.J. Ackerman, Entrapping enzyme in a functionalized nanoporous support, J. Am. Chem. Soc., 124 (2002) 11242-11243.

[231] M. Ramanathan, H.R. Luckarift, A. Sarsenova, J.R. Wild, E.K. Ramanculov, E.V. Olsen, A.L. Simonian, Lysozyme-mediated formation of protein-silica nano-composites for biosensing applications, Colloids Surf., B, 73 (2009) 58-64.

[232] A.E. David, A.J. Yang, N.S. Wang, Enzyme stabilization and immobilization by sol-gel entrapment, Methods Mol Biol, 679 (2011) 49-66.

[233] H.H.P. Yiu, P.A. Wright, Enzymes supported on ordered mesoporous solids: a special case of an inorganic-organic hybrid, J. Mater. Chem., 15 (2005) 3690-3700.

[234] X.-Y. Chu, N.-F. Wu, M.-J. Deng, J. Tian, B. Yao, Y.-L. Fan, Expression of organophosphorus hydrolase OPHC2 in Pichia pastoris: Purification and characterization, Protein Expression Purif., 49 (2006) 9-14.

[235] P. Mulchandani, W. Chen, A. Mulchandani, J. Wang, L. Chen, Amperometric microbial biosensor for direct determination of organophosphate pesticides using recombinant microorganism with surface expressed organophosphorus hydrolase, Biosens. Bioelectron., 16 (2001) 433-437.

[236] H.R. Luckarift, L. Betancor, Bioinspired enzyme encapsulation for biocatalysis, Trends Biotechnol., 26 (2008) 566-572.

[237] V. Stepankova, S. Bidmanova, T. Koudelakova, Z. Prokop, R. Chaloupkova, J. Damborsky, Strategies for Stabilization of Enzymes in Organic Solvents, ACS Catal., 3 (2013) 2823-2836.

[238] C.B. Faulds, M. Pérez-Boada, Á.T. Martínez, Influence of organic co-solvents on the activity and substrate specificity of feruloyl esterases, Bioresour. Technol., 102 (2011) 4962-4967.

[239] W.F. Busby, J.M. Ackermann, C.L. Crespi, Effect of methanol, ethanol, dimethyl sulfoxide, and acetonitrile on in vitro activities of cDNA-expressed human cytochromes P-450, Drug Metab. Dispos., 27 (1999) 246-249.

[240] L.A.S. Gorman, J.S. Dordick, Organic solvents strip water off enzymes, Biotechnol. Bioeng., 39 (1992) 392-397.

[241] A. Zaks, A.M. Klibanov, Enzyme-catalyzed processes in organic solvents, Proc. Natl. Acad. Sci. U. S. A., 82 (1985) 3192-3196.

[242] N. Doukyu, H. Ogino, Organic solvent-tolerant enzymes, Biochem. Eng. J., 48 (2010) 270-282.

[243] R.A. Sheldon, Enzyme Immobilization: The Quest for Optimum Performance, Adv. Synth. Catal., 349 (2007) 1289-1307.

[244] H.R. Luckarift, S. Balasubramanian, S. Paliwal, G.R. Johnson, A.L. Simonian, Enzyme-encapsulated silica monolayers for rapid functionalization of a gold surface, Colloids Surf., B, 58 (2007) 28-33.

[245] L. Wang, L. Wei, Y. Chen, R. Jiang, Specific and reversible immobilization of NADH oxidase on functionalized carbon nanotubes, J. Biotechnol., 150 (2010) 57-63.

[246] E.T. Hwang, H. Gang, J. Chung, M.B. Gu, Carbonic anhydrase assisted calcium carbonate crystalline composites as a biocatalyst, Green Chem., 14 (2012) 2216-2220.

[247] E.T. Hwang, R. Tatavarty, J. Chung, M.B. Gu, New Functional Amorphous Calcium Phosphate Nanocomposites by Enzyme-Assisted Biomineralization, ACS Appl. Mater. Interfaces, 5 (2013) 532-537.

[248] Z. Gu, A. Biswas, M. Zhao, Y. Tang, Tailoring nanocarriers for intracellular protein delivery, Chem. Soc. Rev., 40 (2011) 3638-3655.

[249] D.S. Watson, A.N. Endsley, L. Huang, Design considerations for liposomal vaccines: Influence of formulation parameters on antibody and cell-mediated immune responses to liposome associated antigens, Vaccine, 30 (2012) 2256-2272.

[250] T. Akagi, F. Shima, M. Akashi, Intracellular degradation and distribution of protein-encapsulated amphiphilic poly(amino acid) nanoparticles, Biomaterials, 32 (2011) 4959-4967.

[251] R.C. Mundargi, V.R. Babu, V. Rangaswamy, P. Patel, T.M. Aminabhavi, Nano/micro technologies for delivering macromolecular therapeutics using poly(d,l-lactide-co-glycolide) and its derivatives, J. Controlled Release, 125 (2008) 193-209.

[252] I.I. Slowing, B.G. Trewyn, S. Giri, V.S.Y. Lin, Mesoporous Silica Nanoparticles for Drug Delivery and Biosensing Applications, Adv. Funct. Mater., 17 (2007) 1225-1236.

[253] N.W.S. Kam, H. Dai, Carbon Nanotubes as Intracellular Protein Transporters: Generality and Biological Functionality, J. Am. Chem. Soc., 127 (2005) 6021-6026.

[254] M. Zorko, Ü. Langel, Cell-penetrating peptides: mechanism and kinetics of cargo delivery, Adv. Drug Delivery Rev., 57 (2005) 529-545.

[255] V. Torchilin, Intracellular delivery of protein and peptide therapeutics, Drug Discovery Today: Technologies, 5 (2008) e95-e103.

[256] E.A. Simone, T.D. Dziubla, F. Colon-Gonzalez, D.E. Discher, V.R. Muzykantov, Effect of Polymer Amphiphilicity on Loading of a Therapeutic Enzyme into Protective Filamentous and Spherical Polymer Nanocarriers, Biomacromolecules, 8 (2007) 3914-3921.

[257] D. Bhadra, S. Bhadra, S. Jain, N.K. Jain, A PEGylated dendritic nanoparticulate carrier of fluorouracil, Int. J. Pharm., 257 (2003) 111-124.

[258] C.M. Ensor, F.W. Holtsberg, J.S. Bomalaski, M.A. Clark, Pegylated Arginine Deiminase (ADI-SS PEG20,000 mw) Inhibits Human Melanomas and Hepatocellular Carcinomas in Vitro and in Vivo, Cancer Res., 62 (2002) 5443-5450.

[259] M. Manuela Gaspar, D. Blanco, M.E.M. Cruz, M.a. José Alonso, Formulation of l-asparaginase-loaded poly(lactide-co-glycolide) nanoparticles: influence of polymer properties on enzyme loading, activity and in vitro release, J. Controlled Release, 52 (1998) 53-62.

[260] J.A. Rodríguez-Martínez, I. Rivera-Rivera, R.J. Solá, K. Griebenow, Enzymatic activity and thermal stability of PEG-α-chymotrypsin conjugates, Biotechnol. Lett., 31 (2009) 883-887.

[261] C. Lei, Y. Shin, J. Liu, E.J. Ackerman, Entrapping enzyme in a functionalized nanoporous support, J. Am. Chem. Soc., 124 (2002) 11242-11243.

[262] M. Persson, E. Wehtje, P. Adlercreutz, Immobilisation of lipases by adsorption and deposition: high protein loading gives lower water activity optimum, Biotechnol. Lett., 22 (2000) 1571-1575.

[263] S. Kaliberov, S. Chiz, L. Kaliberova, V. Krendelchtchikova, D. Della Manna, T. Zhou, D. Buchsbaum, Combination of cytosine deaminase suicide gene expression with DR5 antibody treatment increases cancer cell cytotoxicity, Cancer gene therapy, 13 (2006) 203-214.

[264] E.S. Lee, Z. Gao, Y.H. Bae, Recent progress in tumor pH targeting nanotechnology, J. Controlled Release, 132 (2008) 164-170.

[265] N. Carelle, E. Piotto, A. Bellanger, J. Germanaud, A. Thuillier, D. Khayat, Changing patient perceptions of the side effects of cancer chemotherapy, Cancer, 95 (2002) 155-163.

[266] C. Müller, P.A. Schubiger, R. Schibli, In vitro and in vivo targeting of different folate receptor-positive cancer cell lines with a novel 99mTc-radiofolate tracer, Eur J Nucl Med Mol Imaging, 33 (2006) 1162-1170.

[267] R.A. Daniels, H. Turley, F.C. Kimberley, X.S. Liu, J. Mongkolsapaya, P. Ch'En, X.N. Xu, B. Jin, F. Pezzella, G.R. Screaton, Expression of TRAIL and TRAIL receptors in normal and malignant tissues, Cell Res, 15 (2005) 430-438.

[268] A. Albanese, P.S. Tang, W.C. Chan, The effect of nanoparticle size, shape, and surface chemistry on biological systems, Annual review of biomedical engineering, 14 (2012) 1-16.

[269] J. Harris, F. Veronese, Peptide and protein pegylation II-clinical evaluation, Adv Drug Deliv Rev, 55 (2003) 1259-1260.

[270] J.M. Harris, R.B. Chess, Effect of pegylation on pharmaceuticals, Nature Reviews Drug Discovery, 2 (2003) 214-221.

[271] K. Knop, R. Hoogenboom, D. Fischer, U.S. Schubert, Poly (ethylene glycol) in drug delivery: pros and cons as well as potential alternatives, Angewandte Chemie International Edition, 49 (2010) 6288-6308.

[272] F.M. Veronese, Peptide and protein PEGylation: a review of problems and solutions, Biomaterials, 22 (2001) 405-417.

[273] J.K. Armstrong, G. Hempel, S. Koling, L.S. Chan, T. Fisher, H.J. Meiselman, G. Garratty, Antibody against poly (ethylene glycol) adversely affects PEG‐asparaginase therapy in acute lymphoblastic leukemia patients, Cancer, 110 (2007) 103-111.

[274] T. Ishihara, M. Takeda, H. Sakamoto, A. Kimoto, C. Kobayashi, N. Takasaki, K. Yuki, K.-i. Tanaka, M. Takenaga, R. Igarashi, Accelerated blood clearance phenomenon upon repeated injection of PEG-modified PLA-nanoparticles, Pharmaceutical research, 26 (2009) 2270-2279.

[275] K. Ishihara, H. Nomura, T. Mihara, K. Kurita, Y. Iwasaki, N. Nakabayashi, Why do phospholipid polymers reduce protein adsorption?, Journal of biomedical materials research, 39 (1998) 323-330.

[276] L. Zhang, Z. Cao, T. Bai, L. Carr, J.-R. Ella-Menye, C. Irvin, B.D. Ratner, S. Jiang, Zwitterionic hydrogels implanted in mice resist the foreign-body reaction, Nature biotechnology, 31 (2013) 553-556.

[277] Y. Iwasaki, K. Ishihara, Phosphorylcholine-containing polymers for biomedical applications, Analytical and bioanalytical chemistry, 381 (2005) 534-546.

[278] Y. Bae, N. Nishiyama, S. Fukushima, H. Koyama, M. Yasuhiro, K. Kataoka, Preparation and biological characterization of polymeric micelle drug carriers with intracellular pH-triggered drug release property: tumor permeability, controlled

subcellular drug distribution, and enhanced in vivo antitumor efficacy, Bioconjugate chemistry, 16 (2005) 122-130.

[279] E.S. Lee, K. Na, Y.H. Bae, Polymeric micelle for tumor pH and folate-mediated targeting, Journal of Controlled Release, 91 (2003) 103-113.

[280] Z. Gao, D. Lee, D. Kim, Y. Bae, Doxorubicin loaded pH-sensitive micelle targeting acidic extracellular pH of human ovarian A2780 tumor in mice, Journal of drug targeting, 13 (2005) 391-397.

[281] E.R. Gillies, J.M. Fréchet, pH-responsive copolymer assemblies for controlled release of doxorubicin, Bioconjugate chemistry, 16 (2005) 361-368.

[282] K. Engin, D. Leeper, J. Cater, A. Thistlethwaite, L. Tupchong, J. McFarlane, Extracellular pH distribution in human tumours, International Journal of Hyperthermia, 11 (1995) 211-216.

[283] R. van Sluis, Z.M. Bhujwalla, N. Raghunand, P. Ballesteros, J. Alvarez, S. Cerdán, J.-P. Galons, R.J. Gillies, In vivo imaging of extracellular pH using 1 H MRSI, Magnetic resonance in medicine, 41 (1999) 743-750.

[284] D.B. Leeper, K. Engin, A.J. Thistlethwaite, H.D. Hitchon, J.D. Dover, D.-J. Li, L. Tupchong, Human tumor extracellular pH as a function of blood glucose concentration, International Journal of Radiation Oncology* Biology* Physics, 28 (1994) 935-943.

[285] A.S. Ojugo, P.M. McSheehy, D.J. McIntyre, C. McCoy, M. Stubbs, M.O. Leach, I.R. Judson, J.R. Griffiths, Measurement of the extracellular pH of solid tumours in mice by magnetic resonance spectroscopy: a comparison of exogenous 19F and 31P probes, NMR in Biomedicine, 12 (1999) 495-504.